An-Najah National University

Faculty of Graduate studies

Purification of Groundwater from Heavy Toxic Metals using Suspended Polydentate Supported Ligands

By

Bayan Mohammad Mahmoud Khalaf

Supervisor

Prof. Shehdeh Jodeh

Co- Supervisor

Prof. Ismail Warad

This Thesis is Submitted in Partial Fulfillment of the Requirements for the Degree of Master of Chemistry, Faculty of Graduate Studies, An-Najah National University, Nablus, Palestine.

2016

Purification of Groundwater from Heavy Toxic Metals using Suspended Polydentate Supported Ligands

By

Bayan Mohammad Mahmoud Khalaf

This Thesis was defended successfully on 14/2/2016 and approved by:

Defense Committee Members	**Signature**
– **Prof. Shehdeh Jodeh/Supervisor**	.....
– **Prof. Ismail Warad/Co-Supervisor**	.....
– **Dr. Subhi Samhan /External Examiner**	.....
– **Dr. Nidal Zatar /Internal Examiner**	.....

Dedication

I dedicate this thesis to my family for supporting and encouraging me to believe in myself, and to my friends who have been in my side all the way.

Acknowledgments

I would like to express my gratitude for everyone who helped me in this research starting with endless thanks for my supervisors, Prof. Shehdeh Jodeh and Prof. Ismail Warad, since they didn’t keep any effort in encouraging me to do a great job, providing me with valuable information and advices to be better each time. Thanks for the continuous support and kind communication which had a great effect regarding to feel interesting about what I am working on.

In addition, I would like to thank both Palestinian Water Authority and MEDRC for their financial funding for my master degree works. Also, I would like to thank MENA for their funding for support of grant No - WIF 04 under prime contract / To No - AID - OAA - TO - 11 - 00049. Special thanks go to both Sara Hillars and Dr. Ghazi Abu rumman from MENA for their help and guidelines.

Furthermore, I would like to thank my family for supporting me all the way, and I wish that I made them proud of me and of my hard work.

Finally, I won't also forget to present my special thanks for my friends who have been in my side during this research.

الإقرار

أنا الموقعة أدناه مقدمة الرسالة التي تحمل العنوان :

Purification of Groundwater from Heavy Toxic Metals using Suspended Polydentate Supported Ligands

أقر بأنّ ما اشتملت عليه هذه الرسالة إنما هي نتاج جهدي الخاص ، باستثناء ما تمّت الإشارة إليه حيثما ورد ، وأنّ هذه الرسالة ككل ، أو أي جزء منها لم يُقدّم لنيل أي درجة أو لقب علمي أو بحثي لدى أي مؤسسة تعليمية أو بحثية أخرى.

Declaration

The work provided in this thesis, unless otherwise referenced, is the researcher's own work and has not been submitted elsewhere for any other degree or qualification.

Student's name: Bayan Mohammad Khalaf **اسم الطالبة :**

Signature: Bayan **التوقيع :**

Date: 14-2-2016 **التاريخ :**

List of Contents

List of Tables

List of Figures

List of Abbreviations

Symbol	Abbreviation
SEM	Scanning Electron Micrograph
UV	Ultra-Violet
IR	Infrared
B.E.T	Brunauer-Emmett-Teller
B.J.H	Barrett-Joyner-Halenda
TGA	Thermogravimetric Analysis
AAS	Atomic Absorption Spectroscopy
ICP	Inductively Coupled Plasma
^{13}C NMR	Carbon 13 Nuclear Magnetic Resonance
TLV	Threshold Limit Value
WHO	World Health Organization
DO	Dissolved Oxygen
TOC	Total Organic Carbon
WH	Water Hardness
C_e	The equilibrium concentration of the adsorbate (mg/L).
C_o	The initial concentration of the adsorbate (mg/L).
q_e	The amount of adsorbate per unit mass of adsorbent (mg/g).
b	The Langmuir affinity constant (L/mg).
Q_o	The adsorption capacity at equilibrium (mg/g).
V	The volume of the solution (L).
m	The mass of the adsorbent (g).
K_F	The Freundlich constant related to adsorption capacity (mg/g).
n	The heterogeneity coefficient that gives an indication of how favorable the adsorption process (g/L).
q_t	The mass of adsorbate per unit mass of adsorbent at time t (mg/g).
K_1	The rate constant of pseudo first-order adsorption model ($mg.g^{-1}.min^{-1}$).
K_2	The equilibrium rate constant of pseudo second-order adsorption model ($g.mg^{-1}.min^{-1}$).
K_p	The diffusion rate constant ($mg.g^{-1}.min^{0.5}$).
C	Constant that gives an indication of the thickness of the boundary layer (mg/g).
ΔG	Gibbs free energy change (J).
ΔH	Enthalpy change (J).

ΔS	Entropy change (J/K).
T	The absolute temperature (K).
R	The universal gas constant (8.314 $J.mol^{-1}.K^{-1}$).
K_d	The thermodynamic equilibrium constant (L/g).

Purification of Groundwater from Heavy Toxic Metals using Suspended Polydentate Supported Ligands

By

Bayan Khalaf

Supervisor

Prof. Shehdeh Jodeh

Co- Supervisor

Prof. Ismail Warad

Abstract

This study aims to prepare several vehicles chelation polydentate supported ligands in order to be susceptible to imply conjunction with the highly toxic heavy metal ions in the water including lead, nickel and cadmium ions, as the process of interaction between ligands and heavy metals depends on the circumstances surrounding conditions which are treated in this research.

Metal ion uptake through complexation can be affected by hydrophilic-hydrophobic balance, the nature of chelate ligands and the extent of cross-linking of macromolecular supports. Ligand function also dictates reactivity, complexation ability and efficiency of polymer supported ligands in the present case expected to be good solution for such problem.

This research involves the synthesis of new polysiloxane surfaces modified with ortho-, meta-, or para-nitrophenyl moieties. The resulting adsorbents have been characterized by SEM, IR, UV, ^{13}C solid state NMR, BET surface area, B.J.H. pore sizes, TGA and nitrogen adsorption-desorption

isotherm. These porous materials showed a very good thermal and chemical stability and hence they can be used as perfect adsorbents to uptake toxic heavy metal ions including Cd(II), Pb(II) and Ni(II) from groundwater taking from Burqin town in Palestine. The concentrations of each adsorbate in the filtrate were determined using Atomic Absorption Spectrophotometer. The results showed that all of the three resulting products have high adsorption efficiency. Also, it showed strong complexation properties with heavy metal ions.

In order to investigate the adsorption efficiency for the adsorption of Cd(II), Pb(II) or Ni(II) onto (Si-o-NO_2), (Si-m-NO_2) or (Si-p-NO_2), the effect of solution conditions on each adsorption process were studied. These conditions involve the effect of contact time, pH value, temperature, adsorbent dose and the initial concentration of adsorbate.

The maximum extent of adsorption was for (Si-p-NO_2) polymer in the presence of lead ions. This adsorption process needed only 1 minute of shaking to have 99.95% as percent of Pb(II) removal at solution conditions of 20°C temperature, pH value equals 8, 5 mg adsorbent dose, 50 ppm of Pb(II) solution as initial concentration and 7 mL solution volume. For cadmium and nickel ions, the maximum percent of removal was 98.99% in the presence of (Si-m-NO_2) adsorbent.

The best equilibrium isotherm model for each adsorption process was investigated according to the value of the correlation coefficient of Langmuir and Freundlich isotherm adsorption models. The kinetics of adsorption were also investigated using pseudo first-order, pseudo second-

order and intra-particle diffusion kinetic models. In addition, Van't Hoff plot for each adsorption was investigated in order to determine the values of enthalpy change and entropy change, and hence determining if the adsorption process is spontaneous or not, and if it is exothermic or endothermic one. The results showed that all of these adsorptions followed Langmuir adsorption isotherm and the mechanism of all of these reactions followed pseudo second-order kinetic adsorption model. The thermodynamic parameters of all the adsorptions proved that these processes are endothermic ($\Delta H > 0$) and non spontaneous ($\Delta S < 0$).

Each of the synthesized polymers was also regenerated, and the percentage removal before and after adsorbent recovery is determined. The results showed a promising percent of removal for Cd(II), Pb(II) and Ni(II).

Chapter One

Introduction

1.1 Overview

The increasing levels of heavy metal ions in the water resources and environment represent a serious threat to human health, ecological systems and living resources. Although there are many sources of heavy metals in addition to the natural ones, some industrial sectors are at present those which contribute the most to environmental pollution with these toxic elements. Among such industrial sectors the metal finishing industry is an important one, due to the large number of enterprises by which is integrated as well as their geographical dispersion. The main way of pollution of these industries is the emission of liquid effluents with relatively low, although harmful metal concentrations (up to some hundreds of mg/L), mostly, mercury, lead, chromium, cadmium, copper, zinc and nickel. These seven elements are considered ‘‘priority metals’’ from the standpoint of potential hazard to human health.

Environmental pollution with heavy metal ions is a considerable problem owing to their tendency to accumulate in living organisms and toxicities in relatively low concentration [1-3]. Many methods, such as reduction and precipitation, ion exchange, reverse osmosis and adsorption, have been proposed to remove heavy metal ions from water [2-7]. Among these technologies, many researches concentrated on metal ion recovery using

appropriate chelate polymer surfaces, because they are reusable, easy handing and have higher adsorption capacities, efficiencies as well as high selectivity to some metal ions [2, 3, 6, 7]. Hence, numerous chelating resins have been prepared through the polymerization of conventional chelating monomers, such as acrylic acid [8], allylthiourea [9], vinyl pyrrolidone [10], and vinyl imidazole [11]. Additionally modification of a synthetic polymer [2, 5, 12-17] or a natural polymer matrix [3, 18-21] by functionlization reactions has also been used to form a chelating polymer. Around the vinyl monomers, Glycidyl MethAcrylate (GMA) is a commercial industrial material, which is cheaper than any other vinyl monomers possessing an epoxy ring in the side chain. Thus, numerous chelating resins have been successfully prepared via an epoxy group reaction of poly(glycidyl methacrylate) with amines. In addition, glycine is a low-priced amino acid that possesses an amino and a carboxyl groups to share electron pairs with a metal ion [5, 13-15, 20].

In this work, a chelating polysiloxane surfaces derived from carbaldehyde derivatives and 3-aminopropyl trimethoxysilane were synthesized and then functionalized with ortho-,meta-, or para-nitrophenyl moieties for the removal of Pd(II), Ni(II), and Cd(II) from an aqueous solution. The effects of solution conditions including pH value, temperature, contact time, adsorbent dose and metal ion concentration, on the adsorption behaviour were investigated.

1.2 Research Objectives

1.2.1 General Objectives

1. Purify the water from toxic metal ions by coordinate the supported chelate ligand with these metal ions through complexation process.

2. To study the several factors in order to determine the extent and the efficiency of adsorption technique.

1.2.2 Specific Objectives

1. Synthesis and characterization of new supported hybrid material containing chelate part to be as a tited-free ligand.

2. Comparison of the efficiency of ortho-, meta-, and para-nitrophenyl receptors for the adsorption of lead, nickel and cadmium ions in water.

3. De-complexation, which is removal of the metal by de-binding it using chemical or electrochemical method in order to recycle the stationary phase.

1.3 Research Questions

1. What are the optimum conditions of pH, temperature, contact time, concentration of adsorbate and amount of adsorbent for the synthesized polymers to adsorb cadmium, nickel and lead ions efficiently?

2. To which extent the new synthesized polysiloxane surfaces can tolerate and adsorb heavy metal ions in groundwater?

3. Can nitrophenyl-substituted silicas be used to clean up polluted groundwater?

1.4 Significance of Thesis

1. Through this work we find out novel technique which is ready to uptake heavy toxic elements from the water to drinkable degree.

2. The stationary phase supported material can be recycled and be used for several times.

3. Small lab station can be established in order to test the method efficiency.

1.5 Novelty of the Work

This research depends on synthesis and characterization of new polysiloxane surfaces modified with ortho-, meta-, or para-nitrophenyl receptors. The resulting adsorbents have been characterized by IR, BET surface area, ^{13}C NMR solid state, SEM, UV, B.J.H. pore sizes, TGA and nitrogen adsorption-desorption isotherm.

Each of the synthesized products was used to uptake toxic heavy metal ions including cadmium, nickel and lead from groundwater.

The porous silica-immobilized ligands showed very strong complexation properties in the presence of heavy metal ions. The concentrations of toxic minerals in the filtrate were determined using Atomic Absorption

Spectrophotometer. The results showed that all of the three resulting products have very high efficiency for the adsorption of Ni(II), Pb(II) and Cd(II) in water.

The maximum extent of adsorption was for the modified polysiloxane surfaces with functional para-nitrophenyl moieties in the presence of lead ions. This adsorption process needed only one minute of shaking to have 99.95% as percent of Pb(II) removal.

1.6 Methodology

The efficient method that was used in this work in order to remove Pd(II), Cd(II) and Ni(II) from water and hence make it safe for drinking includes the following steps.

1- Modified polysiloxane surfaces with functional ortho-, meta-, or para-nitrophenyl receptors are synthesized using complexation technique as in scheme (Figure 1.1).

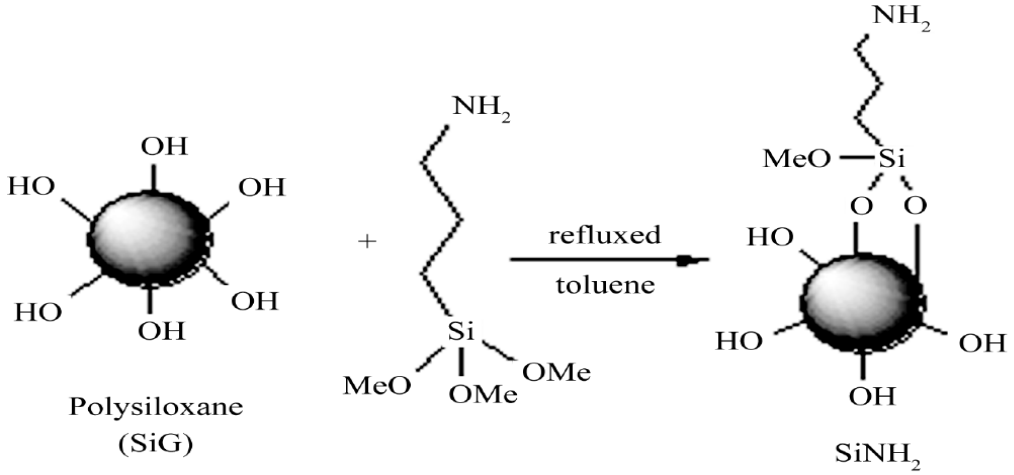

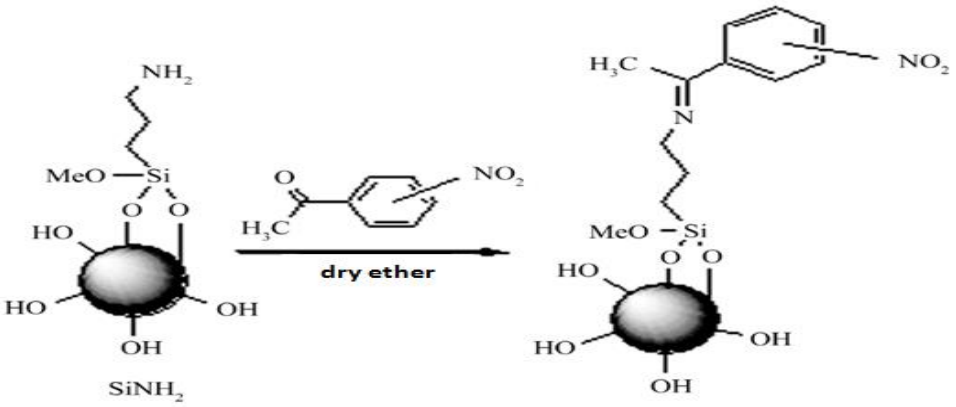

Figure 1.1: The synthesis route of modified nitrophenyl-substituted silicas.

2- The ions of metal to be separated from the coordination compounds (i.e. the polymeric complexes) with a high molecular weight polyelectrolyte (a chelating agent) added into a solution under separation. Solubility of the complexes so formed is much smaller than that of the unbounded ions. Thus, a polymeric complex remains in the retentate (concentrate) when such a solution is forced through the filtration station.

3- Stationary phase using such polymeric chelate continent will serve as stand columns to coordinate mobile metal ions in suitable milled complexation condition; the process can be carried out under the continuous mode of operation which provides means to automate it (Figure 1.2).

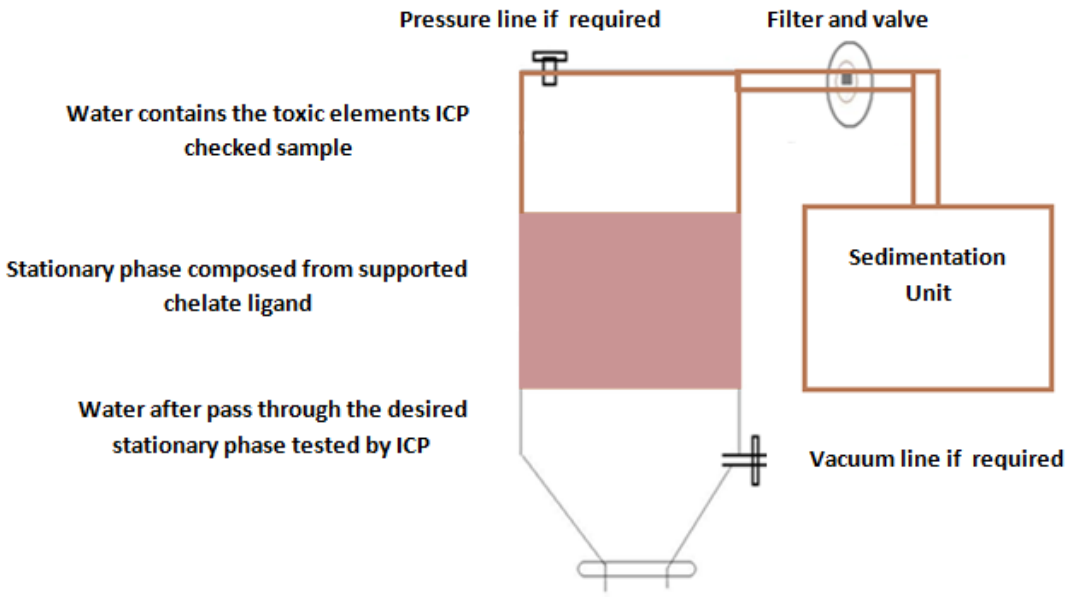

Figure 1.2: An apparatus shows purification process of toxic heavy metal ions from groundwater.

4- Recycling of complexes, this means that the metal/polymer complex can later be decomposed by chemical methods (such as using acidic medium) or electrochemical methods. Then it comes back into the chelation stage without any additional treatment. A multiple reuse of the chelating agent provides means to enhance the economical indexes of the process run aimed at separation of metal ions. The concentrations of toxic metal ions are determined before and after the treatment using Inductively Coupled Plasma (ICP) instrument that can be used for the analysis of many elements at the same time, or Atomic Absorption Spectrophotometer (AAS) that depends on the analysis of one element at a time, in order to verify the effectiveness of this purification method.

Chapter Two

Literature Review

2.1 Groundwater

As Known from the water cycle, there is continuous motion of water through the environment. Evaporation of water from the oceans occurs first, then it condenses into clouds and finally fells as rain on the land surface. Some of rainfall will flow into rivers and back into the sea, but most of it will soak into the soil, which acts like a giant sponge. Some of this water will be taken up by plants through transpiration and then returning to the atmosphere. While the other part of it will soak under the ground as groundwater in infiltration process [22].

The geological formations in which groundwater flows through them may be impermeable where water can hardly flow. And be permeable, in which these formations contain fine holes that allow water to flow and hence acting as aquifers of groundwater [23].

2.1.1 Importance of Groundwater

Groundwater is one of the most major sources of freshwater in the world. It makes up approximately 30% of all the world's freshwater, such that; freshwater makes up about 2.5% of all the world’s water. The quality of groundwater in most of the areas is very good, and it usually needs much less treatment than surface water in order to make it safe for drinking. This

is because of flowing of groundwater through the soil and rocks which play an important role in removing different types of pollutants [24].

2.1.2 Groundwater Pollution

Water is considered a universal solvent; it can tolerate many types of materials. Only, when a concentration of a solute inside water increases to a level that adversely affect living organisms. Then, this solute is considered a pollutant. So that; in order to avoid water contamination, the amount of this substance should not be allowed to cross a specific concentration that depends on the type and toxicity of the pollutant. This concentration is called Threshold Limit Value (TLV) which shows the average concentration to which any person with good health may be exposed for seven to eight hours per week for lifetime without showing an adverse health effect [25].

About six hundred chemicals have been listed with threshold limit values ranging from very low concentrations. Such as, 0.001 ppm for mercury to high values. For example, 1000 ppm for platinum. In general, TLV for the same substance will decrease with increasing temperature [26, 27].

Groundwater can be considered the most important source of drinking water. This source is usually clean and suitable for human usage, but it becomes contaminated in the presence of industrial activities. Many environmental agencies, of which the most important the World Health Organization (WHO) have set standards limiting the levels of dangerous

chemicals in drinking water. Any water source exceeding these values is not supposed to be used for drinking. Threshold limits vary slightly from one agency to another and from one year to another, according the most recent finding of researchers and to the most recent trends of pollution [28-30].

Several parameters can be used to investigate pollution of groundwater. For example; pH, salinity, Dissolved Oxygen (DO), nitrates, phosphates, heavy metals, oil derivatives, Water Hardness (WH), Total Organic Carbon (TOC) and organic residues [31-33].

2.1.3 Purification of Groundwater

Pollution of groundwater with heavy metal ions occurs when these pollutants are discharged directly or indirectly into water bodies beneath earth's surface in soil pore spaces, and in the fractures of rock formations without adequate treatment to be rid off [34].

In general, purification of polluted groundwater aims to remove undesirable chemicals, suspended solids and biological contaminants in order to make groundwater fit for drinking, agricultural or other purposes [35].

Any process of groundwater treatment needs to follow a number of steps. These are, identify the exact source of the groundwater that needs to be treated by determining location, cost, sustainability, and the quality and quantity of water. Then this polluted water must be protected from further

contamination. After that, finding the most appropriate purification technique of having usable water [36, 37].

2.2 Heavy Metals

Among the 88 metals present in the periodic table, about 30 elements may be considered as toxic heavy metals. Such as, Co, Ni, Cu, Ag, Au, Pd, TI, Cd, Re, Mo, Ta, Bi, Zn, Os and others. All of the heavy metals have a specific gravity (density) greater than 5.0 g/cm^3 [38].

Many of the heavy metals are common and are found in many living organisms. Unwanted heavy metal ions often find their way into water from many sources. Inevitably, some of these chemicals find their way into groundwater from which drinking water is taken. Generally, when heavy metals exist as free elements, they are not toxic as the forms that result from existing as cations or organometallic compounds [39].

Heavy metals are used in many industrial processes. For example, textile, tanning, pickling, electroplating, plastic and battery industries. Because of their many uses in society; heavy metal ions often find their way into solid waste and wastewater where they are difficult to be removed and become dangerously concentrated [40].

2.2.1 Toxicity of Heavy Metals

There are many types for the toxicities of heavy metals. Some have cumulative toxicity, these are; lead, mercury, cadmium, and arsenic. These

four elements are very toxic, such that; they have extremely low threshold limit values. They are excreted from human body so slowly; thus even very low concentrations of these pollutants can accumulate in the body until they become harmful [41].

There are other types of toxicities in addition to the accumulative. Such as, synergistic toxicity; in which the total toxicity of two toxins is more than the sum of the independent toxicities of them. For example, zinc and cadmium show up five times toxicity more than the sum of their independent toxicities. While in the other type of toxicity, that is antagonistic toxicity, the total toxicity of two toxins is less than the sum of their independent toxicities. For example, copper and zinc [42].

In general, heavy metals toxicity depends on a number of factors. These are, the total dose absorbed, speciation, the route of exposure and the age of person. For example, young children are more susceptible to the effects of lead exposure because their organs absorb several times the percent ingested compared with adults [43].

Large amounts of any heavy metal may cause acute toxicity with a short time effect or chronic toxicity with a long time effect [44].

Some of the heavy metals may be harmless or even be necessary to life in trace quantities but toxic in larger amounts. This is true for copper and zinc as examples which are essential in trace concentrations for living organisms, but which in larger ones have toxic effects to the same

organism. The toxicity of a heavy metal is inversely proportional to its TLV, so that; metals with low threshold limit values will have more toxicity compared with that for a metal with larger ones [45, 46].

2.2.2 Cadmium

Cadmium is ductile and lustrous material with a silver-white color. It is soluble in acids but not in alkali medias. This element is very toxic. Such that, it has accumulative toxicity and very low TLV equals 0.003 ppm. There are several uses of cadmium compounds in life. For example, Ni-Cd batteries, pigments, coatings, plating and as stabilizers for plastics [47, 48].

2.2.2.1 Health Effects of Cadmium

Human uptake of cadmium takes place mainly through food. Such as; liver, mushrooms, shellfish, mussels and dried seaweed. These foods can greatly increase the amount of this metal in the body. Also, an exposure to a significantly high cadmium levels occurs through tobacco smoking that firstly transports cadmium into the lungs. Then, blood will transport this toxic material to the rest of human organs. In addition, another important source of cadmium exposure occurs with people who work in factories or hazardous waste sites that release this substance into the air or with people living near these sites [49]. High concentrations of cadmium in human body can cause many adversely health effects. For example; bone fracture, damage to the central nervous system, diarrhoea, Kidney damage,

psychological disorders, damage to the immune system and possibly DNA damage or cancer development [50].

2.2.2.2 Environmental Effects of Cadmium

When cadmium exists in soils, it can be very dangerous. Soils that are acidified enhance the cadmium uptake by plants. So that, this is a major hazard to the animals that are dependent upon plants for survival [51]. Earthworms and other essential soil organisms are extremely susceptive to cadmium poisoning. They can die at very low cadmium concentrations, and this has consequences for the soil structure. Such that, when there are high concentrations of cadmium in soils, this can influence soil processes of microorganisms, and hence threat the whole soil ecosystem [52].

In aquatic ecosystem. The susceptibility to cadmium can vary greatly between aquatic organisms. For example, freshwater organisms are usually less resistant to cadmium poisoning than salt-water organisms [53].

2.2.3 Lead

Lead is a soft and malleable metal. This accumulative toxic element has TLV of 0.01 mg/L. Releasing of lead into water and soil usually occurs in the form of lead oxides, hydroxides or lead metal oxyanion complexes. There are many sources of lead compounds. For example; flaking, chipping and improper renovation of buildings [54].

2.2.3.1 Health Effects of Lead

This toxic metal can enter the human body through uptake of water, air and food containing lead. For example, lead can enter drinking water through corrosion of pipes. This is more likely to be happened when water is slightly acidic. Lead can cause several adversely health effects like: disruption of nervous systems, declined fertility of men through sperm damage and kidney damage [55, 56].

2.2.3.2 Environmental Effects of Lead

The major sources of lead entering an ecosystem are atmospheric lead that results primarily from automobile emissions, lead-acid batteries, paint chips, fertilizers, pesticides and many other industrial products. It is known that lead accumulates in the soil especially that with a high organic content. Hence, displacing many other metals from the binding sites on the organic matter and hindering the chemical breakdown of inorganic soil fragments. As a result, lead in the soil may become more soluble, thus more readily to be taken up by plants [57].

2.2.4 Nickel

Nickel is silvery-white, hard and ductile metal. This substance is a good conductor of heat and electricity. Nickel is usually bivalent in its compounds, although it assumes other valences. Most nickel compounds are usually blue or green. This metal dissolves slowly in dilute acids but becomes passive when treated with nitric acid. Nickel is essential to life in

very small quantities, but if the uptake of this mineral is greater than its TLV (0.02 ppm). Then, it becomes toxic and hence affects negatively on health [58].

The main use of nickel is in the preparation of alloys that are characterized by ductility strength and resistance to corrosion and heat. Other examples of using nickel in society are rechargeable batteries, coinage, foundry products, plating, synthesis of catalysts and many other chemicals [59].

2.2.4.1 Health Effects of Nickel

Humans may be exposed to nickel by drinking water, eating food, breathing air or smoking cigarettes. Skin contact with nickel-contaminated water or soil may also result in nickel exposure. The uptake of too large amounts of nickel can result in the following adversely health effects: asthma and chronic bronchitis, respiratory failure, heart disorders, lung embolism and higher chances for the development of different types of cancers like; nose, larynx, or prostate cancer [60].

2.2.3.2 Environmental Effects of Nickel

Most of the nickel compounds that are released to the environment will adsorb to sediment or soil particles and hence become immobile. Although in acidic ground, nickel is bound to become more mobile and hence it will often rinse out to the groundwater [61].

2.3 Adsorption

2.3.1 Adsorption Definition, Features and Types

Adsorption is a surface phenomenon, which includes the adhesion of the adsorbate on the surface of the adsorbent. The atom, ion or molecule that adsorbs on the pores of the surface is called the adsorbate, while the substance on which adsorption occurs is called the adsorbent. Adsorbate may be gas, liquid, or dissolved solids. Whereas, adsorbent may be a liquid or a solid material [62].

Adsorption technique is an extremely important process of utilitarian significance. It has practical applications in biology, technology, industry and environmental protection. The efficiency of this treatment method depends on a number of factors. These are, the nature of adsorbate and adsorbent, the surface area of the adsorbent and its activation. Also, it depends on experimental conditions. Such as, temperature, pressure and pH value [63].

Adsorption is more useful, effective and suitable purification method for removing industrial effluents over other conventional treatment techniques, this is due to having many advantages. For example, simplicity, low cost, possibility of adsorbent recovery, high efficiency in minimization of many chemical and biological wastes and successful operation over a wide range of temperatures and pH values [64].

This purification method results in forming a new intermolecular attraction forces between the adsorbate and the adsorbent. Depending upon the type of these forces, adsorption can be classified into two types.

1. **Physical Adsorption (Physisorption)**

   There are many characteristics of this type of adsorption. These are; weak intermolecular forces of bonding usually as dipolar interaction. Also, physical adsorption has low heat of adsorption so it requires a little or no activation energy at all. Physisorption forms multi-molecular layers and it is not very specific. In addition, this adsorption type is reversible, as the adsorbate molecule does not remain fixed on a specific location on the adsorbent surface, so it will be free to move from one position to another, and hence making adsorbate recovery is possible [65].

   Physisorption usually takes place at low temperatures and can be easily reversed by heating or by decreasing the pressure [66].

2. **Chemical Adsorption (Chemisorption)**

   The properties of chemisorption include the following: forces of interaction are strong chemical bond forces, such as covalent and ionic bonds. Also, it has relatively high adsorption enthalpy, so that; this adsorption usually requires high activation energy to be happened. Additionally, chemisorption is irreversible, specific and taking place at high temperatures [67].

2.3.2 Equilibrium Isotherm Models

Adsorption process is usually studied through graph known as adsorption isotherm. That is the amount of the adsorbate on the adsorbent as a function of its pressure (if gas) or concentration (if liquid) at constant temperature.

Analysis of the isotherm data is important to develop an equation, which accurately represents the observed results. The most common isotherms that are applied in solid/liquid systems are the theoretical equilibrium isotherm models, which are Langmuir and Freundlich isotherms [68].

2.3.2.1 Langmuir Adsorption Isotherm

This isotherm is called the ideal localized monolayer model; it was developed to represent chemisorption. Langmuir isotherm is based on the following assumptions. These are, adsorption is limited to monolayer coverage, such that; the adsorbed molecule cannot migrate across the surface or interact with neighboring molecules. Also, the surface of the adsorbent is uniform. This means that all the adsorption sites are equivalent in energy [69].

The Langmuir equation relates the coverage of molecules on a solid surface to the concentration of a medium above the solid surface at a fixed temperature. This equation can be written as:

$$\frac{\boldsymbol{C_e}}{\boldsymbol{q_e}} = \frac{\mathbf{1}}{\boldsymbol{bQ_o}} + \frac{\mathbf{1}}{\boldsymbol{Q_o}}\boldsymbol{C_e}$$

Where;

C_e is the equilibrium concentration of the adsorbate (mg/L).

b is the Langmuir affinity constant (L/mg).

Q_o is the adsorption capacity at equilibrium (mg/g).

q_e is the amount of adsorbate per unit mass of adsorbent (mg/g), and it can be calculated using the following relation:

$$\mathbf{q_e = (C_o - C_e)\frac{V}{m}}$$

Where;

C_o is the initial concentration of the adsorbate (mg/L).

V is the volume of the solution (L).

m is the mass of the adsorbent (g).

($C_o - C_e$) represents the adsorbed amount (ppm).

A graph of (C_e/q_e) values versus C_e is used in order to find the Langmuir parameters. Which are, ($1/bQ_o$) as y-intercept and ($1/Q_o$) as slope [70].

2.3.2.2 Freundlich Adsorption Isotherm

This isotherm was interpreted as adsorption to surfaces supporting sites of varied affinities or to heterogeneous surfaces. Freundlich isotherm assumed that stronger binding sites are occupied first, such that; the binding strength decreases with increasing degree of site occupation.

According to this statement, the adsorbed mass per mass of adsorbent can be expressed by the following equation [71].

$$\boldsymbol{logq_e = logK_F + \frac{1}{n} logC_e}$$

Where;

K_F is the Freundlich constant related to adsorption capacity (mg/g).

n is the heterogeneity coefficient that gives an indication of how favorable the adsorption process (g/L).

A plot of $\log q_e$ values versus $\log C_e$ is used to find Freundlich parameters. Which are, $\log K_F$ as y-intercept and (1/n) as a slope.

2.3.3 Adsorption Kinetic Models

The kinetic of adsorption is defined as the process in which adsorbate molecules are transported from bulk solution to a boundary layer of the water surrounding the adsorbent particle by molecular diffusion through the stationary layer of water. Such that, the adsorbate particles are transported into an available site. Hence, an adsorption bond will be formed between the adsorbate and the adsorbent [72, 73].

Several adsorption kinetic models have been established in order to describe adsorption kinetics and rate-limiting step. These models give information about the adsorption system behavior and the rate at which specific constituent is removed using a certain adsorbent. In addition, they determine whether the adsorption process is a chemical or a physical one, and which specifically is the rate determining step. Examples of the adsorption kinetic models include, external mass transfer model, pseudo first-order and pseudo second-order rate models, Adam–Bohart–Thomas relation, Weber and Morris sorption kinetics, first-order reversible reaction

model, first-order equation of Bhattacharya and Venkobachar and Elovich's model [74, 75].

2.3.3.1 Pseudo First–Order Kinetics

This kinetic model is considered as the earliest model developed for describing adsorption kinetics.

The final integrated equation for this model can be written as:

$$\boldsymbol{log(q_e - q_t) = logq_e - \frac{K_1}{2.303}t}$$

Where;

q_e and q_t are the masses of adsorbate per unit mass of adsorbent at equilibrium, and at time t respectively (mg/g).

k_1 is the rate constant of pseudo first-order adsorption model ($mg.g^{-1}.min^{-1}$).

A plot of $log(q_e - q_t)$ versus t will give a straight line for the pseudo first-order adsorption with $logq_e$ as y-intercept and ($-k_1$ /2.303) as the slope of the graph [76].

2.3.3.2 Pseudo Second–Order Kinetics

This model of kinetics depends on the assumption that the rate-determining step may be chemical adsorption involving valence forces through sharing or exchange of electrons between the adsorbate and the adsorbent.

The rate equation for pseudo second-order kinetic model can be written as:

$$\frac{\mathbf{t}}{\mathbf{q_t}} = \frac{\mathbf{1}}{\mathbf{k_2 q_e^2}} + \frac{\mathbf{1}}{\mathbf{q_e}}\mathbf{t}$$

Where; k_2 is the equilibrium rate constant of pseudo second-order adsorption ($g.mg^{-1}.min^{-1}$).

The plot of t/q_t versus t should give a linear relationship that allows the computation of a second-order rate constants, k_2 and q_e [77].

2.3.3.3 Intra-Particle Diffusion Kinetic Model

This model is based on the theory proposed by Weber and Morris. The final equation of this adsorption kinetic model is:

$$\boldsymbol{q_t = K_p t^{0.5} + C}$$

Where;

K_p is the diffusion rate constant ($mg/g.min^{1/2}$).

C is a constant that gives an indication of the thickness of the boundary layer (mg/g) [78].

A plot of q_t versus $t^{0.5}$ should give a linear relationship for intra-particle diffusion kinetic model with constant C as a y-intercept and K_p as a slope.

2.3.4 Adsorption Thermodynamics

Thermodynamic considerations of an adsorption process are necessary to determine whether this process is favorable or not.

This adsorption behavior can be expressed using the thermodynamic parameters including the change in Gibbs free energy (ΔG), enthalpy change (ΔH) and the change in entropy (ΔS). Where; ΔG and ΔH are in (J) and the unit of ΔS is (J/K).

The following equation is the general equation that can be used to relate between the adsorption parameters [79].

$$\Delta G = \Delta H - T\Delta S$$

Where; T is the absolute temperature (K).

The change in Gibbs free energy can be also calculated by the following equation:

$$\Delta G = - RT \, In K_d$$

Where;

R is the universal gas constant that equals 8.314 $J.mol^{-1}.K^{-1}$.

K_d is the thermodynamic equilibrium constant that equals (q_e/C_e) with a unit of mol or (L/g).

The combination of the last two equations will result in the following equation:

$$\mathbf{ln K_d = \frac{\Delta S}{R} - \frac{\Delta H}{RT}}$$

The plot of InK_d versus (1/T) will give a straight line with (-ΔH/R) as slope and (ΔS/R) as y-intercept. The resulting graph is known as Van't Hoff plot.

2.4 Polysiloxanes

Polysiloxanes are one of the most important organosilicon polymers that are used in polymer chemistry. The silanol $SiO(CH_3)_2$ is the key functional group for the synthesis of these polymers. Silicon (Si) is a semi-metallic element. It makes up 27% of the earth's crust by mass, and it is the second in abundance in the world (after oxygen). Silicon plays an important role in industry. Such as; solar energy and computers.

It is very rare to find silicon by itself in nature; it is usually bound to oxygen to form silicon dioxide that has many different forms. Chains are more readily made from silicon oxide; called siloxanes that can be made by step-growth polymerization or ring-opening copolymerization [80].

There are many useful properties of polysiloxanes. Such as, low glass transition temperature, permeability to gases, low surface energy and flexibility.

The high flexibility of polysiloxanes is due to the ability of the atoms to rotate around a chemical bond. Such that, it considers that the bond length and angles remain unchanged throughout the process, this is called torsion flexibility. Also, flexibility can occur when there is a large hindrance between the non-bonded atoms where there are unfavorable torsion angles, called bending flexibility [81, 82].

2.4.1 Functionalized Polysiloxane Surfaces

There are two common methods used to prepare functionalized polysiloxane ligand systems. The first method called the sol-gel process which involves hydrolysis and condensation of $Si(Oet)_4$ with the appropriate silane coupling agent $(RO)_3SiX$, where; X represents an organofunctionalized ligand. The second method is the chemical modification of the pre-prepared functionalized polysiloxane. This method is used mainly for substitution of organofunctionalized groups especially when the appropriate chelating silane agents are difficult to prepare. The most commonly attached chelate ability for this purpose is devoted for donor atoms which have a large capability in forming complexes with a series of heavy metal ions, and in some cases forcing a distinguishable selective extraction property [83-85].

There are many advantages for using functionalized inorganic supports. For example; lack of swelling in solvents, high hydrolytic, thermal and mechanical stability [86].

Many of the functionalized systems have been used in many useful applications. Such as; separation of metal cations from organic solvents and aqueous solutions, chemisorption and recovery. Also, they are widely used as heterogeneous catalysts and as stationary phases in chromatography [87-90].

2.4.2 Polysiloxane Surfaces Modified with Functional ortho-, meta-, or para-Nitrophenyl Moieties

These days, the preparation of porous materials as adsorbents has generated considerable interest, because of their regular pore structure, unique large specific surface area and well-modified surface properties. In addition, these substances can be regenerated for many times after adsorption saturation [91].

This research involves the modification of porous SiO_2 with functional *ortho*-, *meta*-, or *para*-nitrophenyl receptors using heterogeneous route that involves reaction of carbaldehyde derivatives with 3-aminopropyl trimethoxysilane prior to immobilization on the support [92].

In general, porous silicas are usually modified by post-synthesis or one-pot synthesis. In both methods, the organic functional groups are used. The aptitude of the resulting attached chelate is mainly owed to the presence of sulfur, oxygen or nitrogen donor atoms [93-95].

Chapter Three

Experimental Part

3.1 Chemical Materials

All of the chemical substances that are employed in this work were of analytical grade and are used without any further purification. The required chemicals involve: silica gel (E. Merck) with particle size in the range of (70–230) mesh, and a median pore diameter of 60 Å, was activated for 24 hours before use by heating it at 150˚C, 3-aminopropyltrimethoxysilane that is purchased from Janssen Chimica, ethanol, toluene, $SnCl_2$, dichloromethane, acetonitrile, dry diethyl ether, HCl solution, NaOH solution, $Cd(NO_3)_2.4H_2O$, $Pb(NO_3)_2$ and $NiCl_2.6H_2O$.

3.2 Instrumentations

The required instrumentations for this research include the following: shaking water bath (Daihan Labtech, 20 to 250 rpm Digital Speed Control), pH meter (model: 3510, JENWAY), glassware, thermometer, AAS instrument (model ZicE-3000 SERIES Serial number c113500021 designed in UK AA Spectrometer), UV spectrometry (model: UV-1601, SHIMADZU), IR Spectrometer (Nicolet iS5, iD3 ATR, Thermo Scientific), TGA (Q50 V20.10 Build 36 instrument at a heating rate of $10^{\circ}C.min^{-1}$ and in N_2 gaseous atmosphere).

3.3 Preparation of Silica-Immobilized Propylamine (SiNH2)

The first step in the preparation of ($SiNH_2$) was the reaction between the silylating agent (3-aminopropyltrimethoxysilane) and the silanol groups on the silica surface. Such that, 25 g of activated silica gel (SiG) suspended in

150 mL of toluene was refluxed and mechanically stirred under nitrogen atmosphere for 3 hours. Then, 10 mL of aminopropyltrimethoxysilane was added dropwise. After that, 1 g of $SnCl_2$ was used as catalyst and the mixture was kept under reflux for 48 hours.

The resulting solid matrix was filtered, washed with toluene and ethanol. Then, it was soxhlet extracted with a (1:1) mixture of ethanol and dichloromethane for 24 hours in order to remove the silylating reagent residue. The obtained immobilized silica gel was dried in vacuum at 20°C.

3.4 Synthesis of Nitrophenyl-Substituted Silicas (Si-o-NO2), (Si-m-NO2) and (Si-p-NO2)

A mixture of 10 g of 3-aminopropylsilica ($SiNH_2$) with 3 g of each of *ortho*-nitroacetophenone, meta-nitroacetophenone or para-nitroacetophenone respectively in 100 mL of dry diethyl ether was stirred at room temperature for 24 hours. This process results in the formation of the three required adsorbents including (Si-o-NO_2), (Si-m-NO_2) and (Si-p-NO_2) respectively. After being filtered, the solid products were soxhlet extracted with acetonitrile, methanol and dichloromethane for 15 hours. Then, these products were dried under vacuum at 70˚C over 40 hours.

3.5 Preparation of Standard Solutions

Cadmium nitrate tetrahydrate $Cd(NO_3)_2.4H_2O$ with molar mass equals 318.48192 $g.mol^{-1}$, was used to prepare several standard solutions of Cd(II) at different initial concentrations depending on dilution calculations ($M_1*V_1 = M_2*V_2$).

Also, the same method of calculation was used for lead nitrate $Pb(NO_3)_2$ (331.2098 g/mol) and nickel chloride hexahydrate $NiCl_2.6H_2O$ (237.69108 g/mol) in order to prepare several standard solutions of Pb(II) and Ni(II) respectively. Such that, the used solvent for all of these salts was groundwater from Burqin village in Palestine.

The prepared initial concentrations of cadmium, nickel and lead ions are: 5, 10, 15, 20, 25, 30, 35, 40, 45 and 50 ppm. These standard solutions of calibration are used in batch experiments in order to study the effect of different factors such as; time, pH and temperature on each adsorption process. And hence to know what are the optimum conditions for having effectient adsorption of Cd(II), Pb(II) or Ni(II) on ortho-, meta-, or para-nitrophenyl silicas.

By using AAS measurements and depending upon the resulting calibration curves, the concentrations of cadmium, lead and nickel ions in the used groundwater (without any treatment) equal zero.

3.6 Calibration Curves

Atomic Absorption Spectrophotometer was used to construct the calibration curves of Cd(II), Pb(II) and Ni(II) through measuring the absorbance and the concentration for each prepared calibration standard. According to Beer-Lambert law, solution with high concentration absorbs more light than solution of lower concentration. Since concentration and absorbance are directly proportional. This law can be used to determine an unknown concentration depending on using the calibration curve of standard solutions of the same material.

3.6.1 Calibration Curve of Cadmium

To prepare Cd(II) solution with 1000 ppm concentration, 2.7442 g of $Cd(NO_3)_2.4H_2O$ was dissolved in about 100 mL water in a small beaker, then transferred into 1 L volumetric flask. The volume was completed to the mark with water. The flask was shaken several times. Then dilution calculations are used to prepare several solutions with different initial concentrations (5, 10, 15, 20, 25, 30, 35, 40, 45 and 50 ppm).

After that, atomic absorption measurements of these standard solutions were investigated in order to have a calibration curve of cadmium as shown in (Figure 3.1).

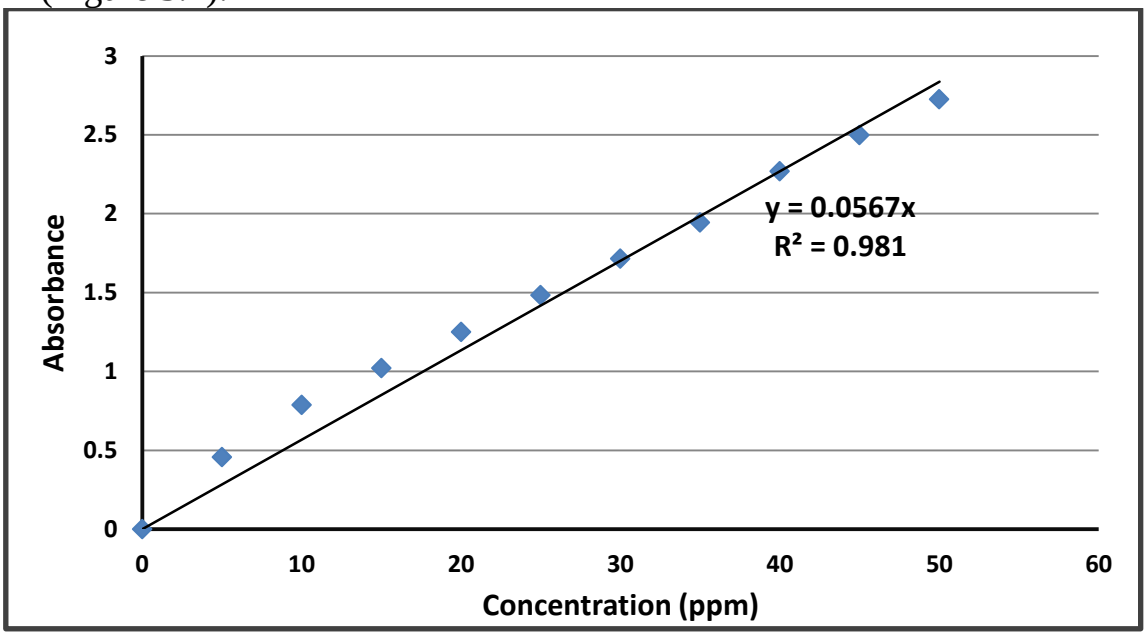

Figure 3.1: Calibration curve of Cd(II).

3.6.2 Calibration Curve of Lead

In order to prepare Pb(II) solution with 1000 ppm initial concentration, 1.5985 g of $Pb(NO_3)_2$ dissolved in about 100 mL water in a small beaker, then transferred into 1 L volumetric flask. The volume was completed to

the mark with water. The flask was shaken several times. Then dilution calculations are used to prepare several standards with different initial concentrations.

The calibration curve of lead was obtained by using AAS measurements of the prepared lead standard solutions as shown in (Figure 3.2).

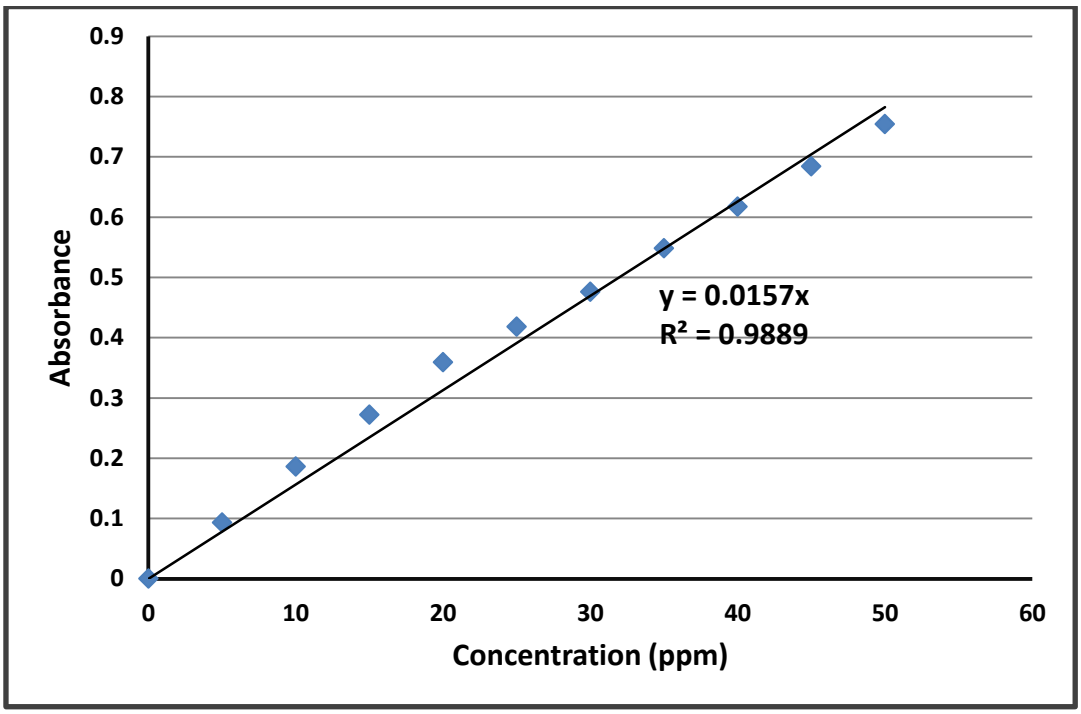

Figure 3.2: Calibration curve of Pb(II).

3.6.3 Calibration Curve of Nickel

To prepare Ni(II) solution with a concentration of 1000 ppm, 4.0497 g of $NiCl_2.6H_2O$ was dissolved in about 100 mL water in a small beaker, then transferred into 1 L volumetric flask. The volume was completed to the mark with water. The flask was shaken several times. Then dilution calculations are used to prepare several solutions with different initial nickel concentrations.

After that, atomic absorption measurements of the prepared standard solutions were investigated and hence the calibration curve of nickel is obtained as shown in (Figure 3.3).

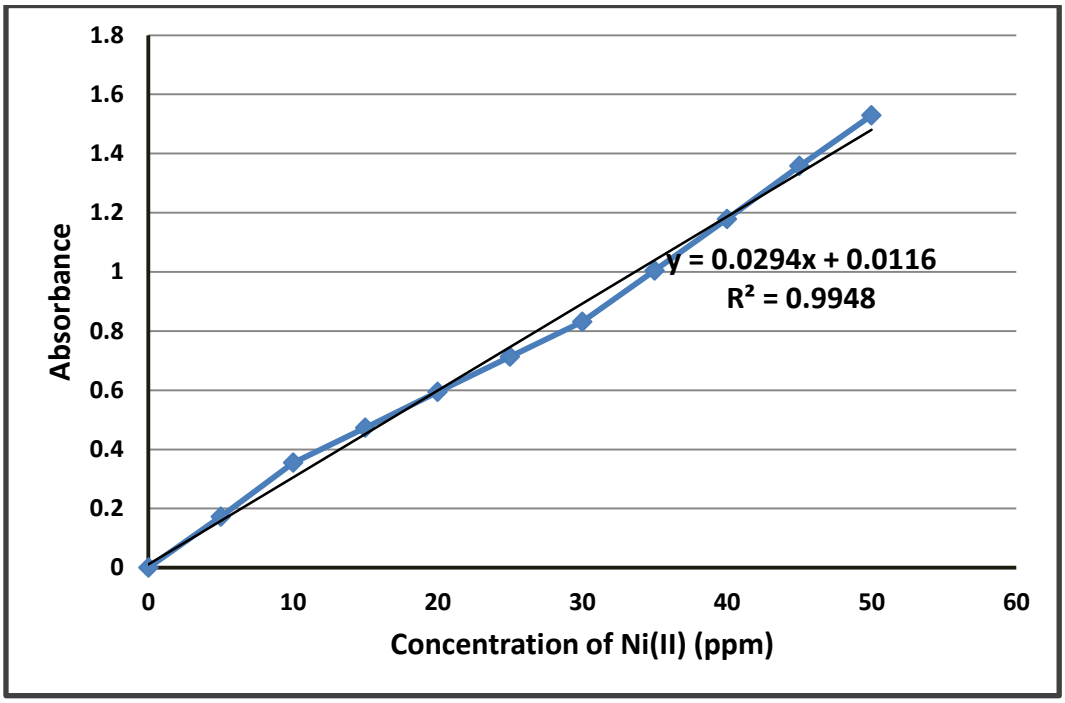

Figure 3.3: Calibration curve of Ni(II).

3.7 Batch Experiments

A mixture of 1 mg sample of (Si-o-NO_2), (Si-m-NO_2) or (Si-p-NO_2) adsorbent with 7 mL of groundwater containing known concentration of Cd(II), Ni(II) or Pb(II) toxic metal was shaken.

The effect of solution conditions including; contact time, temperature, pH value, the amount of modified polymer and the concentration of toxic metal ion was discussed.

Atomic absorption measurements were used for the filtrate mixture of each sample in order to determine the remained amount of the toxic metal ion and hence investigating the extent of the adsorption efficiency.

3.7.1 Effect of Contact Time

The adsorption of toxic heavy metals on each adsorbent was studied as a function of shaking time at 20 ^{o}C. A sample of 10 ppm of standard solutions at pH value equals 6 was taken in a volumetric flask and shaken with 1 mg of an adsorbent. At the end of time intervals (1 minute to 30 hours), each sample was filtered off and the amount of each adsorbate is determined using AAS apparatus.

3.7.2 Effect of pH

The effect of pH value on the adsorption behavior was investigated using different pH values ranging from 2 to 12. The pH value was adjusted using roughly concentrations of 0.1 M HCl and 0.1 M NaOH solutions.

A 1 mg of an adsorbent sample was added to 7 mL of the prepared standard solution with a concentration of 10 ppm. The prepared mixtures were placed in shaking water bath at constant temperature (20°C), with considering into account the resulting optimum time for each previous adsorption process.

3.7.3 Effect of Temperature

To study the effect of temperature on each adsorption process. 1 mg of the adsorbent was added to 7 mL of the standard solution of Cd(II), Ni(II) or Pb(II) with a concentration of 10 ppm at the optimum value of pH.

Each mixture was placed in shaking water bath at desired temperature (the range was 5 to 80°C) for optimum contact time. At the end of time

intervals, each sample is filtered off and the amount of each adsorbate is determined using AAS instrument.

3.7.4 Effect of Adsorbent Dose

In order to find out the optimum amount of adsorbent that is required for the adsorption of Ni(II), Cd(II) and Pb(II) on modified silicas, (1, 2, 3, 4 or 5 mg) of the modified silica was added to five vials containing 7 mL of 10 ppm of toxic metal standard solution. The mixtures were placed in shaking water bath at the optimum temperature, pH and time.

Then, the concentration of the ions in the filtrate is measured using AAS instrument.

3.7.5 Effect of Adsorbate Concentration

To find the optimum concentration of cadmium, nickel and lead metal ions. The resulting optimum mass of each adsorbent was added to a number of vials, each contains 7 mL of different standard concentrations of Cd(II), Pb(II) and Ni(II). Such that, all optimum condition of pH, contact time, temperature and the amount of adsorbent must be taken in consideration. After that, the concentration of the ions in each filtrate is measured using AAS.

3.8 Adsorbent Regeneration

A mixture of 20 mg sample of (Si-o-NO_2), (Si-m-NO_2) or (Si-p-NO_2) adsorbent with 20 mL of groundwater containing 10 ppm concentration of Cd(II), Ni(II) or Pb(II) metals was shaken for 5 minutes at 20 °C and pH value of 6.

Then, AAS measurements for the filtrate were determined, and the adsorbent after each adsorption process is washed with 0.1M HCl solution then with distilled water. After that, each regenerated polymer left to dry for 24 hours before second using. The same technique of recovery is then used for each regenerated adsorbent in order to prove that the three modified silicas can be used for several times with approximately no effect on the percentage removal of heavy metal ions in groundwater.

Chapter Four

Results and Discussion

4.1 Materials Characterization

4.1.1 Elemental Analysis

In order to characterize the modification on the surface of the synthesized silica gel, microanalysis of nitrogen and carbon (are not present in the initial activated silica gel SiG) of aminopropyl silica ($SiNH_2$) was investigated, as shown in (Table 4.1).

Table 4.1: Texture and adsorption parameters of the starting (SiG) and of the modified samples ($SiNH_2$), (Si-o-NO_2), (Si-m-NO_2) and (Si-p-NO_2).

Parameters	SiG	$SiNH_2$	Si-o-NO_2	Si-m-NO_2	Si-p-NO_2
S_{BET} (m^2/g)	305	241	240	223	232
Pore volume (cm^3/g)	0.77	0.67	0.65	0.54	0.63
Nitrogen content (w%)	-	1.60	1.76	1.72	1.64
Carbon content (w%)	-	4.12	4.92	5.70	5.75

The results showed that the two methoxy groups were substituted by silanol and the (-NH_2) group content of $SiNH_2$ was 1.14 $mmol.g^{-1}$. The new synthesized chelating adsorbents (Si-o-NO_2), (Si-m-NO_2) and (Si-p-NO_2) are also indicated an increase in the percentages of nitrogen and carbon that are attributed to the nitrophenyl fraction immobilized on silica gel surface support.

4.1.2 SEM Characterization

Scanning Electron Micrographs of the original silica gel (SiG) and of the new modified materials ($SiNH_2$), (Si-o-NO_2), (Si-m-NO_2) and (Si-p-NO_2) showed that nitrophenyl-substituted silicas can be strongly employed as perfect adsorbents for removing toxic heavy metal ions. Such that, these chelating polymers display an increased porous and rough nature, as shown in the following Figures (4.1-4.5).

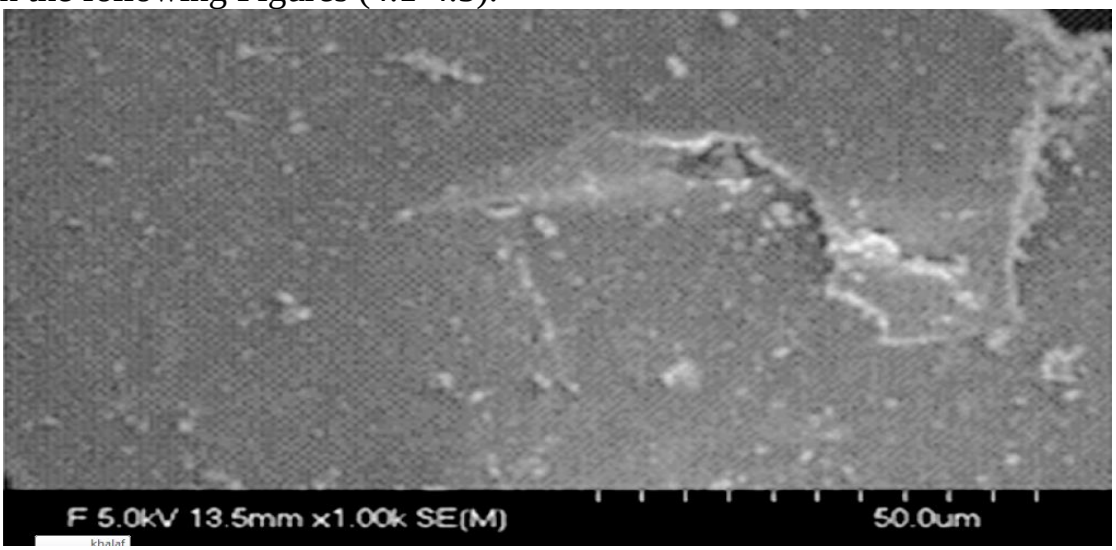

Figure 4.1: SEM photograph of silica gel (SiG).

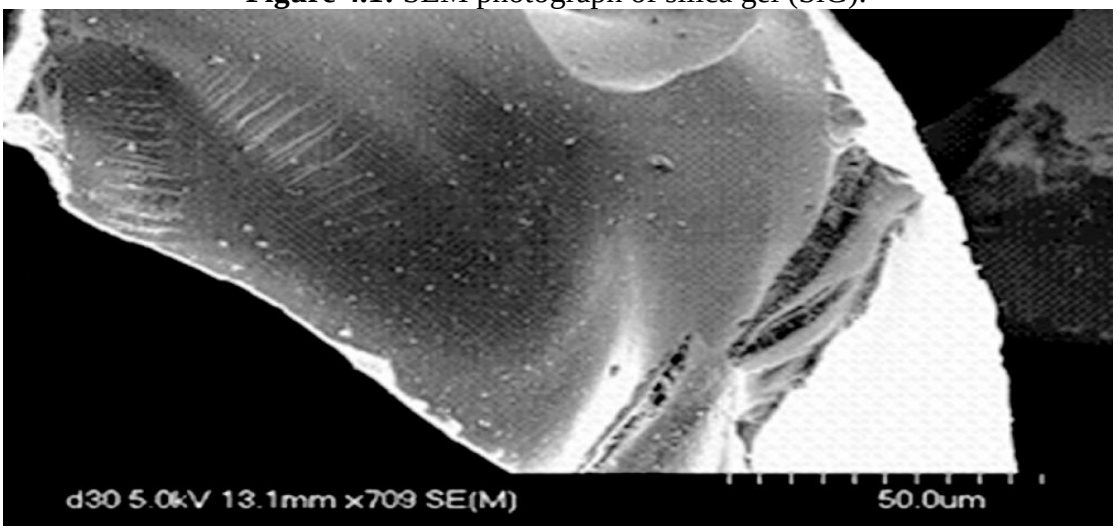

Figure 4.2: SEM photograph of ($SiNH_2$).

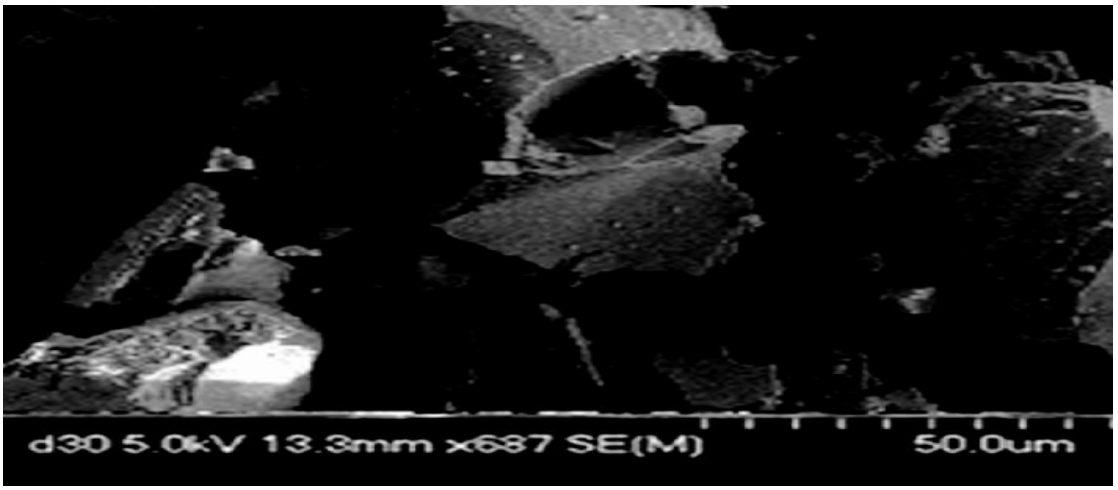

Figure 4.3: SEM photograph of (Si-o-NO_2).

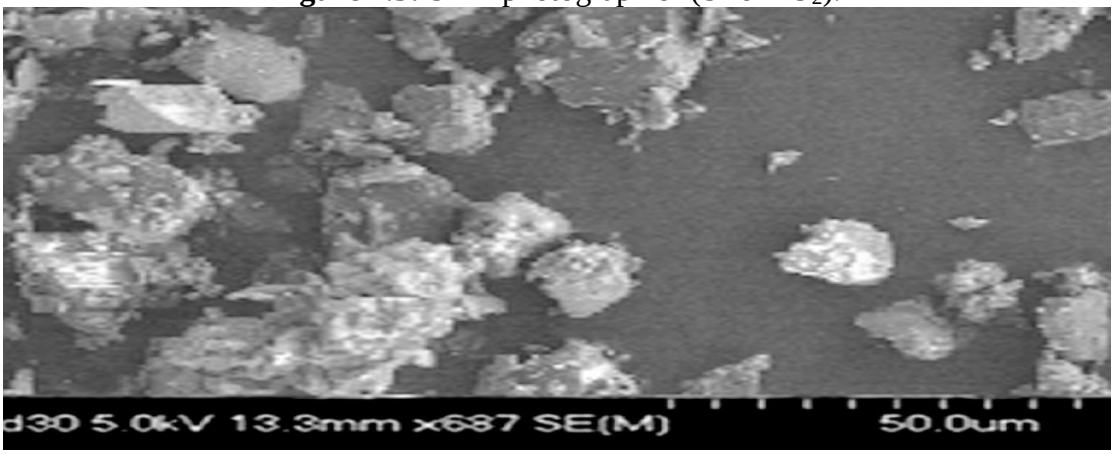

Figure 4.4: SEM photograph of (Si-m-NO_2).

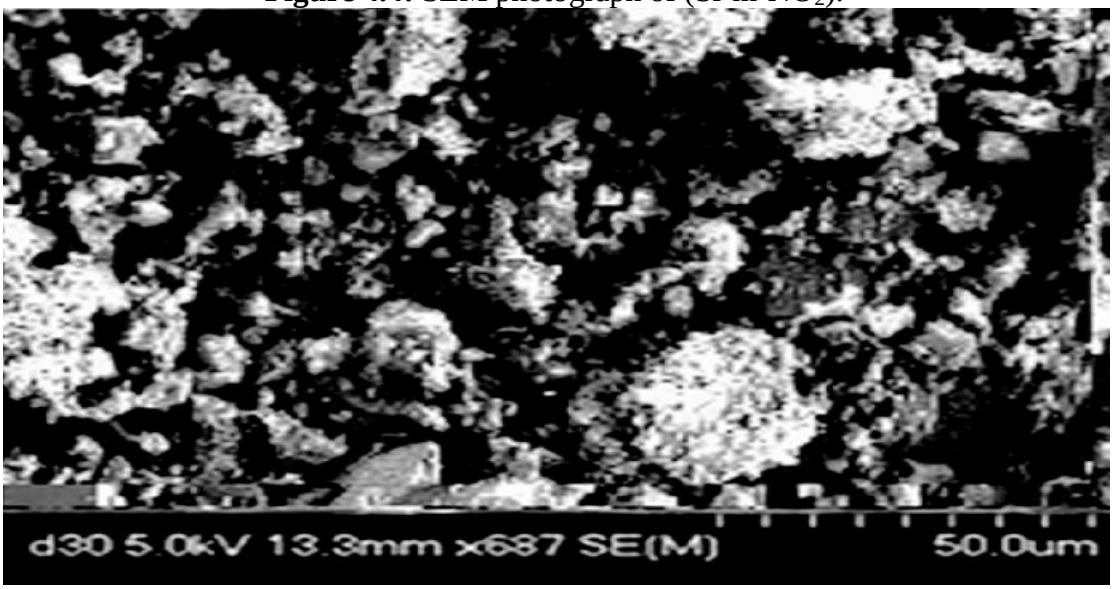

Figure 4.5: SEM photograph of (Si-p-NO_2).

4.1.3 IR Characterization

As shown in (Figure 4.6), the most important characteristic feature when comparing 3-aminopropyl silica ($SiNH_2$) with the native silica (SiG) was the appearance of a ν(C-H) weak bands at 2700 cm^{-1} and a ν(NH_2) around 1580 cm^{-1}, corresponding to the carbon chain of the pendant group attached to the inorganic matrix of silica.

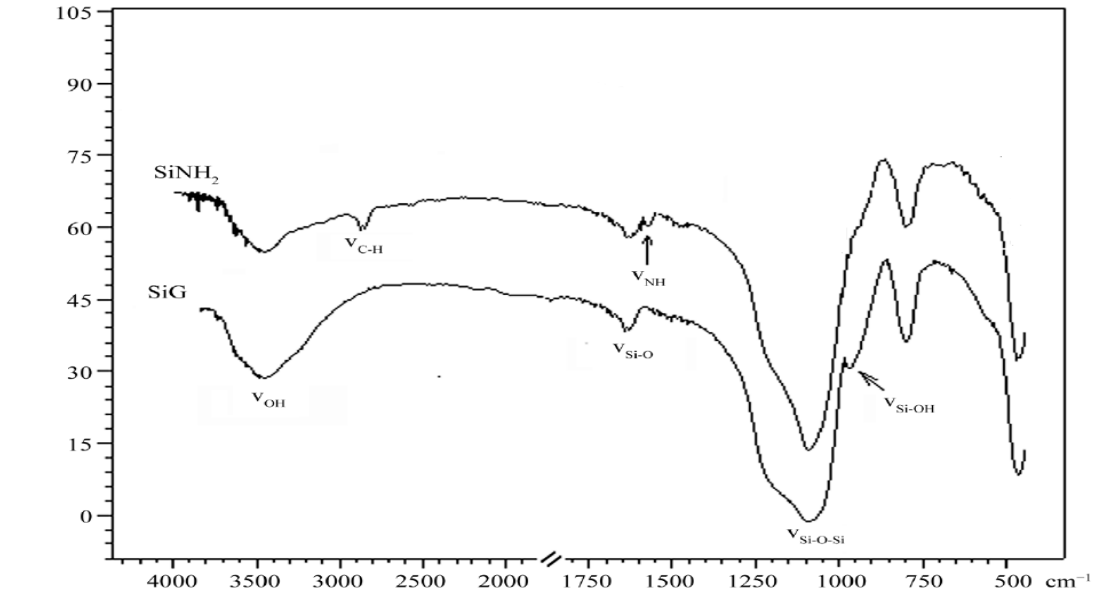

Figure 4.6: IR spectra of silica gel (SiG) and of the modified sample ($SiNH_2$).

For each of the final synthesized chelating materials, there is appearance of new characteristic band, due to the presence of (N-O) groups. For example, the main feature for (Si-m-NO_2) spectra is the disappearance of the absorption band at 1580 cm^{-1}, which testifies the reactivity of the primary amine group (-NH_2). Also, we note the appearance of the new characteristic band around 1520 cm^{-1} as a result of (C=N) vibrations, as shown in (Figure 4.7).

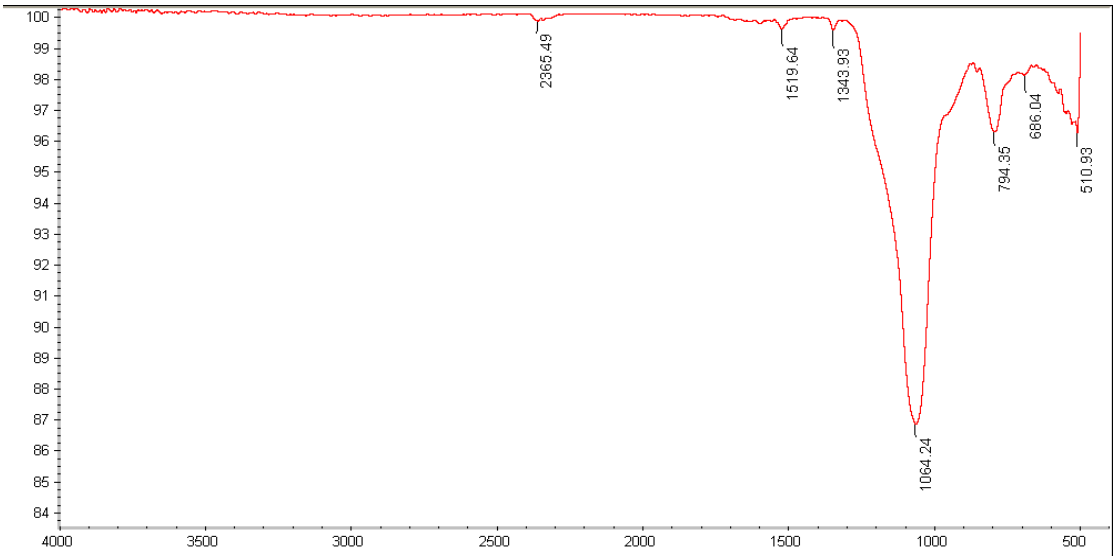

Figure 4.7: IR spectrum of (Si-m-NO_2).

The other modified adsorbents (Si-o-NO_2) and (Si-p-NO_2) are also revealed the appearance of new characteristic bands. These spectra showed that nitrophenyl-substituted units had been grafted onto the surface of inorganic silica gel after modification process as shown in (Figure 4.8 and 4.9).

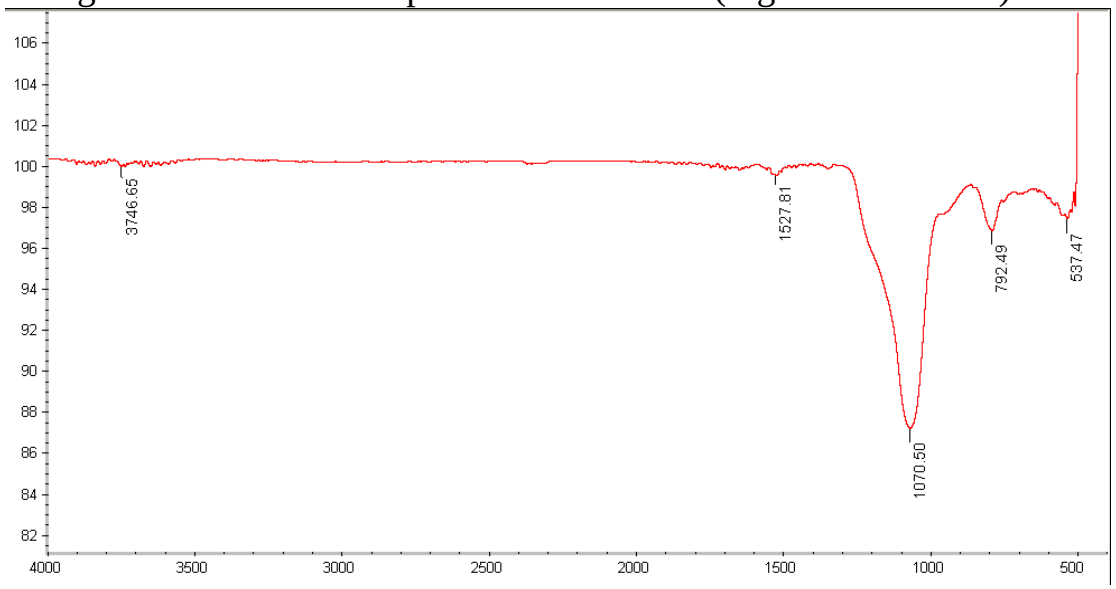

Figure 4.8: IR spectrum of (Si-o-NO_2).

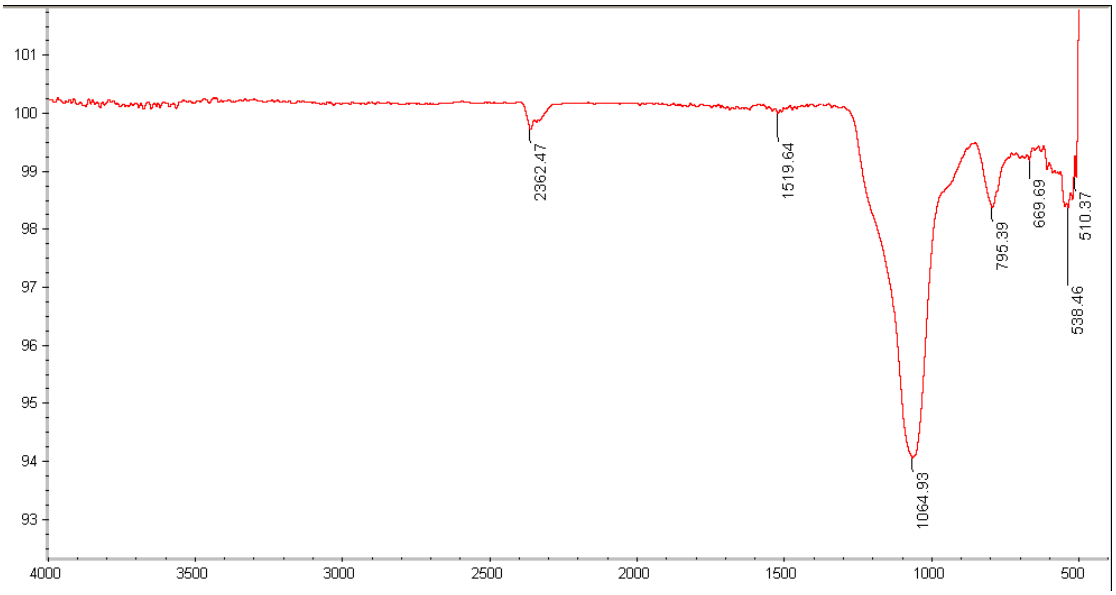

Figure 4.9: IR spectrum of (Si-p-NO_2).

4.1.4 UV Characterization

Each of the three synthesized silicas was dissolved in ethanol in order to characterize its Ultra-Violet spectrum. The lowest solubility was for para-nitrophenyl silica, and this is probably due to having very strong surface properties.

At wavelengths lower than 300 nm. The highest absorbance was for ortho-nitrophenyl silica compared with (Si-m-NO_2) and (Si-p-NO_2) that showed very low light absorbance. While for wavelengths higher than 500 nm, all of the prepared polymers showed approximately a straight line relationship between absorbance and wavelengths, as shown in (Figure 4.10).

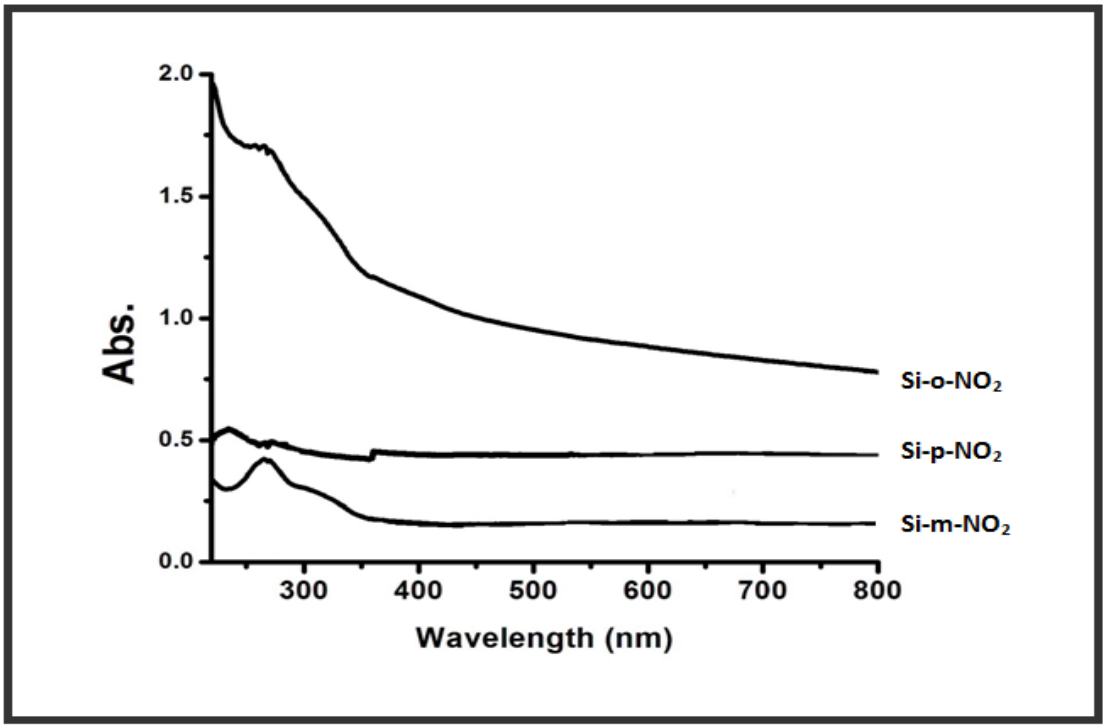

Figure 4.10: UV-Visible Spectra of (Si-o-NO_2), (Si-m-NO_2) and (Si-p-NO_2).

4.1.5 ^{13}C NMR Characterization

This technique of characterization was used to show the presence of the organic spacer arm on the inorganic polysiloxane. As shown in (Figure 4.11), the ^{13}C solid state NMR spectra of $SiNH_2$ modified sample indicated the presence of three well-formed peaks, at 9.4, 25.0 and 42.6 ppm. These peaks were attributed to the propyl carbon, (Si-CH_2), (-CH_2-) and (N-CH_2) respectively. While, the signal at 53.1 ppm was assigned to show unsubstituted methoxy group (-OCH_3) as confirmed by microanalysis.

For the (Si-o-NO_2), (Si-m-NO_2) and (Si-p-NO_2) polymers, the spectra reveal other signals ranging from 100 ppm to 160 ppm corresponding to specific carbons of nitrophenyl-substituted units.

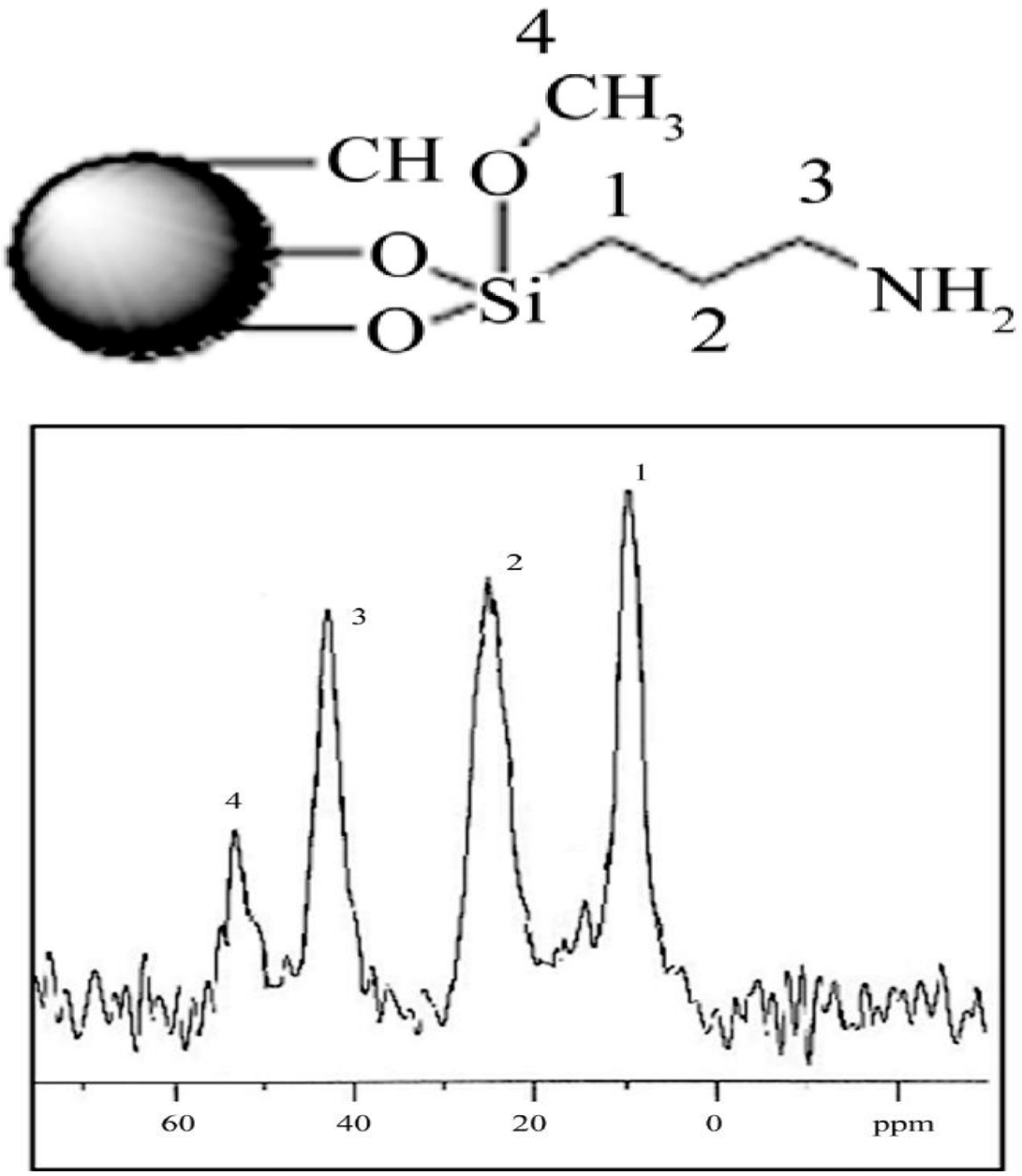

Figure 4.11: ^{13}C solid state NMR spectra of the modified sample ($SiNH_2$).

4.1.6 TGA Analysis and Thermal Stability

The resulting thermogravimetric curves reflect the thermal stability of these new adsorbents. As shown in (Figure 4.12), the quantity decomposed in each stage confirms the amount of the compounds grafted. Silica gel (SiG) indicates two losses attributed to physisorbed water molecules released and to the condensation of silanol groups bonded to the surface. While, the 3-

aminopropyl-silica ($SiNH_2$) presents an additional weight loss compared with native silica gel after the drainage of physically adsorbed water, mainly attributed to the organic spacer arm.

The final materials (Si-o-NO_2), (Si-m-NO_2) and (Si-p-NO_2) are also showed an increase of mass loss allotted to the decomposition of the nitrophenyl-substituted fraction that is immobilized on the surface of silica gel, together with condensation of the remaining silanol groups. This increase in mass loss reflects the higher amount of the anchored organic groups with an order of *ortho*<*meta*<*para* due to steric effects.

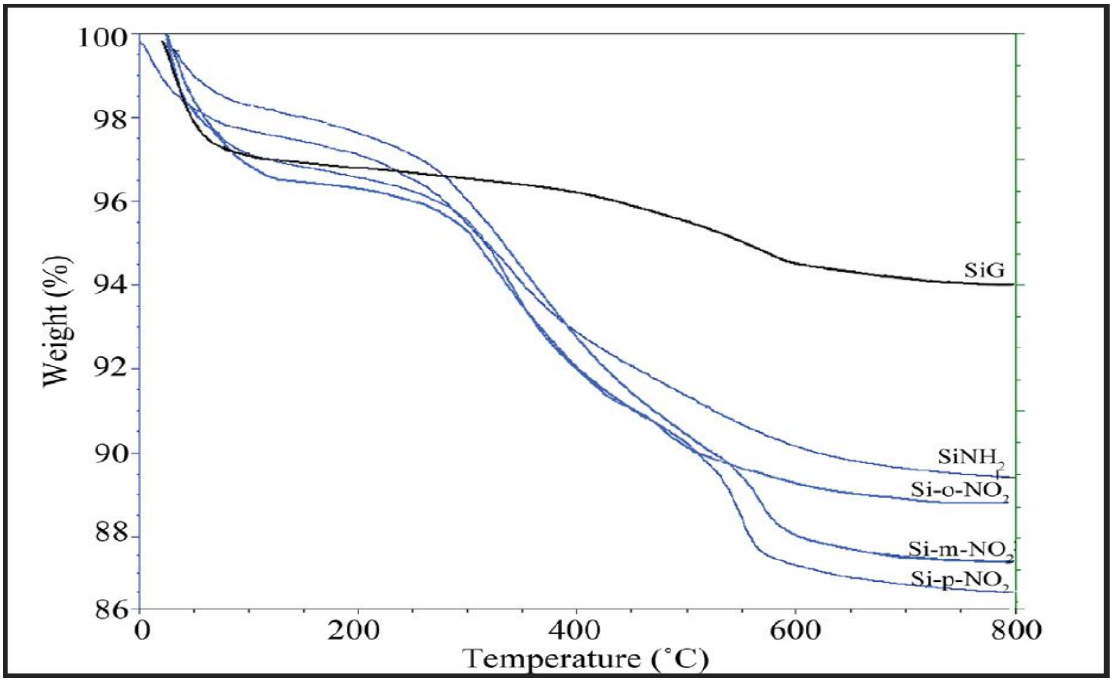

Figure 4.12: TGA curves of native silica gel (SiG) and of the modified samples ($SiNH_2$), (Si-o-NO_2), (Si-m-NO_2) and (Si-p-NO_2).

4.1.7 Chemical Stability

The chemical stability of the new synthesized chelating polymers was examined in various buffer and acidic solutions with pH value ranging

between 1 and 7. The prepared materials were mixed with different concentrations and stirred at 20 °C for 24 hours. The observed result showed no changing in the adsorbent structure.

The observed high stability that is exhibited by the attached organofunctional group is due to the length of the pendant group, which binds the nitrophenyl groups to the silica supported surface.

It is observed that when the length of the hydrocarbon bridge was more than two methylene groups, the rupture of (Si-C) bond did not occur in a mineral acidic medium due to the length of the chain. Such that; longer chains can no longer have a functional handle that can undergo beta-elimination of the Si cation.

4.1.8 Surface Properties

Barrett-Joyner-Halenda (BJH) pore sizes and nitrogen adsorption-desorption isotherms (BET) are used to study the porosity changes of the new modified polysiloxane surfaces induced by the introduction of nitrophenyl-substituted groups. Such that, the surface area and pore volumes of modified silicas ($SiNH_2$), (Si-o-NO_2), (Si-m-NO_2) and (Si-p-NO_2) were measured. BET surface area of the porous polysiloxane (SiG) equals 305 $m^2.g^{-1}$, and the pore volume of it equals 0.77 $cm^3.g^{-1}$. While, the observed result of 3-aminopropyl silica ($SiNH_2$) showed a decrease in BET surface area as immobilization of additional groups takes place to give 241 $m^2.g^{-1}$ and a pore volume of 0.67 $cm^3.g^{-1}$, (Figure 4.13).

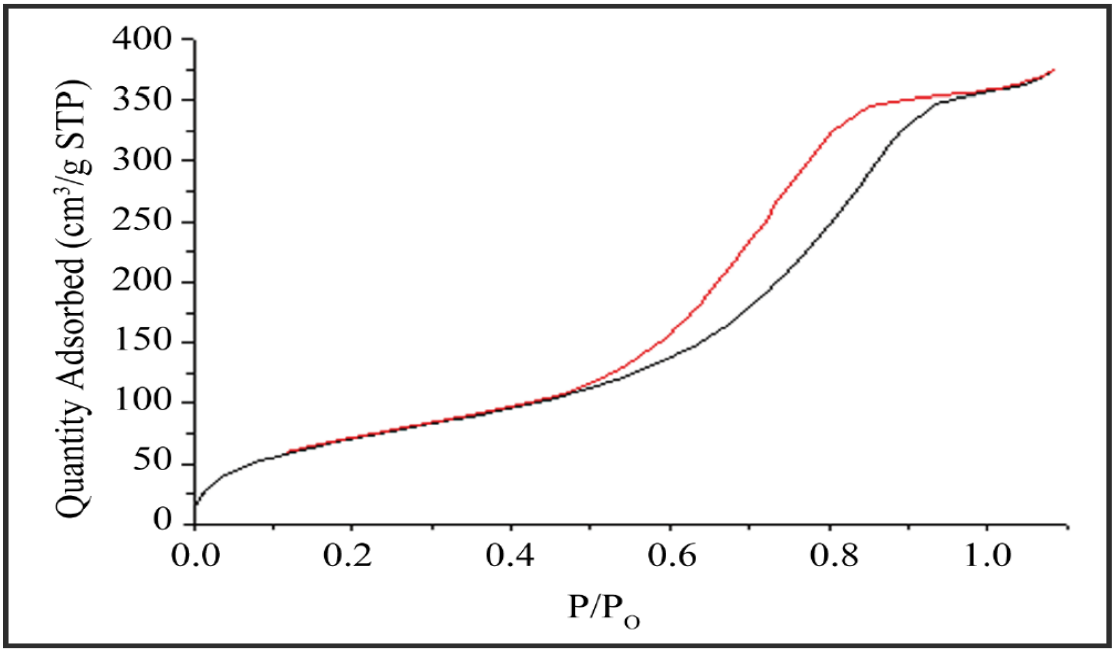

Figure 4.13: BET plot of (Si-NH_2).

In addition, all of the nitrophenyl-substituted silicas (Si-o-NO_2), (Si-m-NO_2) and (Si-p-NO_2) showed a decrease surface area and BJH pore diameters as shown in the following Figures (4.14-4.16).

The pronounced decreased parameters are attributable to the grafted nitrophenyl-substituted units on the porous chelating polysiloxane, as shown in (Table 1). Moreover, the nitrogen adsorption-desorption isotherm for silica derivatives are of type IV according to the IUPAC classification and display a pronounced hysteresis for partial pressures ($0.4 < (P/P_0) < 1.0$) which is the direct evidence of the presence of mesopores. Also, the hysteresis loops of Type H2 indicate the presence of a uniform pore diameter distribution.

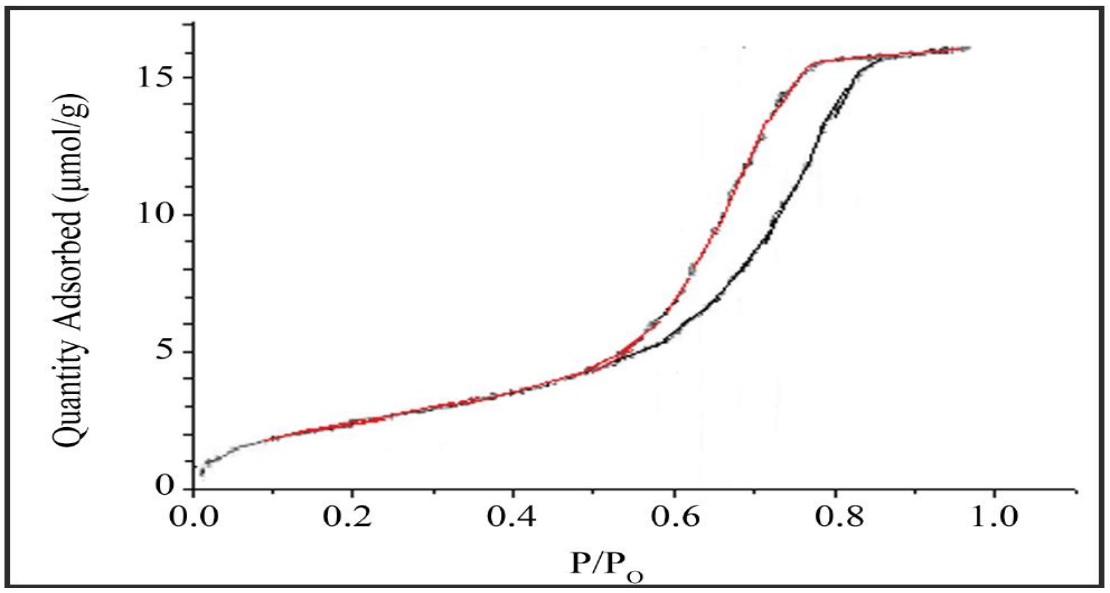

Figure 4.14: BET plot of (Si-o-NO_2).

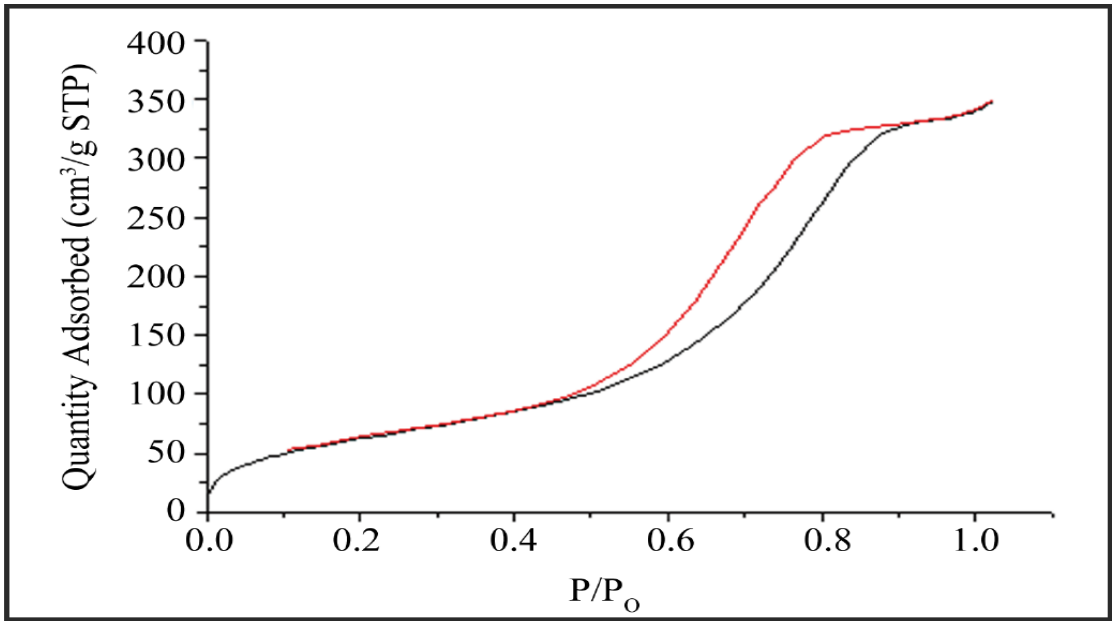

Figure 4.15: BET plot of (Si-m-NO_2).

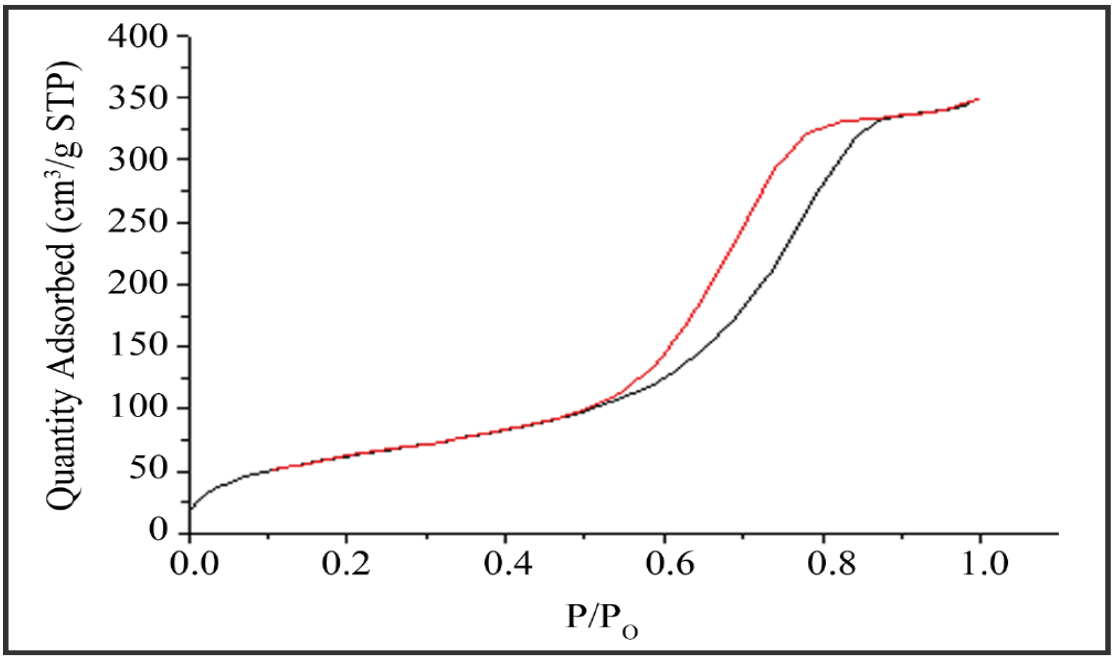

Figure 4.16: BET plot of (Si-p-NO_2).

4.2 Adsorption Results

This research aimed to use the synthesized modified silicas for removing heavy metal ions from groundwater, and hence to compare the adsorption efficiency of these polymers. This process was done by studying the adsorption capacities for nitrophenyl substituted silicas towards cadmium, lead and nickel adsorbates. The extracted concentrations of heavy metal ions were determined using atomic absorption measurements.

After finding the remaining concentrations, the percentage removal for each adsorption process must be determined. This value is defined as the ratio of difference in the adsorbate concentration before and after adsorption ($C_I - C_F$), to the initial concentration of the metal ion in the aqueous solution (C_I), as shown in the following equation:

$$\%\ of\ Removal = \frac{C_I - C_F}{C_I} * 100\%$$

Where;

C_I and C_F are the initial and finial concentrations of heavy metal ion in groundwater, respectively (ppm).

The adsorption processes are compared according to using the same adsorbent with cadmium, lead or nickel ions or using the same heavy metal with different adsorbents including (Si-o-NO_2), (Si-m-NO_2) or (Si-p-NO_2).

4.2.1 Using the Same Adsorbate with Different Adsorbents

4.2.1.1 Adsorption of Cadmium

The effect of solution conditions for the adsorption of cadmium on (Si-o-NO_2), (Si-m-NO_2) or (Si-p-NO_2) adsorbents is determined. As the adsorbent changed, the adsorption dependence on the polymer nature is investigated.

4.2.1.1.1 Effect of Contact Time

In order to establish an appropriate contact time between cadmium ions and each of the adsorbents, adsorption capacities of Cd(II) were measured as a function of time as shown in (Figure 4.17).

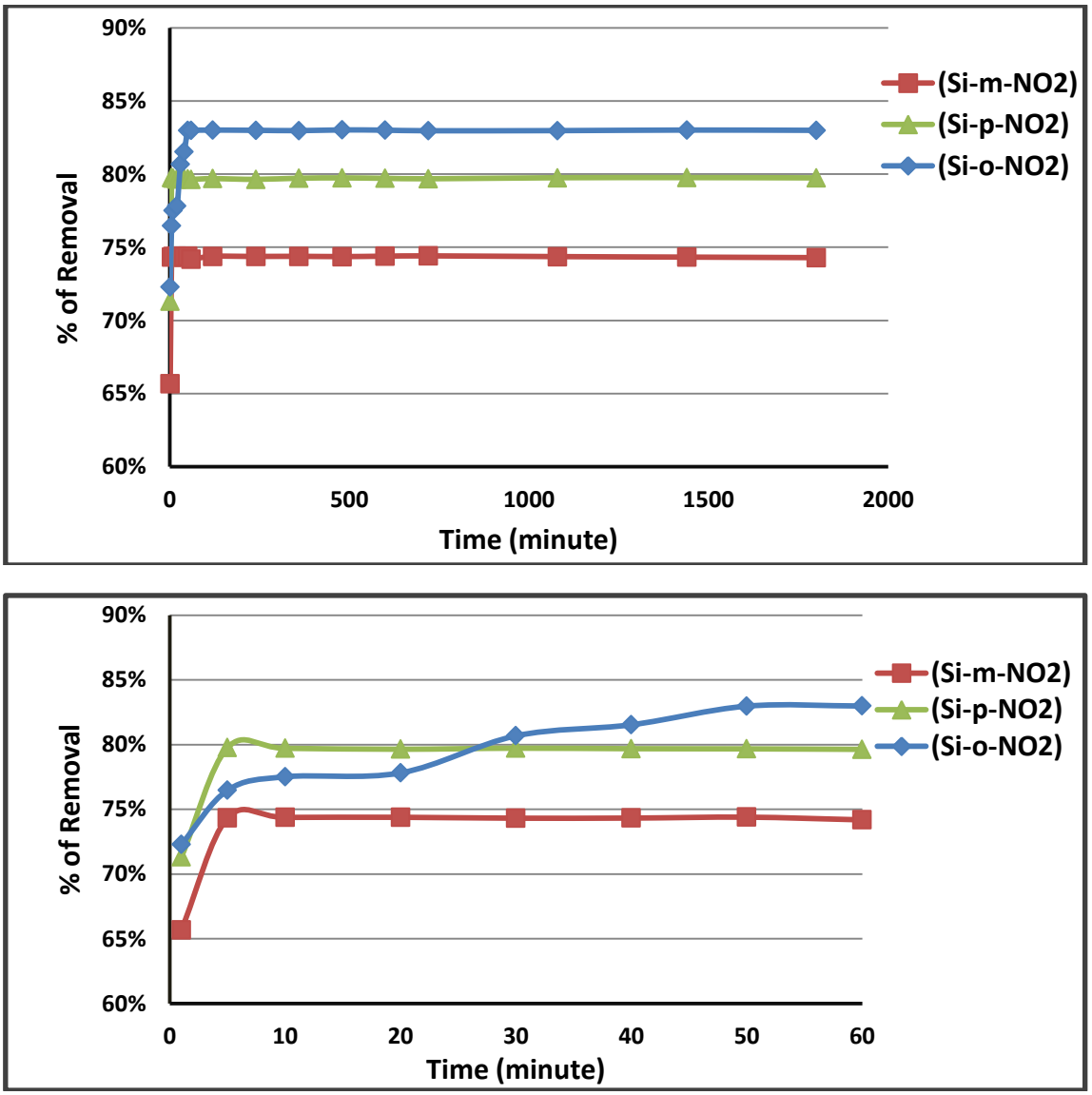

Figure 4.17: Effect of contact time on the adsorption of Cd(II) on ortho-, meta- or para-nitrophenyl silicas (C_I = 10 ppm, adsorbent dose = 1 mg, volume of groundwater = 7 mL, pH = 6, temperature = 20 °C).

This plot shows that the highest percent of Cd(II) removal was for (Si-o-NO_2) after 50 minutes time of shaking as optimum contact time between the adsorbate and the adsorbent, this percentage is 82.98%. While when (Si-p-NO_2) is used for removing cadmium metal ions, the percent of removal is 79.77% and the optimum contact time is after 5 minutes.

The removal of Cd(II) from groundwater using (Si-m-NO_2) has a 74.38% as percent of metal ion removal and an optimum contact time of 10 minutes. For the three synthesized adsorbents, the remaining concentration of the cadmium ions after each optimum contact time becomes approximately constant. The high percents of Cd(II) removal are due to the high availability of vacant sites on the adsorbent external surface. In general, by considering the large required optimum time (50 minutes) for removing cadmium ions using (Si-o-NO_2) polymer matrix, we can consider that (Si-p-NO_2) is better than (Si-o-NO_2) for Cd(II) removing, this is because that it requires small optimum time of shaking (only 5 minutes). Also; the difference between these two percentages is very low (3.21%).

4.2.1.1.2 Effect of pH Value

pH value is one of the most important parameters that controlling the uptake of heavy metal ions from aqueous solutions. (Figure 4.18) shows the effect of pH value on Cd(II) removal efficiency on different adsorbents. These studies were conducted at the optimum contact times for (Si-o-NO_2), (Si-m-NO_2) and (Si-p-NO_2) adsorbents with varying the pH value of the solution.

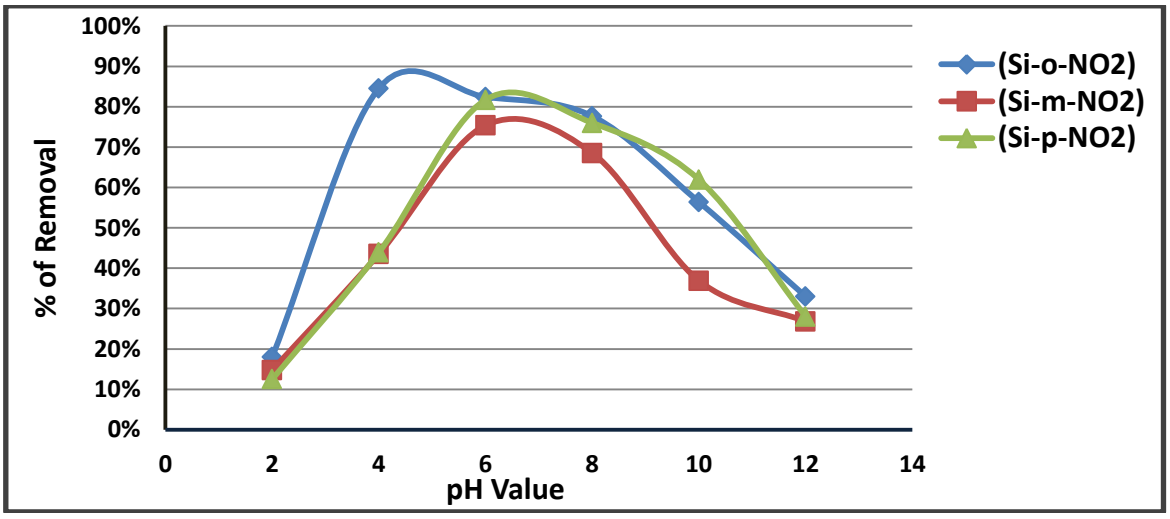

Figure 4.18: Effect of pH value on the adsorption of Cd(II) on ortho-, meta- or para-nitrophenyl silicas (C_I = 10 ppm, adsorbent dose = 1 mg, volume of groundwater = 7 mL, temperature = 20 °C).

For (Si-o-NO_2) matrix, the percentage adsorption increases with pH to attain a maximum at pH 5, and thereafter it decreases with further increase in the value of pH. This adsorbent has the maximum percent of Cd(II) removal that is 84.57% compared with that for (Si-p-NO_2) that equals 81.72% and (Si-m-NO_2) that equals 75.39%.

In addition, the effect of pH value on the adsorption efficiency of (Si-m-NO_2) and (Si-p-NO_2) polymers increases with pH until reaching a maximum at pH 6 and pH 7 respectively, and thereafter the percent of cadmium removal decreases with further increase in pH value.

The increase in metal ion removal as the pH value increases can be explained on the basis of a decrease in competition between proton and cadmium ions for the same functional groups and by the decrease in the positive surface charge, which results in lower electrostatic repulsion between the surface and metal ions. While, the decreasing behavior of the

percentage removal after each optimum pH for the three synthesized adsorbents is probably due to the formation of a soluble hydroxy complexes which lowers the adsorption efficiency to uptake Cd(II) from groundwater.

4.2.1.1.3 Effect of Temperature

To study the effect of temperature on the adsorption of Cd(II) using ortho-, meta- and para nitrophenyl silicas. The optimum conditions of contact time and pH value must be taken in consideration. In general, the adsorption efficiency becomes very low at high temperature values.

As shown in (Figure 4.19), the adsorption of cadmium ions using the three different adsorbents including (Si-o-NO_2), (Si-m-NO_2) and (Si-p-NO_2) has been found to increase with an increase in temperature until reaching a maximum at 25 °C, 10°C and 15 °C respectively, and thereafter the percentage removal decreases with further heating. Such that, the percentages removal at the optimum temperature value are 89.56% for (Si-o-NO_2), 83.95% for (Si-m-NO_2) and 87.94% for (Si-p-NO_2). The low temperature values of the solution enhance the complexation ability between cadmium ions and each of the matrix polymers and hence increase the adsorption efficiency. While, at high temperature values, the adsorption capacity between the adsorbate and the adsorbent is low.

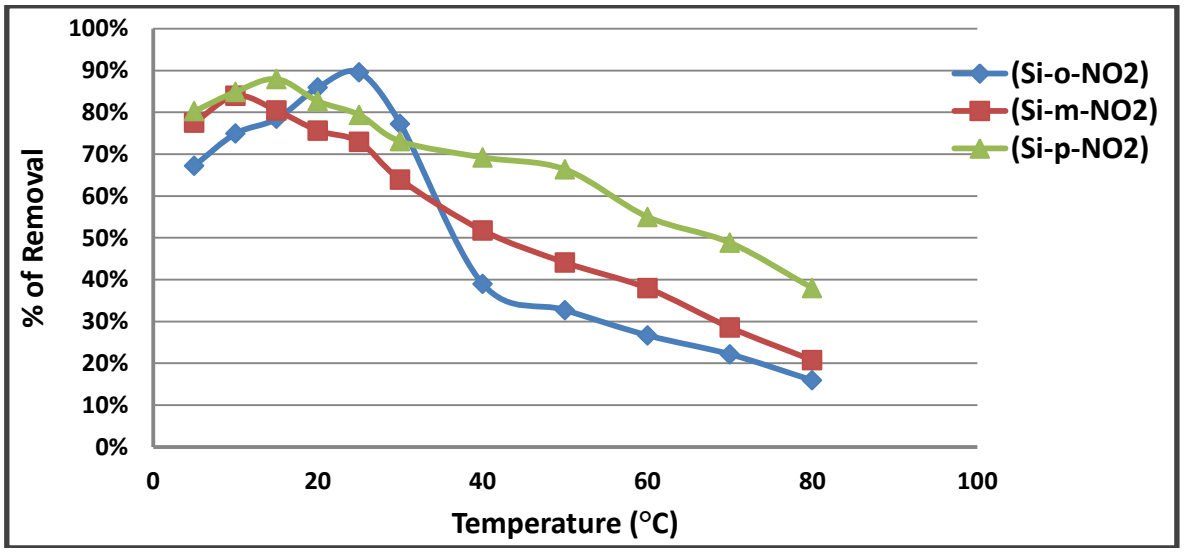

Figure 4.19: Effect of temperature on the adsorption of Cd(II) on ortho-, meta- or para-nitrophenyl silicas (C_I = 10 ppm, adsorbent dose = 1 mg, volume of groundwater = 7 mL).

4.2.1.1.4 Effect of Adsorbent Dose

The experimental results for adsorptive removal of cadmium ions with respect to each dose of (Si-o-NO_2), (Si-m-NO_2) and (Si-p-NO_2) adsorbents are shown in (Figure 4.20) over the range 1 mg to 5 mg, at the optimum values of time, pH and temperature.

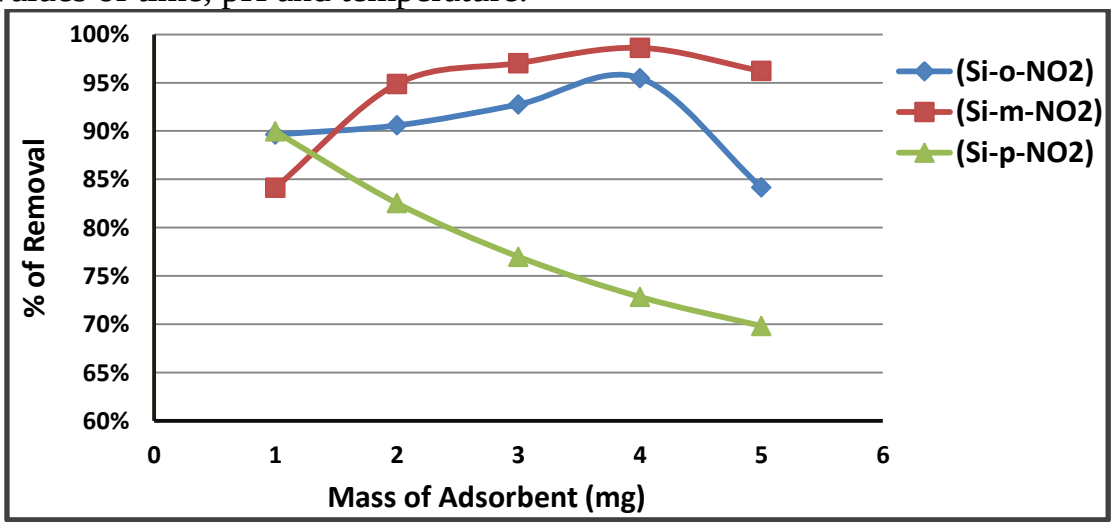

Figure 4.20: Effect of adsorbent dose on the adsorption of Cd(II) on ortho-, meta- or para-nitrophenyl silicas (C_I = 10 ppm, volume of groundwater = 7 mL).

The maximum percent of Cd(II) removal was 98.61% using 4 mg of (Si-m-NO_2). Such that, this polymer showed an increase in percentage removal with increasing the adsorbent dose. Also, the same relation between adsorption efficiency and dosage effect is observed for (Si-o-NO_2) with 4 mg amount of dose and 95.48% as percentage removal.

While (Si-p-NO_2) showed a different effect of adsorbent dose, such that, the maximum observed percent of Cd(II) removal was 89.95% with only 1 mg. The rapidly increased percentage removal of the metal ion with increase in the dose for ortho- and meta-nitrophenyl receptors is due to the greater availability of the exchangeable sites on the adsorbent surface area. While in the case of (Si-p-NO_2), just only very low amount of this adsorbent showed a very high ability to remove Cd(II) from groundwater.

4.2.1.1.5 Effect of Adsorbate Concentration

The effect of the initial concentration of Cd(II) on the percentage removal of heavy metals using the three prepared adsorbents indicated that the adsorptive removal decreases with the increase in the initial heavy metal concentration. The maximum percent of Cd(II) removal was 98.99% for (Si-m-NO_2) by using 15 ppm concentration of cadmium solution. While the observed initial concentrations for having maximum adsorption efficiency for (Si-o-NO_2) and (Si-p-NO_2) polymers are 10 ppm and 5 ppm respectively, with percentage removal of 95.54% for ortho-nitrophenyl silica and 97.98% for para-nitrophenyl silica. Generally, lower initial cadmium ion concentrations results in sufficient adsorption sites to be available for adsorption process (Figure 4.21).

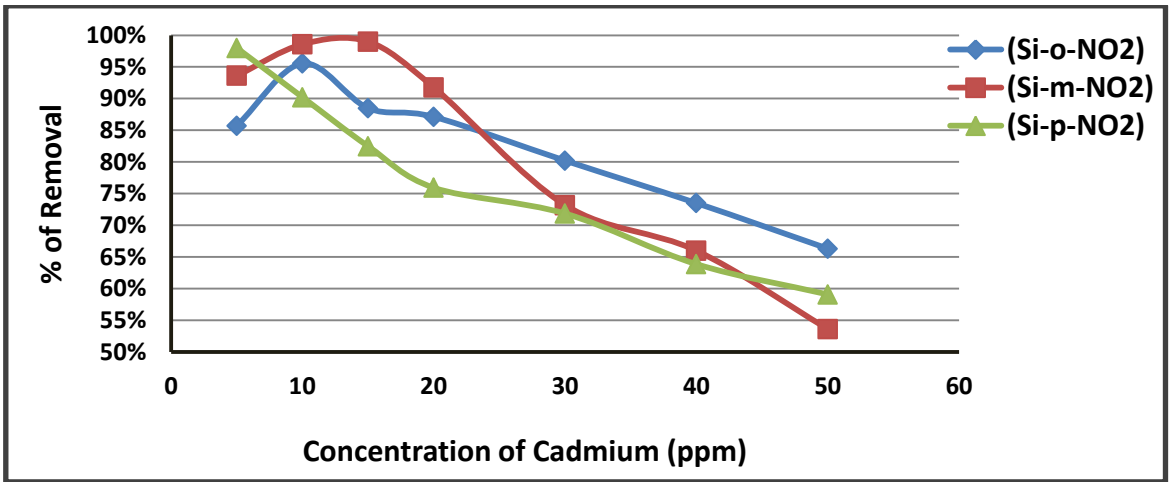

Figure 4.21: Effect of adsorbate concentration on the adsorption of Cd(II) on ortho-, meta- or para-nitrophenyl silicas (volume of groundwater = 7 mL).

The following table represents the adsorption results for removing cadmium ions from groundwater using (Si-o-NO_2), (Si-m-NO_2) or (Si-p-NO_2) adsorbents.

Table 4.2: The adsorption results for removing Cd(II) from groundwater using (Si-o-NO_2), (Si-m-NO_2) and (Si-p-NO_2).

Adsorption of Cd(II)			
Optimum Condition and % of Cd(II) Removal	Si-o-NO_2	Si-m-NO_2	Si-p-NO_2
Contact Time (minute) % of Removal	50 82.98%	10 74.38%	5 79.77%
pH value % of Removal	5 84.57%	6 75.39%	7 81.72%
Temperature (°C) % of Removal	25 89.56%	10 83.95%	15 87.94%
Adsorbent Dose (mg) % of Removal	4 95.48%	4 98.61%	1 89.95%
Adsorbate Concentration(ppm) % of Removal	10 95.54%	15 98.99%	5 97.98%

4.2.1.1.6 Adsorbent Regeneration

(Figure 4.22) shows the effect of adsorbent recovery on the adsorption of cadmium ions on ortho-, meta-, or para-nitrophenyl silicas. As shown in

this plot, the difference between the percents of heavy metal ion removal after the first and second regeneration of each modified polymer is very low. This is strong evidence that the three synthesized adsorbents can be recycled, and hence be used for several times.

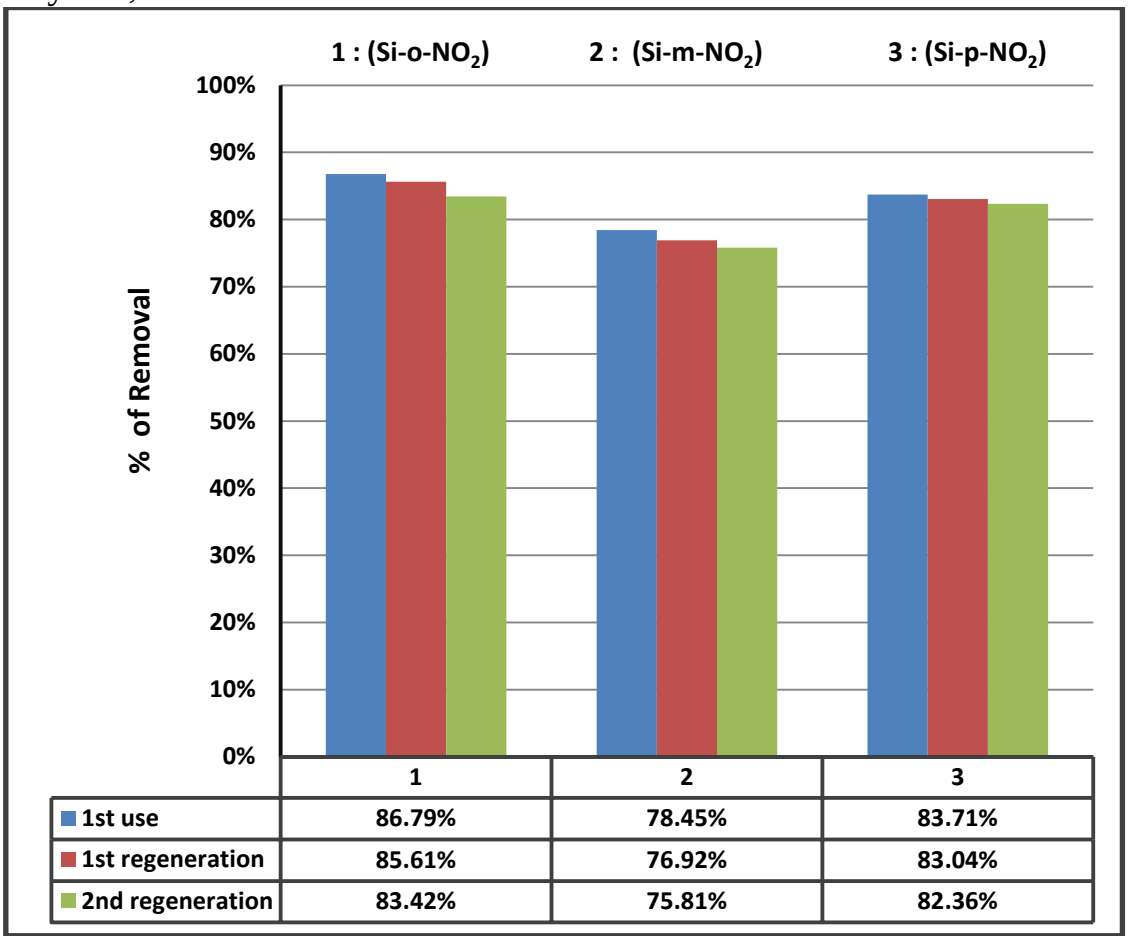

Figure 4.22: Effect of adsorbent recovery on the adsorption of Cd(II) on ortho-, meta-, or para-nitrophenyl silicas (contact time = 5 minute, C_I = 10 ppm, adsorbent dose = 20 mg, volume of groundwater = 20 mL, pH = 6, temperature = 20 °C).

4.2.1.2 Adsorption of Lead

The effect of solution conditions for the adsorption of lead ions on (Si-o-NO_2), (Si-m-NO_2) or (Si-p-NO_2) adsorbents is determined. As the

adsorbent is changed, the adsorption dependence on the polymer nature is investigated.

4.2.1.2.1 Effect of Contact Time

To establish an optimum contact time between lead ions and each of the adsorbents, adsorption capacities of Pb(II) were measured as a function of time (Figure 4.23).

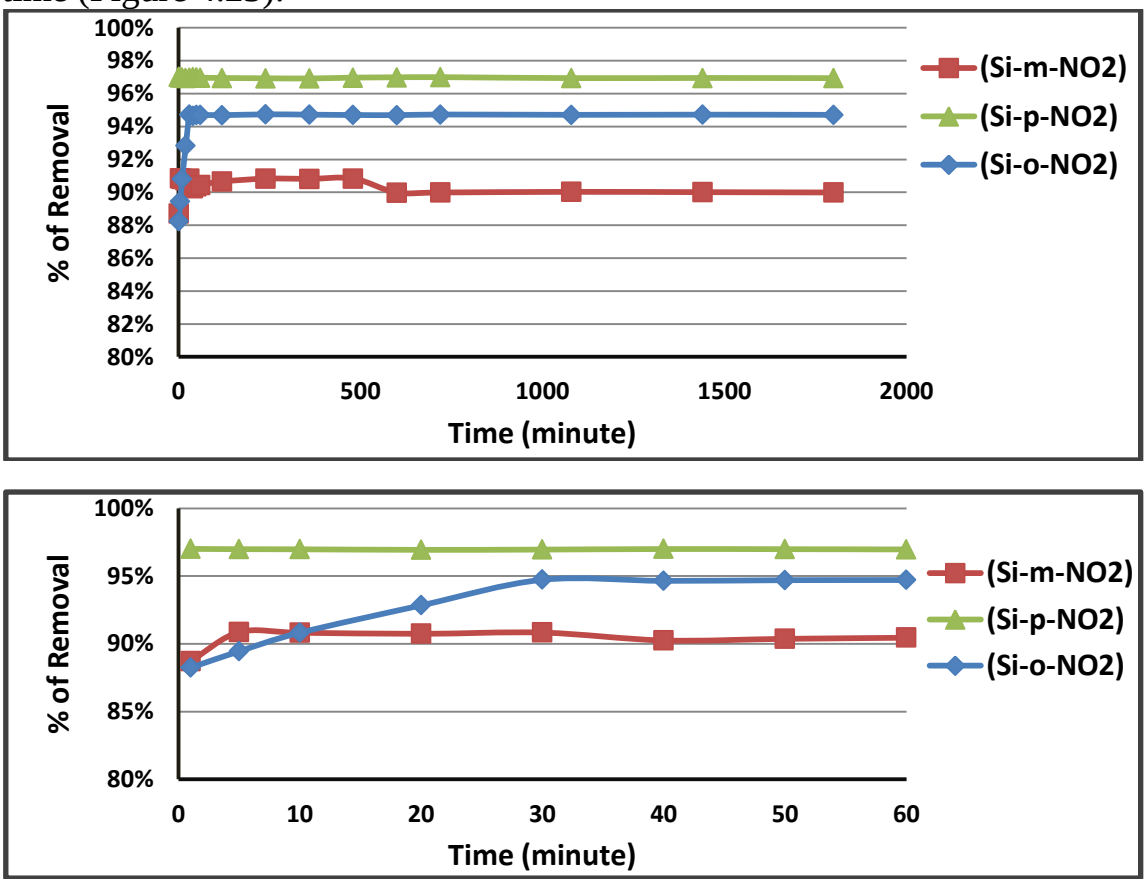

Figure 4.23: Effect of contact time on the adsorption of Pb(II) on ortho-, meta- or para-nitrophenyl silicas (C_I = 10 ppm, adsorbent dose = 1 mg, volume of groundwater = 7 mL, pH = 6, temperature = 20 °C).

As shown in this plot, the highest percent of Pb(II) removal was for (Si-p-NO_2) after only 1 minute of shaking, this percentage is 97.01%. While when (Si-o-NO_2) is used for removing lead metal ions, the percentage

removal is 94.73% and the optimum contact time is after 30 minutes. The removal of Pb(II) from groundwater using (Si-m-NO_2) has a 90.86% as percent of metal ion removal and a optimum contact time of 5 minutes. For the three synthesized adsorbents, the remaining concentration of the lead ions after each optimum contact time becomes approximately constant. The extremely high percents of Pb(II) removal are due to the very high availability of vacant sites on the adsorbent external surface.

4.2.1.2.2 Effect of pH Value

(Figure 4.24) showed the effect of pH value on Pb(II) removal efficiency on different adsorbents. These studies were conducted at the optimum contact times for (Si-o-NO_2), (Si-m-NO_2) and (Si-p-NO_2) with varying the pH value of the solution.

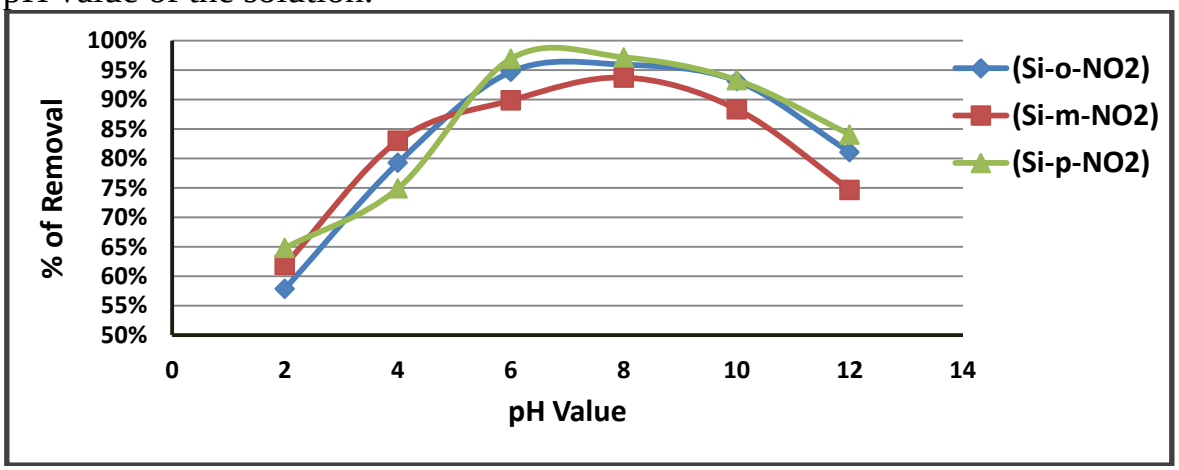

Figure 4.24: Effect of pH value on the adsorption of Pb(II) on ortho-, meta- or para-nitrophenyl silicas (C_I = 10 ppm, adsorbent dose = 1 mg, volume of groundwater = 7 mL, temperature = 20 °C).

For (Si-p-NO_2) matrix, the percentage adsorption increases with pH to attain a maximum at pH 8, and thereafter it decreases with further increase in the value of pH. This adsorbent has the maximum percent of Pb(II)

removal that is 97.14% compared with that for (Si-o-NO_2) that equals 95.89% and (Si-m-NO_2) that equals 93.71%.

Also, the effect of pH value on the adsorption efficiency of (Si-p-NO_2) and (Si-m-NO_2) polymers increases with pH until reaching a maximum at pH 8 and pH 7 respectively, and thereafter the percentage removal decreases with further increase in pH value.

The increase in metal ion removal as the pH increases can be due to decrease in competition between proton and lead ions for the same functional groups and also by the decrease in the positive surface charge, which results in a lower electrostatic repulsion between the surface and lead ions. While the decreasing behavior of the percent of Pb(II) removal after each optimum pH for the three synthesized adsorbents is probably due to the formation of a soluble hydroxy complexes which lowers the adsorption efficiency to uptake lead ions from groundwater.

4.2.1.2.3 Effect of Temperature

To study the effect of temperature on the adsorption of Pb(II) using ortho-, meta-, and para-nitrophenyl silicas. The optimum conditions of contact time and pH value must be taken in consideration. In general, the adsorption efficiency becomes very low at high temperature values.

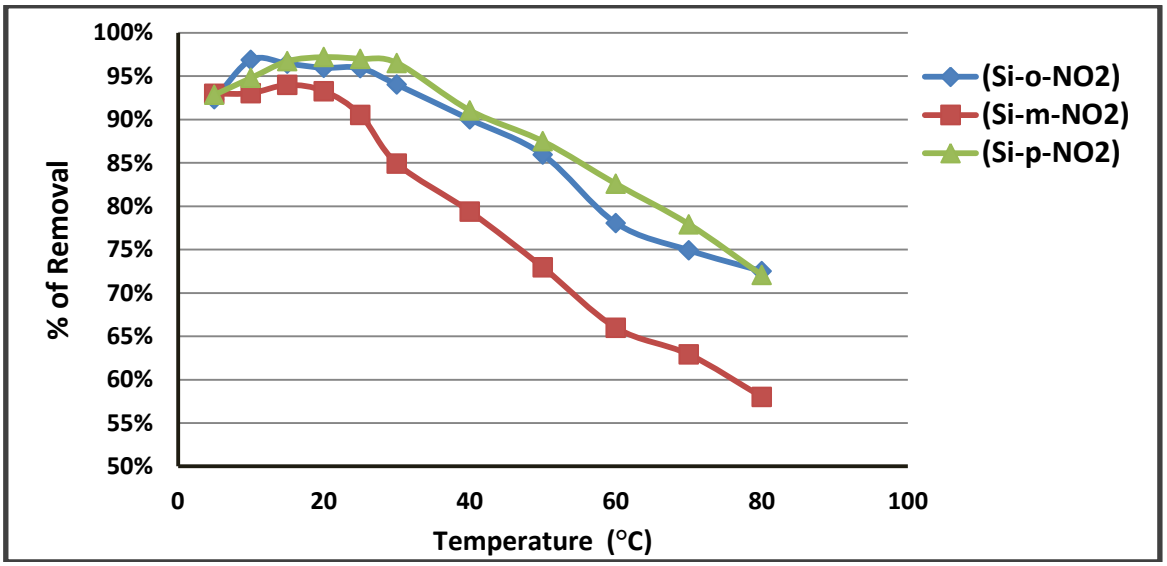

Figure 4.25: Effect of temperature on the adsorption of Pb(II) on ortho-, meta- or para-nitrophenyl silicas (C_I = 10 ppm, adsorbent dose = 1 mg, volume of groundwater = 7 mL).

As shown in (Figure 4.25), the adsorption of lead ions using the three different adsorbents including (Si-o-NO_2), (Si-m-NO_2) and (Si-p-NO_2) has been found to increase with an increase in temperature until reaching a maximum at 10 °C, 15°C and 20 °C respectively, and thereafter the percentage removal decreases with further heating. Such that; the percentages removal at the optimum temperature value are 96.89% for (Si-o-NO_2), 93.98% for (Si-m-NO_2) and 97.19% for (Si-p-NO_2).

In general, low temperatures of the solution enhance the complexation ability between lead ions and each of the matrix polymers and hence increase the adsorption efficiency.

4.2.1.2.4 Effect of Adsorbent Dose

The experimental results for adsorptive removal of lead ions with respect to each dose of (Si-o-NO_2), (Si-m-NO_2) and (Si-p-NO_2) adsorbents are shown

in (Figure 4.26) over the range 1 mg to 5 mg at the optimum values of time, pH and temperature.

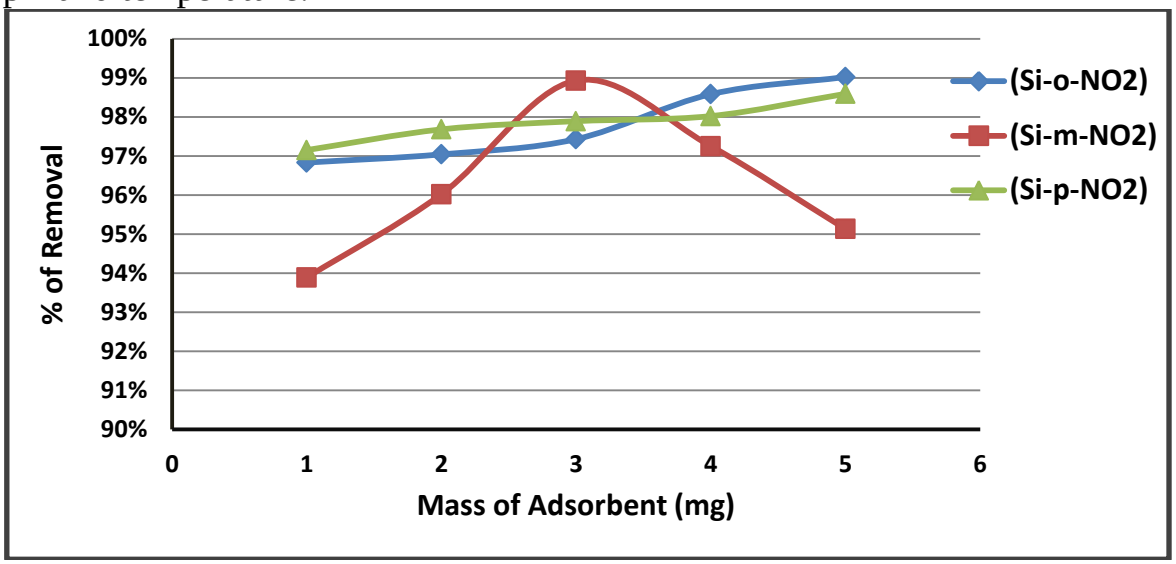

Figure 4.26: Effect of adsorbent dose on the adsorption of Pb(II) on ortho-, meta- or para-nitrophenyl silicas (C_I = 10 ppm, volume of groundwater = 7 mL).

The maximum percent of Pb(II) removal was 99.02% with using 5 mg of (Si-o-NO_2). Such that, this polymer showed an increase in percentage removal with increasing the adsorbent dose. Also, the same relation between adsorption efficiency and dosage effect is observed for (Si-p-NO_2) with 5 mg amount of dose and 98.59% as percentage removal.

While (Si-m-NO_2) showed a different effect of adsorbent dose, such that; the maximum observed percent of Pb(II) removal was 98.59% with 3 mg dose. For ortho-, and para-nitrophenyl silicas, the rapidly increased percentage removal of the metal ion with increase in the adsorbent dose is due to the greater availability of the exchangeable sites on the adsorbent surface area.

4.2.1.2.5 Effect of Adsorbate Concentration

The effect of the initial concentration of Pb(II) on the percentage removal of heavy metals using the three prepared adsorbents is shown in (Figure 4.27).

As shown in this plot. For para-nitrophenyl silica, the adsorptive removal increases with the increase in the initial heavy metal concentration. The maximum percent of Pb(II) removal was 99.95% for (Si-p-NO_2) by using 50 ppm lead concentration. While the observed initial concentration for having maximum adsorption efficiency for (Si-o-NO_2) and (Si-m-NO_2) polymers is 50 ppm, and 10 ppm with percents of Pb(II) removal of 99.84% and 98.91% respectively.

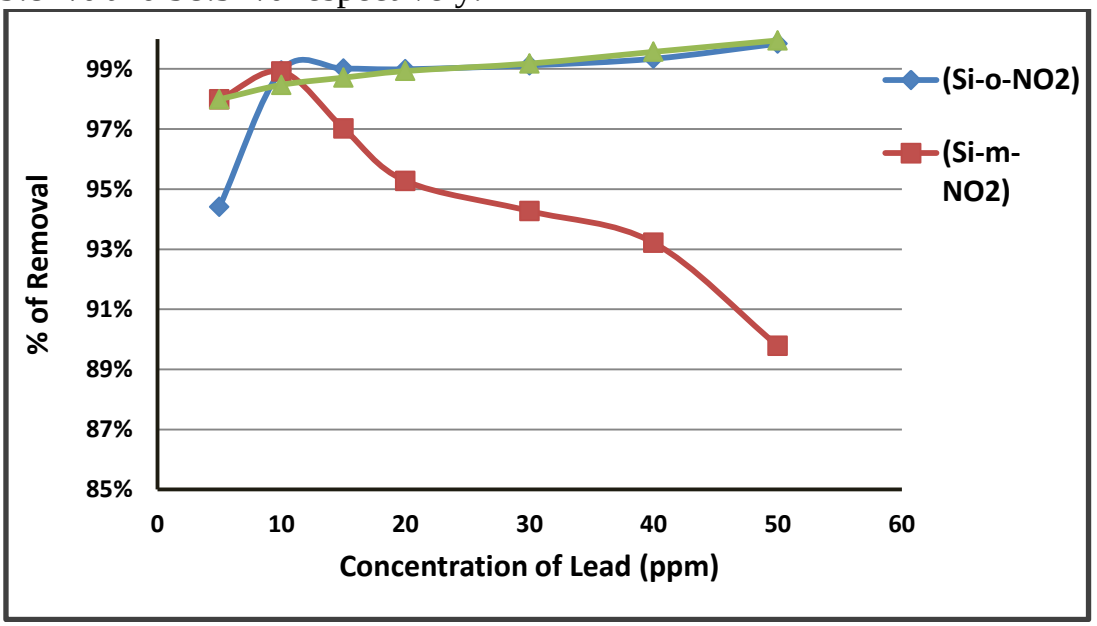

Figure 4.27: Effect of adsorbate concentration on the adsorption of Pb(II) on ortho-, meta- or para-nitrophenyl silicas (volume of groundwater = 7 mL).

The following table represents the adsorption results for removing lead ions from groundwater using (Si-o-NO_2), (Si-m-NO_2) and (Si-p-NO_2) as adsorbents.

Table 4.3: The adsorption results for removing Pb(II) from groundwater using (Si-o-NO_2), (Si-m-NO_2) and (Si-p-NO_2).

Adsorption of Pb(II)			
Optimum Condition and % of Pb(II) Removal	Si-o-NO_2	Si-m-NO_2	Si-p-NO_2
Contact Time (minute) % of Removal	30 94.73%	5 90.86%	1 97.01%
pH value % of Removal	8 95.89%	7 93.71%	8 97.14%
Temperature (°C) % of Removal	10 96.89%	15 93.98%	20 97.19%
Adsorbent Dose (mg) % of Removal	5 99.02%	3 98.93%	5 98.59%
Adsorbate Concentration(ppm) % of Removal	50 99.84%	10 98.91%	50 99.95%

4.2.1.2.6 Adsorbent Regeneration

(Figure 4.28) shows the effect of adsorbent recovery on the adsorption of lead ions on ortho-, meta-, or para-nitrophenyl silicas. As shown in this plot, the difference between the percents of heavy metal ion removal after the first and second regeneration of each modified polymer is very low. This is strong evidence that the three synthesized adsorbents can be recycled, and hence be used for several times.

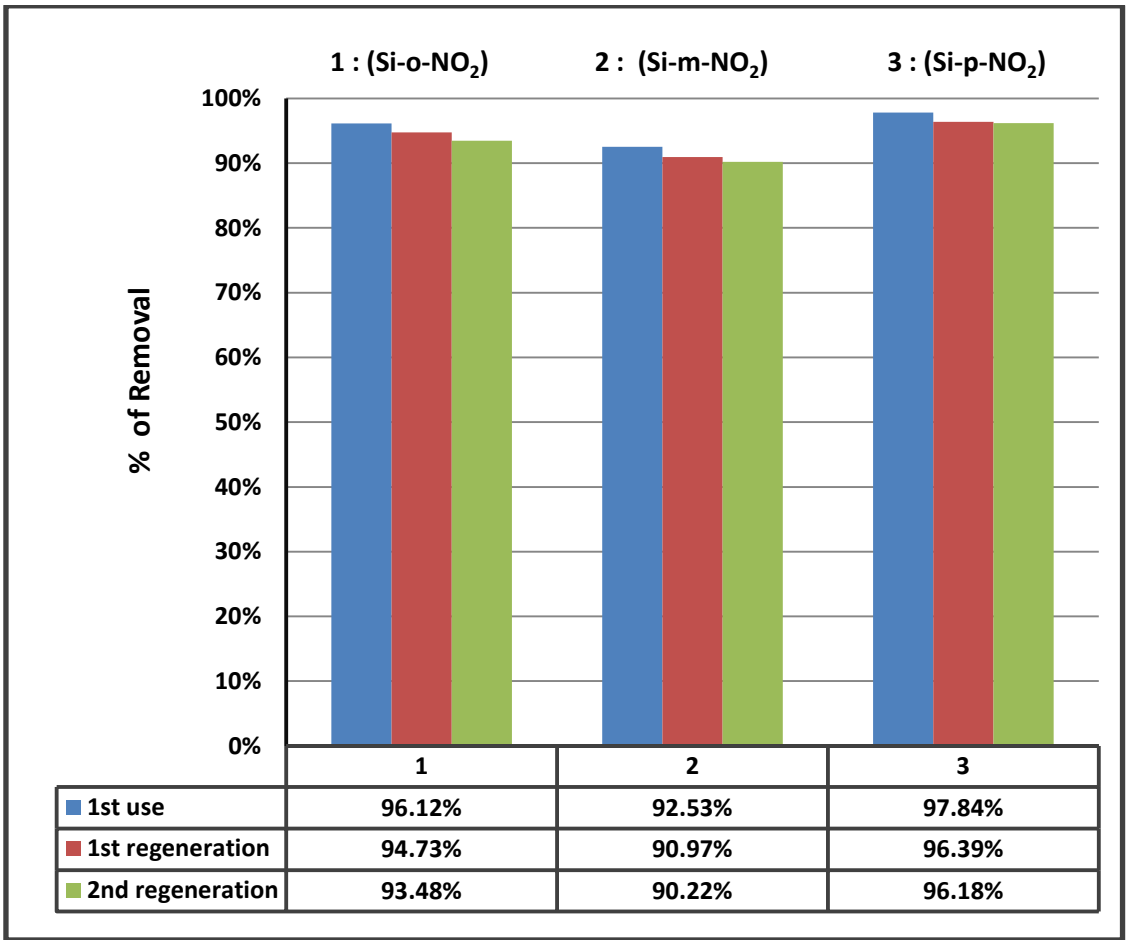

	1	2	3
1st use	96.12%	92.53%	97.84%
1st regeneration	94.73%	90.97%	96.39%
2nd regeneration	93.48%	90.22%	96.18%

Figure 4.28: Effect of adsorbent recovery on the adsorption of Pb(II) on ortho-, meta-, or para-nitrophenyl silicas (contact time = 5 minute, C_I = 10 ppm, adsorbent dose = 20 mg, volume of groundwater = 20 mL, pH = 6, temperature = 20 °C).

4.2.1.3 Adsorption of Nickel

The effect of solution conditions for the adsorption of Ni(II) on (Si-o-NO_2), (Si-m-NO_2) or (Si-p-NO_2) adsorbents is determined. As the adsorbent is changed, the adsorption dependence on the polymer nature is investigated.

4.2.1.3.1 Effect of Contact Time

In order to establish an appropriate contact time between nickel ions and each of the adsorbents, adsorption capacities of Ni(II) were measured as a function of time (Figure 4.29).

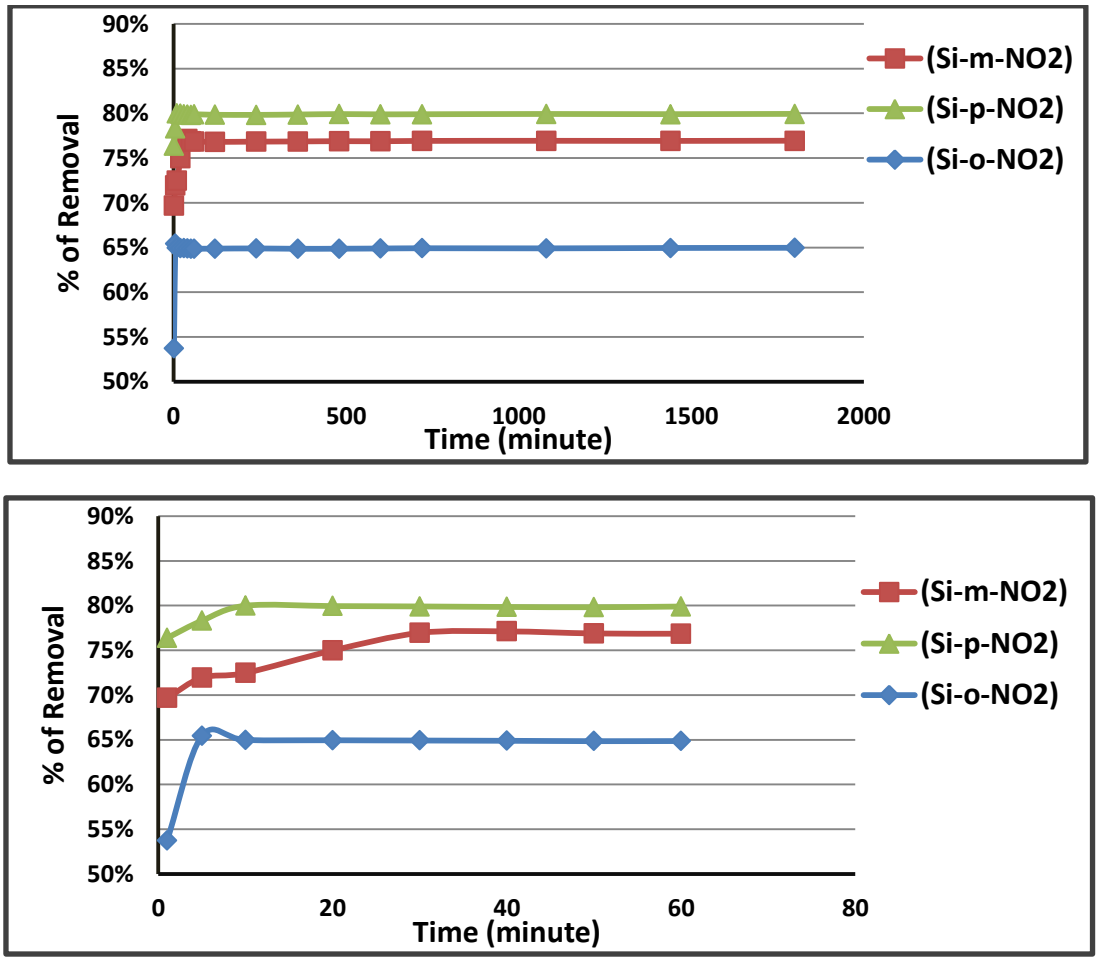

Figure 4.29: Effect of contact time on the adsorption of Ni(II) on ortho-, meta- or para-nitrophenyl silicas (C_I = 10 ppm, adsorbent dose = 1 mg, volume of groundwater = 7 mL, pH = 6, temperature = 20 °C).

As shown in this plot, the highest percent of Ni(II) removal was for (Si-p-NO_2) after 10 minutes time of shaking, this percentage is 79.99%. While when (Si-o-NO_2) is used for removing nickel metal ions, the percent of removal is 64.98% and the optimum contact time is after 10 minutes. The removal of Ni(II) from groundwater using (Si-m-NO_2) has a 76.95% as percent of metal ion removal and a optimum contact time of 20 minutes. For the three synthesized adsorbents, the remaining concentration of the

nickel ions after each optimum contact time becomes approximately constant.

4.2.1.3.2 Effect of pH Value

The effect of pH value on Ni(II) removal efficiency on different adsorbents is shown in (Figure 4.30). These studies were conducted at the optimum contact times for (Si-o-NO_2), (Si-m-NO_2) and (Si-p-NO_2) with varying the pH value of the solution.

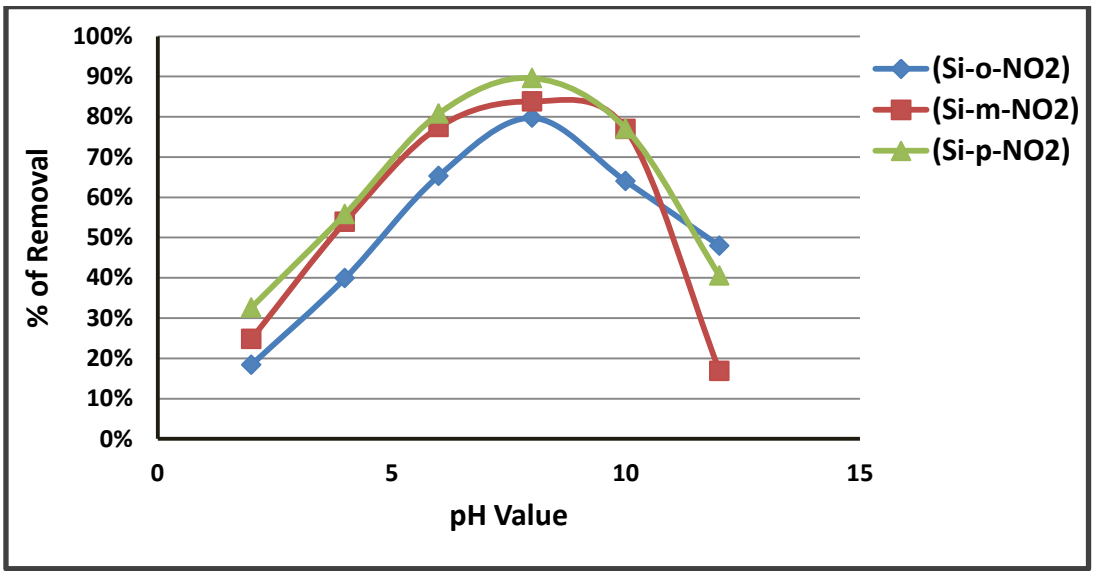

Figure 4.30: Effect of pH value on the adsorption of Ni(II) on ortho-, meta- or para-nitrophenyl silicas (C_I = 10 ppm, adsorbent dose = 1 mg, volume of groundwater = 7 mL, temperature = 20 °C).

For (Si-p-NO_2) matrix, the percentage adsorption increases with pH to attain a maximum at pH 8, and thereafter it decreases with further increase in the value of pH. This adsorbent has the maximum percent of Ni(II) removal that is 89.59% compared with that for (Si-o-NO_2) that equals 79.71% and (Si-m-NO_2) that equals 83.80%. The effect of pH value on the adsorption efficiency of (Si-o-NO_2) and (Si-m-NO_2) polymers increases

with pH until reaching a maximum at pH 7 and thereafter the percent of nickel removal decreases with further increase in pH value.

4.2.1.3.3 Effect of Temperature

To study the effect of temperature on the adsorption of Ni(II) using ortho-, meta-, and para-nitrophenyl silicas. The optimum conditions of contact time and pH value must be taken in consideration. In general, the adsorption efficiency becomes very low at high temperature values.

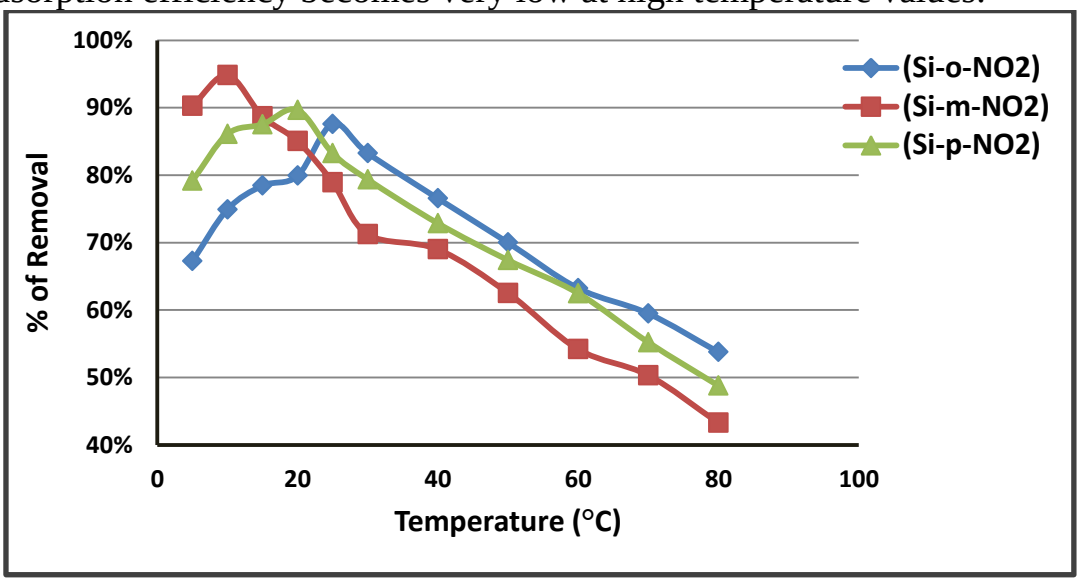

Figure 4.31: Effect of temperature on the adsorption of Ni(II) on ortho-, meta- or para-nitrophenyl silicas (C_I = 10 ppm, adsorbent dose = 1 mg, volume of groundwater = 7 mL).

As shown in (Figure 4.31), the adsorption of nickel ions using the three different adsorbents has been found to increase with an increase in temperature until reaching a maximum at 25 °C, 10°C and 20 °C respectively, and thereafter the percent of Ni(II) removal decreases with increasing temperature. Such that, the percentages removal at the optimum temperature value are 87.59% for (Si-o-NO_2), 94.83% for (Si-m-NO_2) and

89.66% for (Si-p-NO_2). The low temperature values of enhance the complexation ability between nickel ions and each of the matrix polymers and hence increase the adsorption efficiency.

4.2.1.3.4 Effect of Adsorbent Dose

The experimental results for adsorptive removal of nickel ions with respect to each dose of (Si-o-NO_2), (Si-m-NO_2) and (Si-p-NO_2) adsorbents are shown in (Figure 4.32) over the range 1 mg to 5 mg at the optimum values of time, pH and temperature.

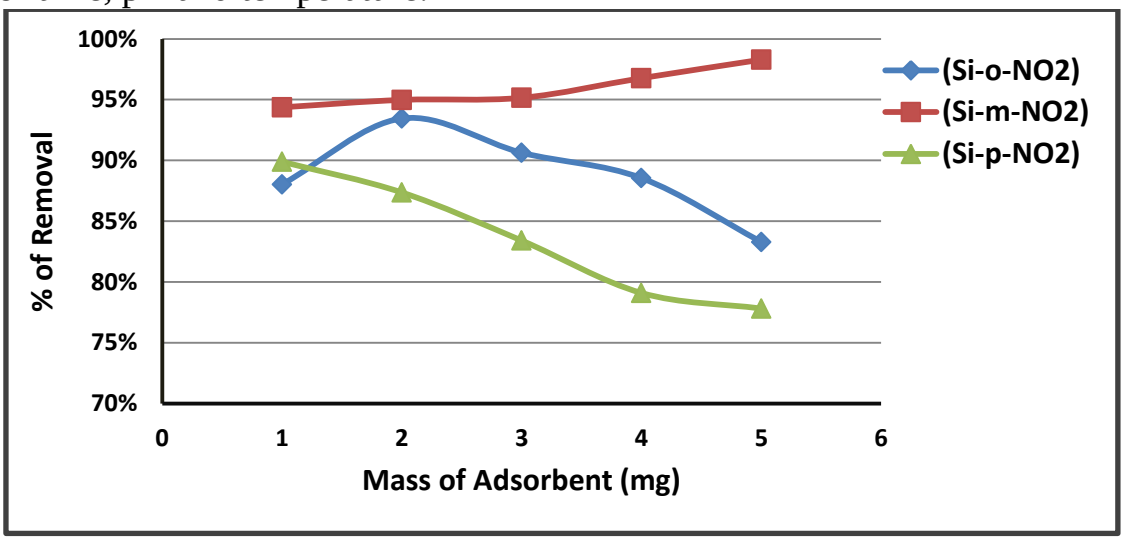

Figure 4.32: Effect of adsorbent dose on the adsorption of Ni(II) on ortho-, meta- or para-nitrophenyl silicas (C_I = 10 ppm, volume of groundwater = 7 mL).

The maximum percent of Ni(II) removal was 98.29% with using 5 mg of (Si-m-NO_2). Such that, this polymer showed an increase in percentage removal with increasing the adsorbent dose. This result is due to that large amount of meta-nitrophenyl silica increases availability of the exchangeable sites on the adsorbent surface area.

For (Si-p-NO_2) and (Si-o-NO_2), they showed a different effect of adsorbent dose compared with (Si-m-NO_2). Such that, the maximum observed percent of Ni(II) removal was 89.89% for para-nitrophenyl silica with only 1 mg adsorbent dose and 93.45% for ortho-nitrophenyl silica with 2 mg dose.

4.2.1.3.5 Effect of Adsorbate Concentration

The effect of the initial concentration of Ni(II) on the percentage removal of heavy metals using the three prepared adsorbents is shown in (Figure 4.33).

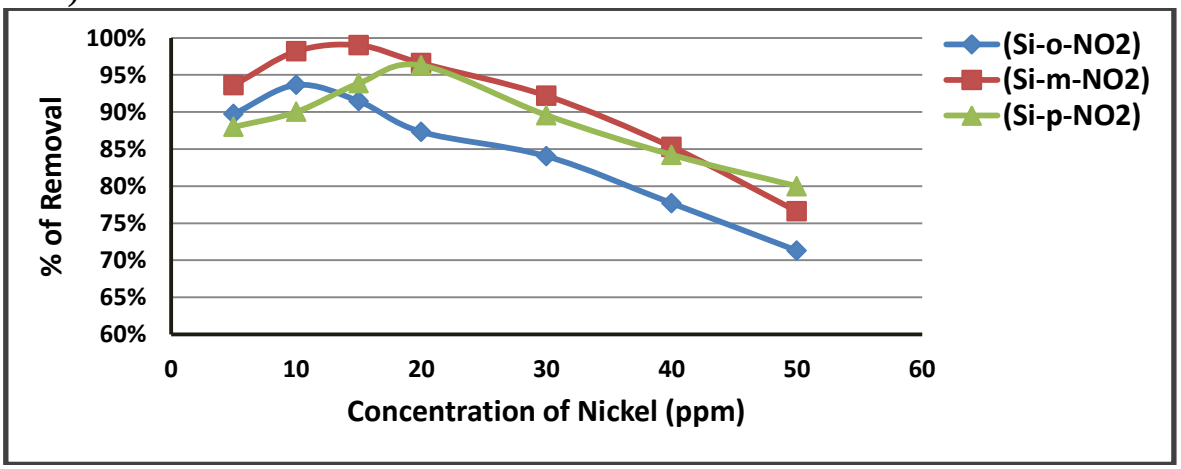

Figure 4.33: Effect of adsorbate concentration on the adsorption of Ni(II) on ortho-, meta- or para-nitrophenyl silicas (volume of groundwater = 7 mL).

As shown in this plot, the adsorptive removal decreases with the increase in the initial heavy metal concentration. The maximum percent of Ni(II) removal was 98.99% for (Si-m-NO_2) by using 15 ppm concentration of Ni(II). While the observed initial concentrations for having maximum adsorption efficiency for (Si-o-NO_2) and (Si-p-NO_2) polymers are 10 ppm and 20 ppm respectively, with percents of removal of 93.64% for ortho-nitrophenyl silica and 96.28% for para-nitrophenyl silica. Such that, lower

initial nickel ion concentrations results in sufficient adsorption sites to be available for adsorption process.

The following table represents the adsorption results for removing nickel ions from groundwater using (Si-o-NO_2), (Si-m-NO_2) and (Si-p-NO_2) as adsorbents.

Table 4.4: The adsorption results for removing Ni(II) from groundwater using (Si-o-NO_2), (Si-m-NO_2) and (Si-p-NO_2).

Adsorption of Ni(II)			
Optimum Condition and % of Ni(II) Removal	Si-o-NO_2	Si-m-NO_2	Si-p-NO_2
Contact Time (minute) % of Removal	10 64.98%	20 76.95%	10 79.99%
pH value % of Removal	7 79.71%	7 83.80%	8 89.59%
Temperature (°C) % of Removal	25 87.59%	10 94.83%	20 89.66%
Adsorbent Dose (mg) % of Removal	2 93.45%	5 98.29%	1 89.89%
Adsorbate Concentration(ppm) % of Removal	10 93.45%	15 98.99%	20 96.28%

4.3.1.3.6 Adsorbent Regeneration

(Figure 4.34) shows the effect of adsorbent recovery on the adsorption of nickel ions on ortho-, meta-, or para-nitrophenyl silicas. As shown in this plot, the difference between the percents of heavy metal ion removal after the first and second regeneration of each modified polymer is very low. This is strong evidence that the three synthesized adsorbents can be recycled, and hence be used for several times.

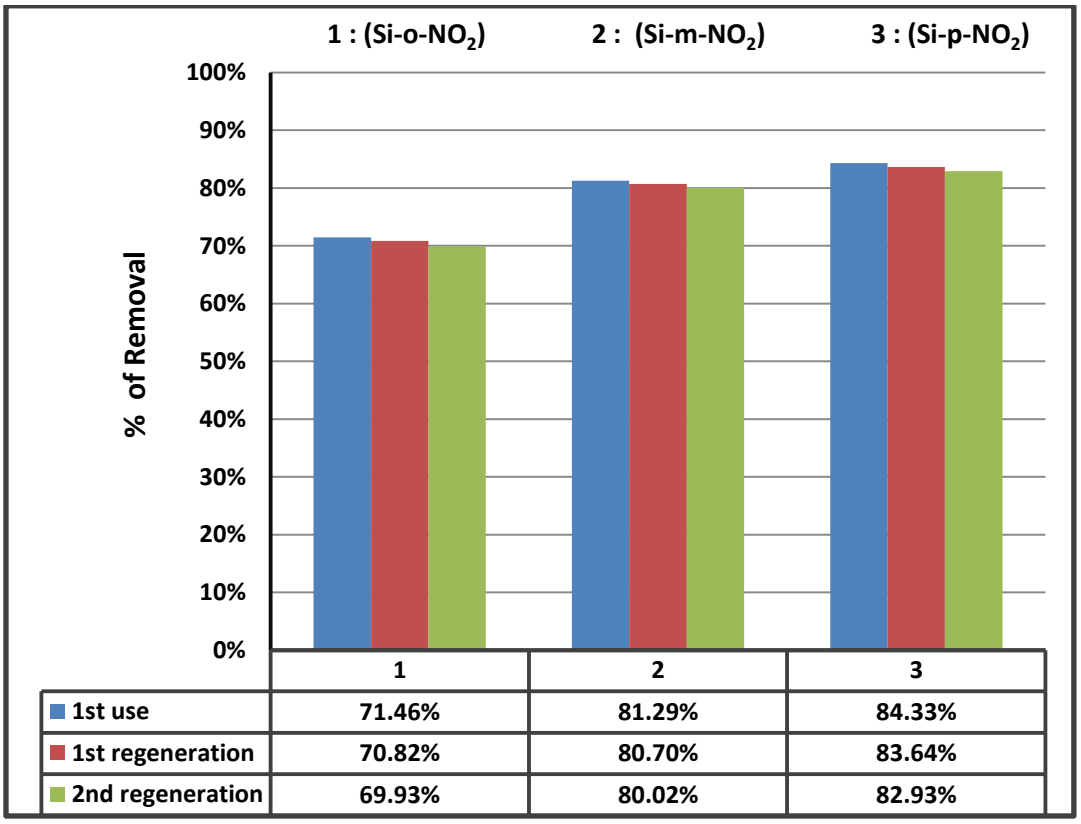

	1	2	3
1st use	71.46%	81.29%	84.33%
1st regeneration	70.82%	80.70%	83.64%
2nd regeneration	69.93%	80.02%	82.93%

Figure 4.34: Effect of adsorbent recovery on the adsorption of Ni(II) on ortho-, meta-, or para-nitrophenyl silicas (contact time = 5 minute, C_I = 10 ppm, adsorbent dose = 20 mg, volume of groundwater = 20 mL, pH = 6, temperature = 20 °C).

4.2.2 Using the Same Adsorbent with Different Adsorbates

4.2.2.1 Adsorption on (Si-o-NO_2)

The effect of solution conditions for the adsorption on (Si-o-NO_2) for the removal of cadmium, lead, or nickel metal ions was investigated, as shown in the following Figures (4.35-4.39).

4.2.2.1.1 Effect of Contact Time

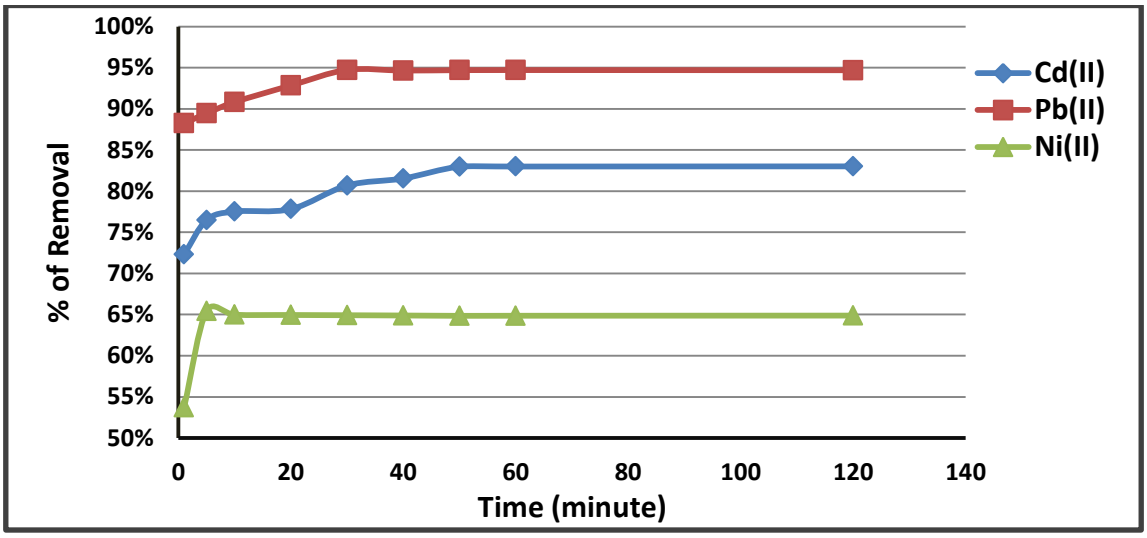

Figure 4.35: Effect of contact time on the adsorption of Cd(II), Pb(II) or Ni(II) on (Si-o-NO_2) (C_I = 10 ppm, adsorbent dose = 1 mg, volume of groundwater = 7 mL, pH = 6, temperature = 20 °C).

4.2.2.1.2Effect of pH Value

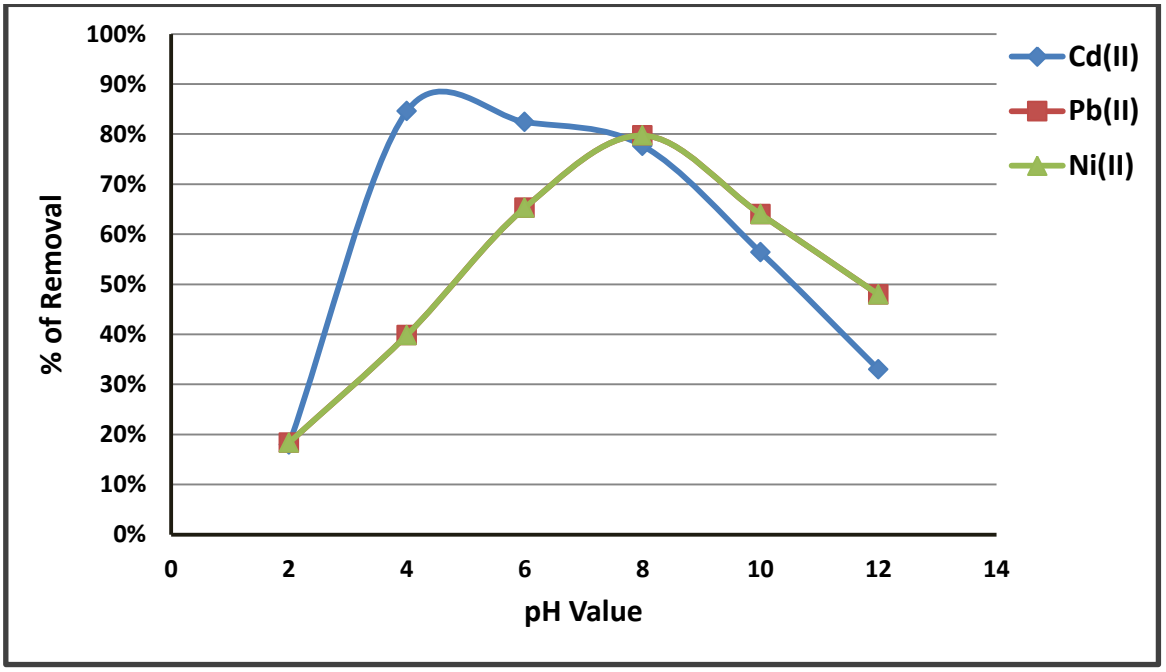

Figure 4.36: Effect of pH value on the adsorption of Cd(II), Pb(II) or Ni(II) on (Si-o-NO_2) (C_I = 10 ppm, adsorbent dose = 1 mg, volume of groundwater = 7 mL, temperature = 20 °C).

4.2.2.1.3 Effect of Temperature

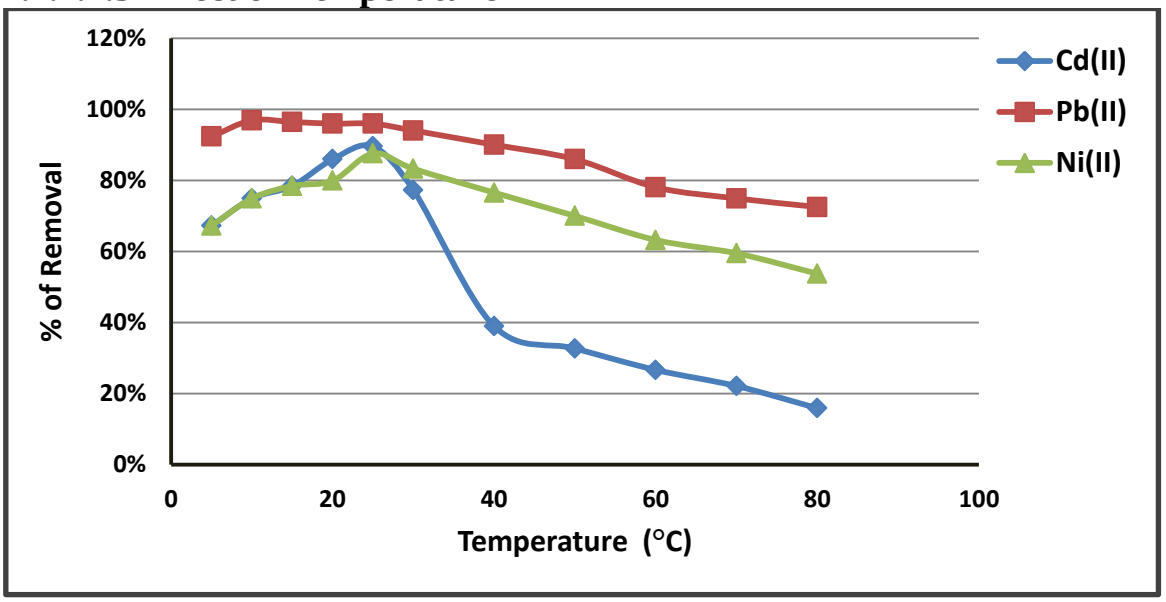

Figure 4.37: Effect of temperature on the adsorption of Cd(II), Pb(II) or Ni(II) on (Si-o-NO_2) (C_I = 10 ppm, adsorbent dose = 1 mg, volume of groundwater = 7 mL).

4.2.2.1.4 Effect of Adsorbent Dose

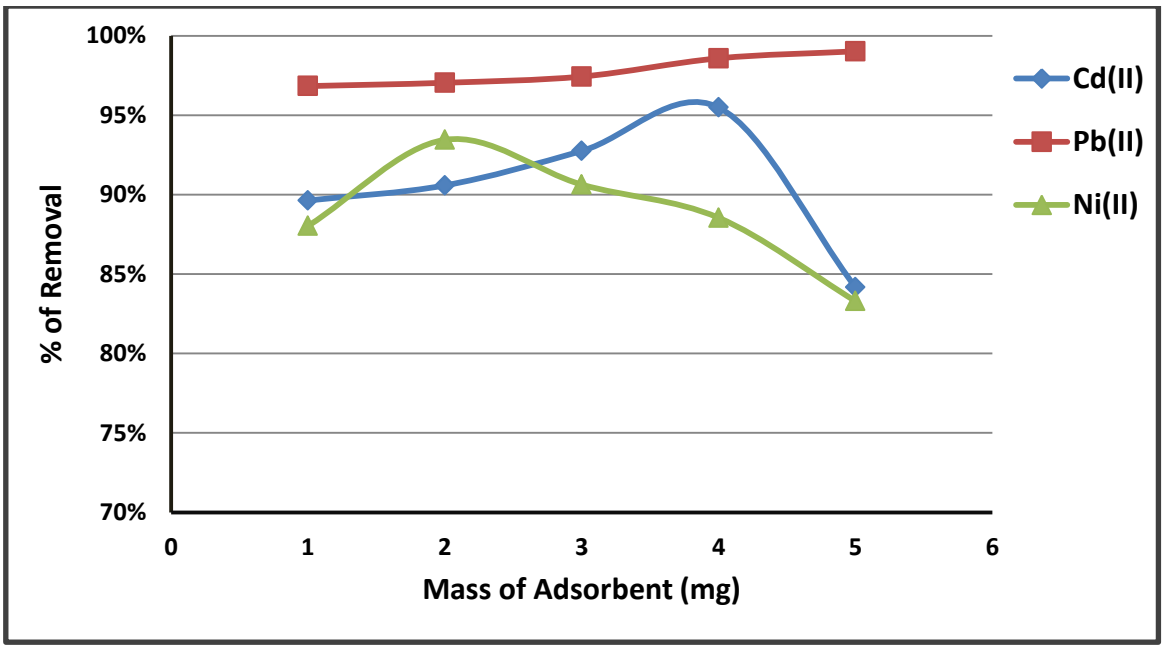

Figure 4.38: Effect of adsorbent dose on the adsorption of Cd(II), Pb(II) or Ni(II) on (Si-o-NO_2)(C_I = 10 ppm, volume of groundwater = 7 mL).

4.2.2.1.5 Effect of Adsorbate Concentration

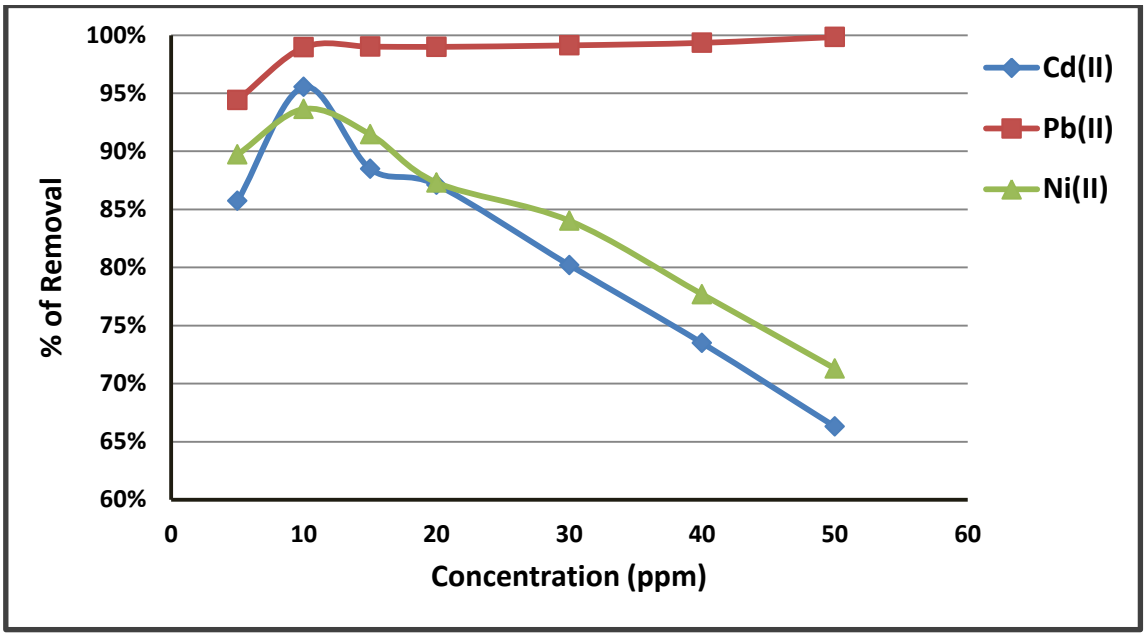

Figure 4.39: Effect of adsorbate concentration on the adsorption of Cd(II), Pb(II) or Ni(II) on (Si-o-NO_2) (volume of groundwater = 7 mL).

The following table shows the adsorption results for removing Cd(II), Pb(II) or Ni(II) from groundwater using (Si-o-NO_2) adsorbent.

Table 4.5: The adsorption results for removing Cd(II), Pb(II) or Ni(II) from groundwater using (Si-o-NO_2).

Adsorption on (Si-o-NO_2)			
Optimum Condition and % of Removal	Cd(II)	Pb(II)	Ni(II)
Contact Time (minute) % of Removal	50 82.98%	30 94.73%	10 64.98%
pH value % of Removal	5 84.57%	8 95.89%	7 79.71%
Temperature (°C) % of Removal	25 89.56%	10 96.89%	25 87.59%
Adsorbent Dose (mg) % of Removal	4 95.48%	5 99.02%	2 93.45%
Adsorbate Concentration(ppm) % of Removal	10 95.54%	50 99.84%	10 93.64%

4.2.2.2 Adsorption on (Si-m-NO_2)

The effect of solution conditions for the adsorption on (Si-m-NO_2) for the removal of cadmium, lead, or nickel metal ions was investigated, as shown in the following Figures (4.40-4.44).

4.2.2.2.1 Effect of Contact Time

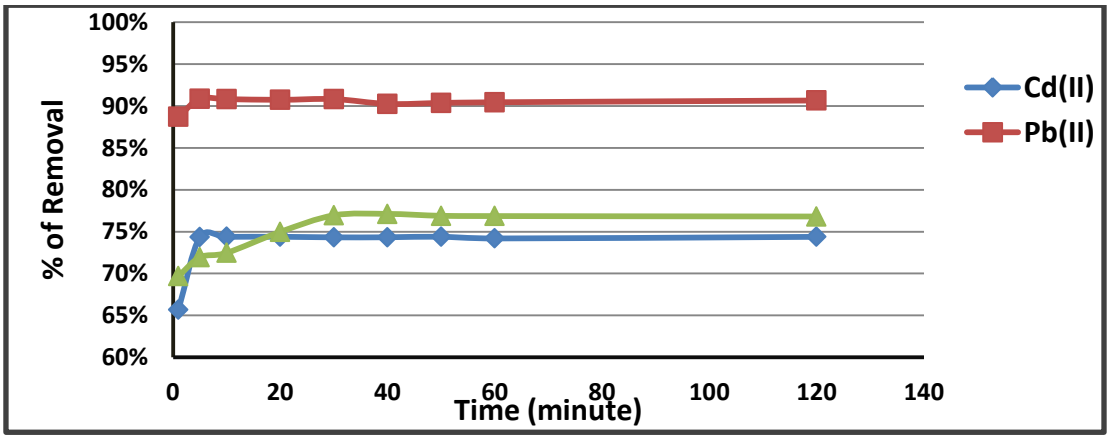

Figure 4.40: Effect of contact time on the adsorption of Cd(II), Pb(II) or Ni(II) on (Si-m-NO_2) (C_I = 10 ppm, adsorbent dose = 1 mg, volume of groundwater = 7 mL, pH = 6, temperature = 20 °C).

4.2.2.2.2 Effect of pH Value

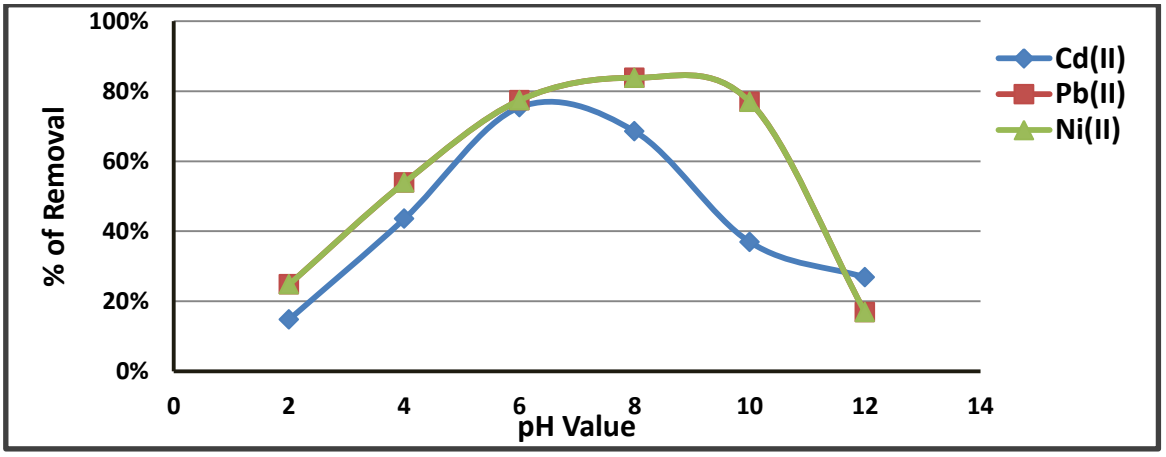

Figure 4.41: Effect of pH value on the adsorption of Cd(II), Pb(II) or Ni(II) on (Si-m-NO_2) (C_I = 10 ppm, adsorbent dose = 1 mg, volume of groundwater = 7 mL, temperature = 20 °C).

4.2.2.2.3 Effect of Temperature

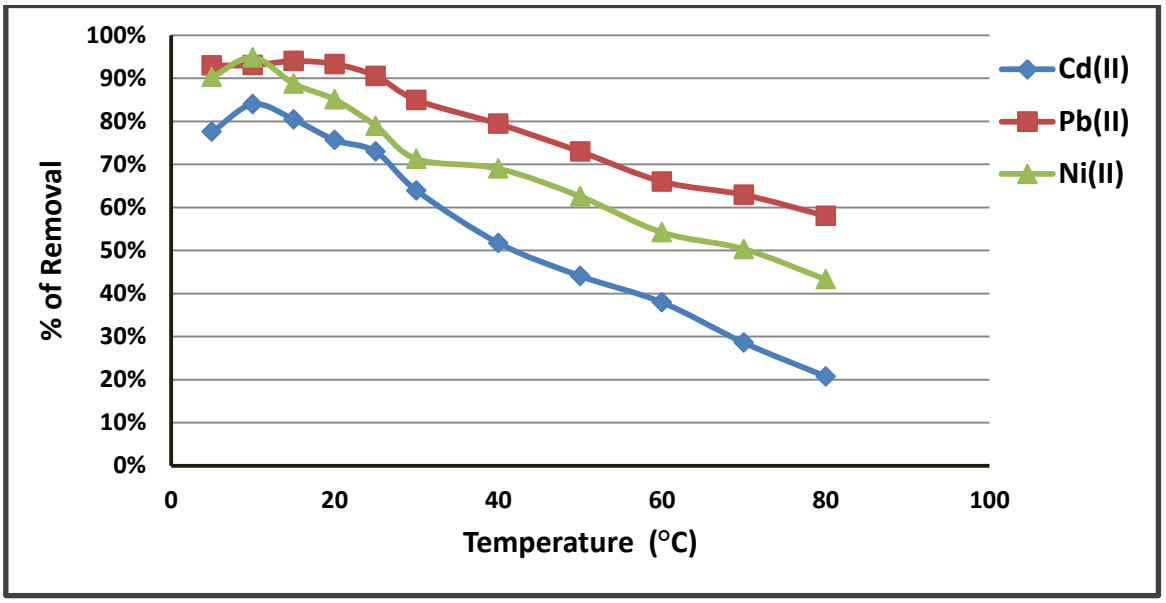

Figure 4.42: Effect of temperature on the adsorption of Cd(II), Pb(II) or Ni(II) on (Si-m-NO_2) (C_I = 10 ppm, adsorbent dose = 1 mg, volume of groundwater = 7 mL).

4.2.2.2.4 Effect of Adsorbent Dose

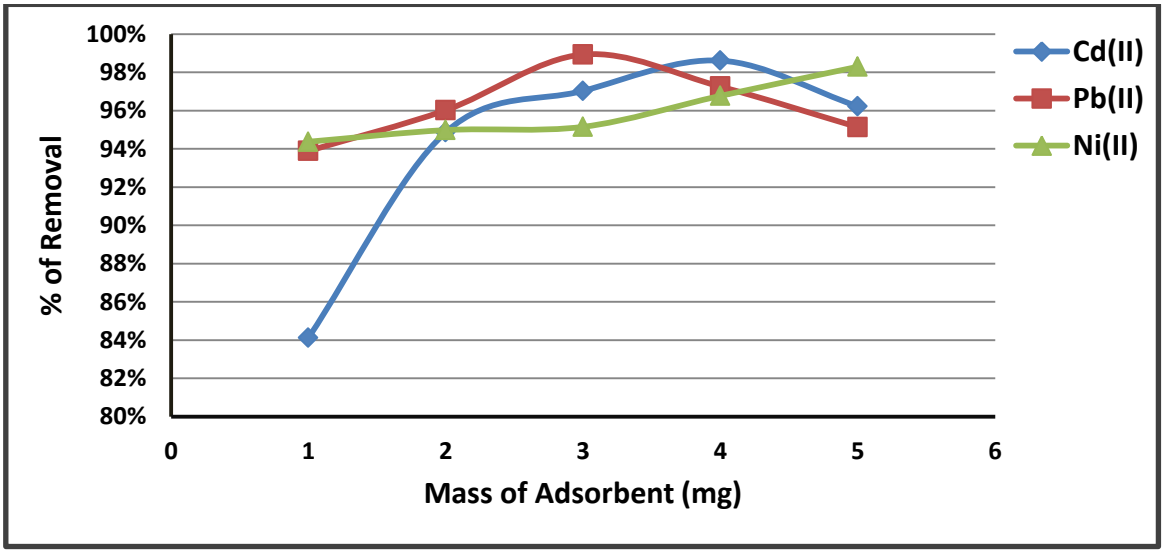

Figure 4.43: Effect of adsorbent dose on the adsorption of Cd(II), Pb(II) or Ni(II) on (Si-m-NO_2) (C_I = 10 ppm, volume of groundwater = 7 mL).

4.2.2.2.5 Effect of Adsorbate Concentration

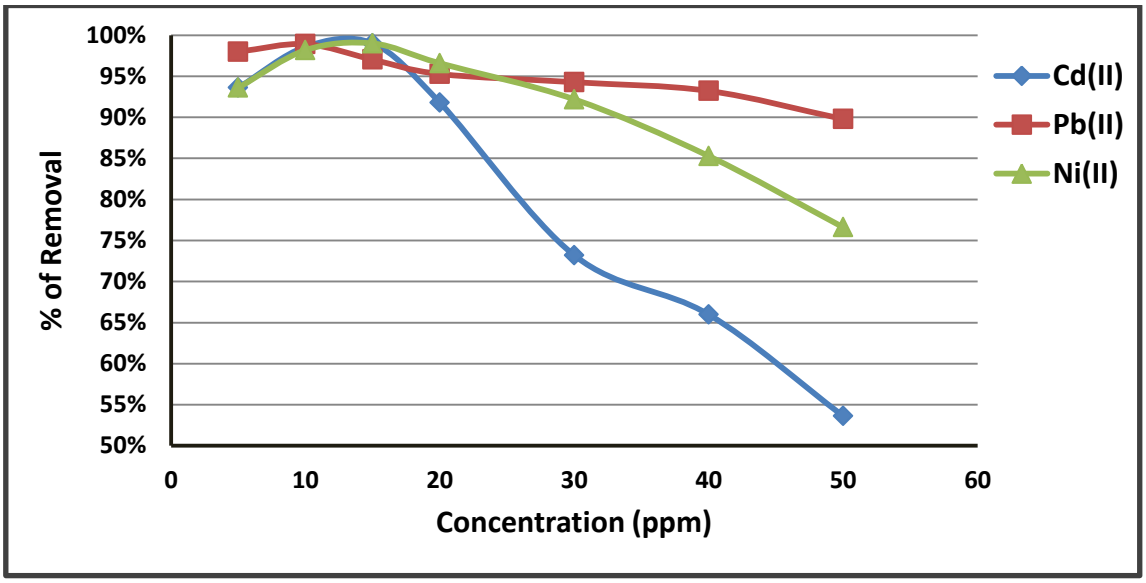

Figure 4.44: Effect of adsorbate concentration on the adsorption of Cd(II), Pb(II) or Ni(II) on (Si-m-NO_2) (volume of groundwater = 7 mL).

The following table shows the adsorption results for removing Cd(II), Pb(II) or Ni(II) from groundwater using (Si-m-NO_2) adsorbent.

Table 4.6: The adsorption results for removing Cd(II), Pb(II) or Ni(II) from groundwater using (Si-m-NO_2).

Adsorption on (Si-m-NO_2)			
Optimum Condition and % of Removal	Cd(II)	Pb(II)	Ni(II)
Contact Time (minute) % of Removal	10 74.38%	5 90.86%	20 76.95%
pH value % of Removal	6 75.39%	7 93.71%	7 83.80%
Temperature (°C) % of Removal	10 83.95%	15 93.98%	10 94.83%
Adsorbent Dose (mg) % of Removal	4 98.61%	3 98.93%	5 98.29%
Adsorbate Concentration(ppm) % of Removal	15 98.99%	10 98.91%	15 98.99%

4.2.2.3 Adsorption on (Si-p-NO_2)

The effect of solution conditions on the adsorption on (Si-p-NO_2) for the removal of cadmium, lead, or nickel metal ions was investigated, as shown in the following Figures (4.45-4.49).

4.2.2.3.1 Effect of Contact Time

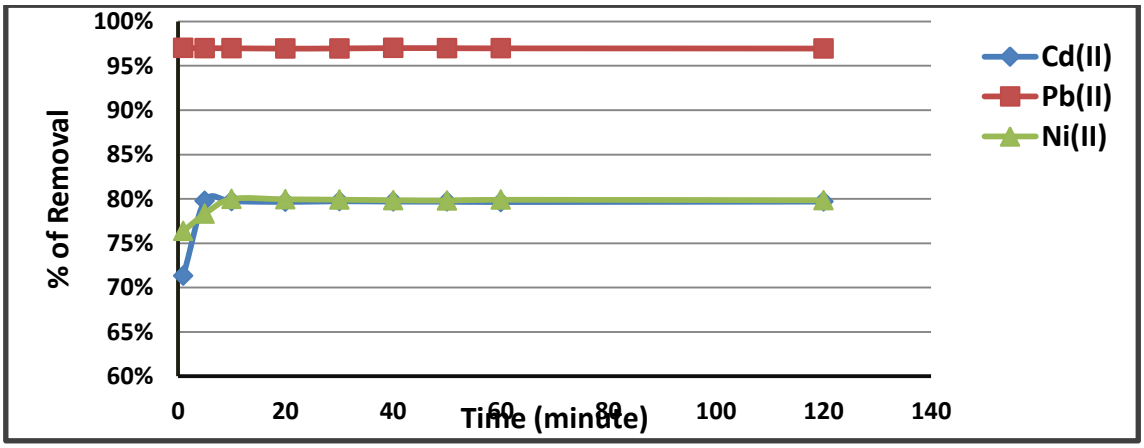

Figure 4.45: Effect of contact time on the adsorption of Cd(II), Pb(II) or Ni(II) on (Si-p-NO_2) (C_I = 10 ppm, adsorbent dose = 1 mg, volume of groundwater = 7 mL, pH = 6, temperature = 20 °C).

4.2.2.3.2 Effect of pH Value

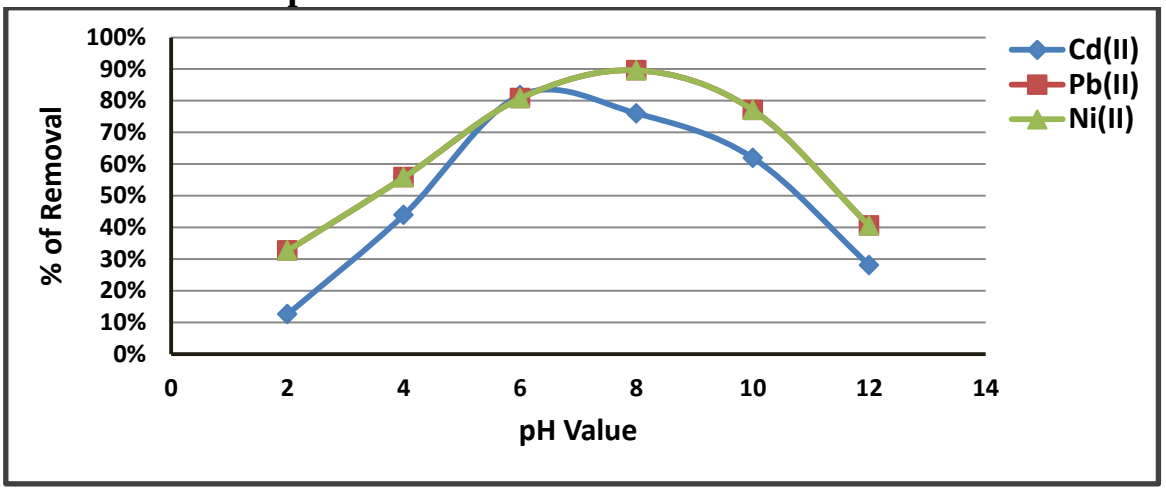

Figure 4.46: Effect of pH value on the adsorption of Cd(II), Pb(II) or Ni(II) on (Si-p-NO_2) (C_I = 10 ppm, adsorbent dose = 1 mg, volume of groundwater = 7 mL, temperature = 20 °C).

4.2.2.3.3 Effect of Temperature

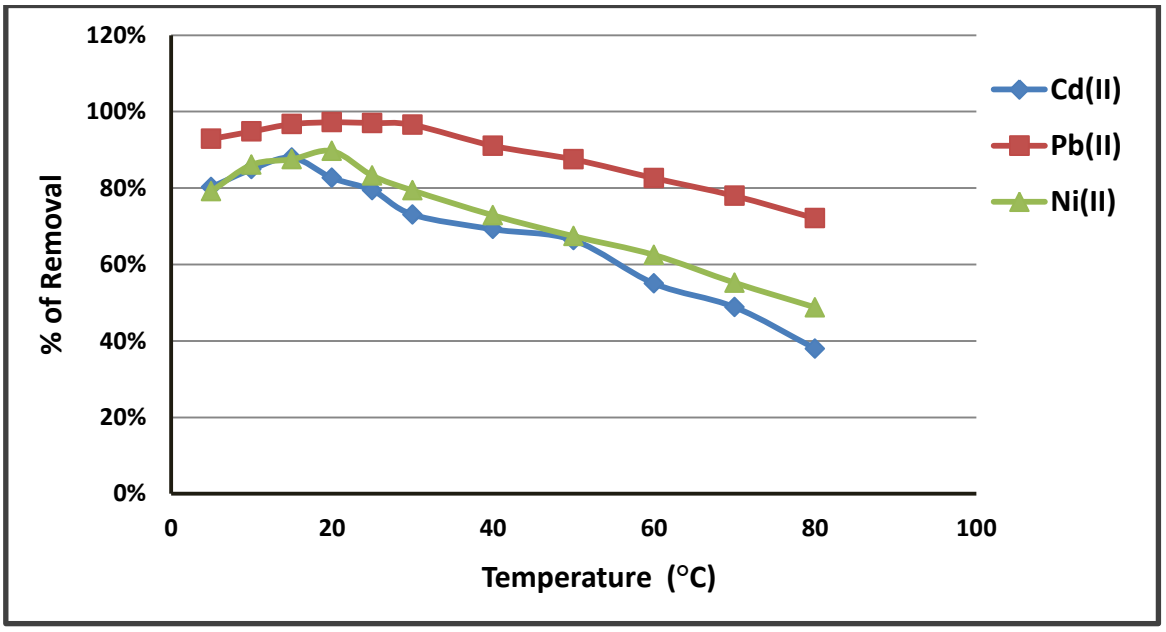

Figure 4.47: Effect of temperature on the adsorption of Cd(II), Pb(II) or Ni(II) on (Si-p-NO_2) (C_I = 10 ppm, adsorbent dose = 1 mg, volume of groundwater = 7 mL).

4.2.2.3.4 Effect of Adsorbent Dose

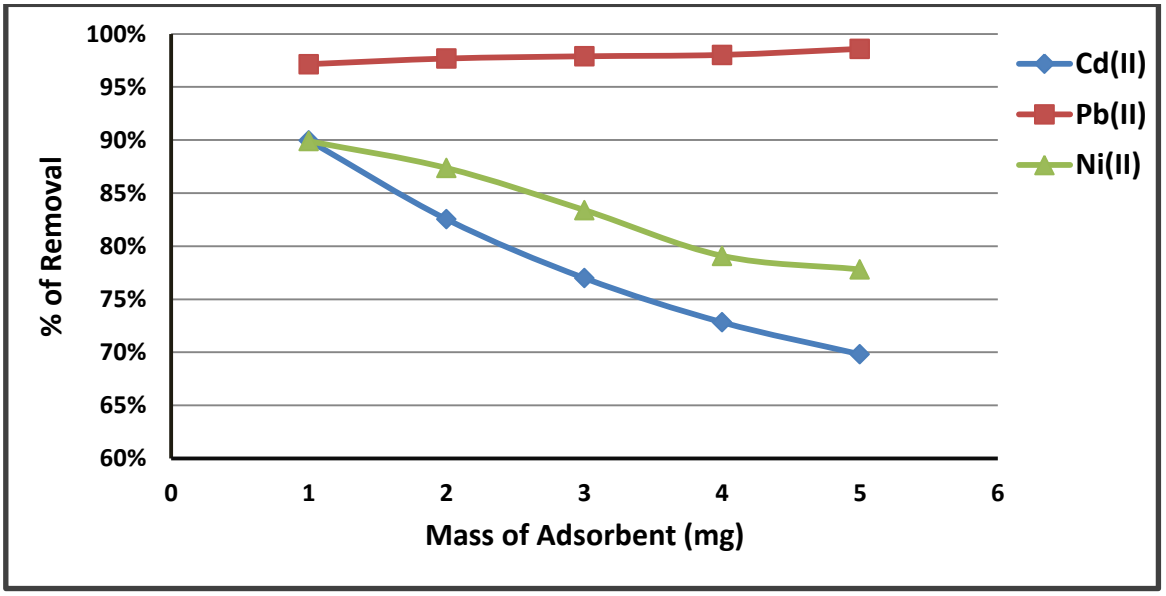

Figure 4.48: Effect of adsorbent dose on the adsorption of Cd(II), Pb(II) or Ni(II) on (Si-p-NO_2) (C_I = 10 ppm, volume of groundwater = 7 mL).

4.2.2.3.5 Effect of Adsorbate Concentration

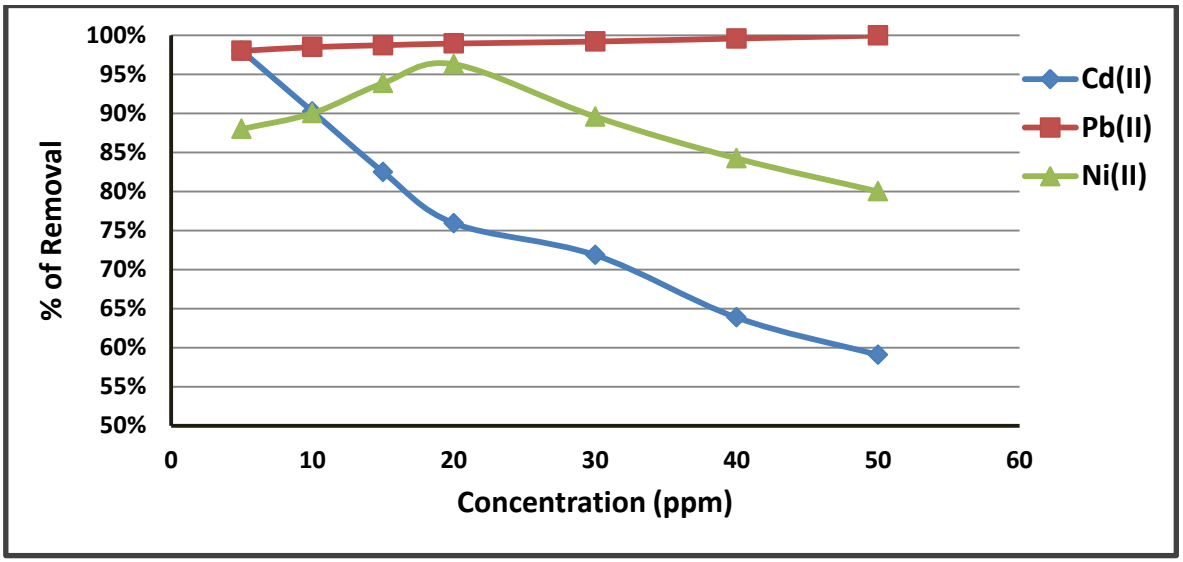

Figure 4.49: Effect of adsorbate concentration on the adsorption of Cd(II), Pb(II) or Ni(II) on (Si-p-NO_2) (volume of groundwater = 7 mL).

The following table shows the adsorption results for removing Cd(II), Pb(II) or Ni(II) from groundwater using (Si-p-NO_2).

Table 4.7: The adsorption results for removing Cd(II), Pb(II) or Ni(II) from groundwater using (Si-p-NO_2).

Adsorption on (Si-p-NO_2)			
Optimum Condition and % of Removal	Cd(II)	Pb(II)	Ni(II)
Contact Time (minute) % of Removal	5 79.77%	1 97.01%	10 79.99%
pH value % of Removal	7 81.72%	8 97.14%	8 89.59%
Temperature (°C) % of Removal	15 87.94%	20 97.19%	10 89.66%
Adsorbent Dose (mg) % of Removal	1 89.95%	5 98.93%	1 89.89%
Adsorbate Concentration(ppm) % of Removal	5 97.98%	50 99.95%	20 96.28%

The following table shows the adsorption results for the adsorption of Cd(II), Pb(II) or Ni(II) on (Si-o-NO_2), (Si-m-NO_2) or (Si-p-NO_2) adsorbent.

Table 4.8: Adsorption results for the adsorption of Cd(II), Pb(II) or Ni(II) on (Si-o-NO_2), (Si-m-NO_2) or (Si-p-NO_2).

Using the same adsorbate with different adsorbents	
Adsorption order for Cd(II)	(Si-m-NO_2) > (Si-p-NO_2) > (Si-o-NO_2)
Adsorption order for Pb(II)	(Si-p-NO_2) > (Si-o-NO_2) > (Si-m-NO_2)
Adsorption order for Ni(II)	(Si-m-NO_2) > (Si-p-NO_2) > (Si-o-NO_2)
Using the same adsorbent with different adsorbates	
Adsorption order for (Si-o-NO_2)	Pb(II) > Cd(II) > Ni(II)
Adsorption order for (Si-m-NO_2)	[Cd(II) , Ni(II)] > Pb(II)
Adsorption order for (Si-p-NO_2)	Pb(II) > Cd(II) > Ni(II)

4.3 Investigation of Adsorption Parameters

In order to investigate the adsorption efficiency for the adsorption of Cd(II), Pb(II) or Ni(II) onto each of the synthesized polymers. The effect of solution conditions on the adsorption process were studied. These conditions involve the effect of shaking time, pH value, temperature, adsorbent dose and the concentration of adsorbate.

The best equilibrium isotherm model for each adsorption process was investigated according to the value of the correlation coefficient of Langmuir and Freundlich models. The kinetics of adsorption were also investigated using pseudo first-order, pseudo second-order and intra-particle diffusion kinetic models. In addition, Van't Hoff plot for each adsorption process was investigated in order to determine the values of enthalpy change and entropy change, and hence determining if the

adsorption is spontaneous ($\Delta S > 0$) or not ($\Delta S < 0$), and if it is exothermic ($\Delta H < 0$) or endothermic one ($\Delta H > 0$).

Finally the effect of adsorbent recovery on the percent of heavy metal ion removal was investigated, and hence the adsorption process with the best regeneration is determined.

4.3.1 Using the Same Adsorbate with Different Adsorbents

4.3.1.1 Adsorption of Cadmium

4.3.1.1.1 Equilibrium Isotherm Models

In order to determine the best adsorption isotherm for the adsorption of cadmium ions onto ortho-, meta-, or para-nitrophenyl silicas, the observed data were fitted to Langmuir and Freundlich isotherms which describe the relationship between the amounts of Cd(II) adsorbed and its equilibrium concentration in solution. The adsorption parameters were investigated by plotting C_e/q_e versus C_e for Langmuir adsorption isotherm, and $\log q_e$ versus $\log C_e$ for Freundlich adsorption isotherm, as shown in Figures (4.50-4.55).

4.3.1.1.1.1 Langmuir Adsorption Isotherm

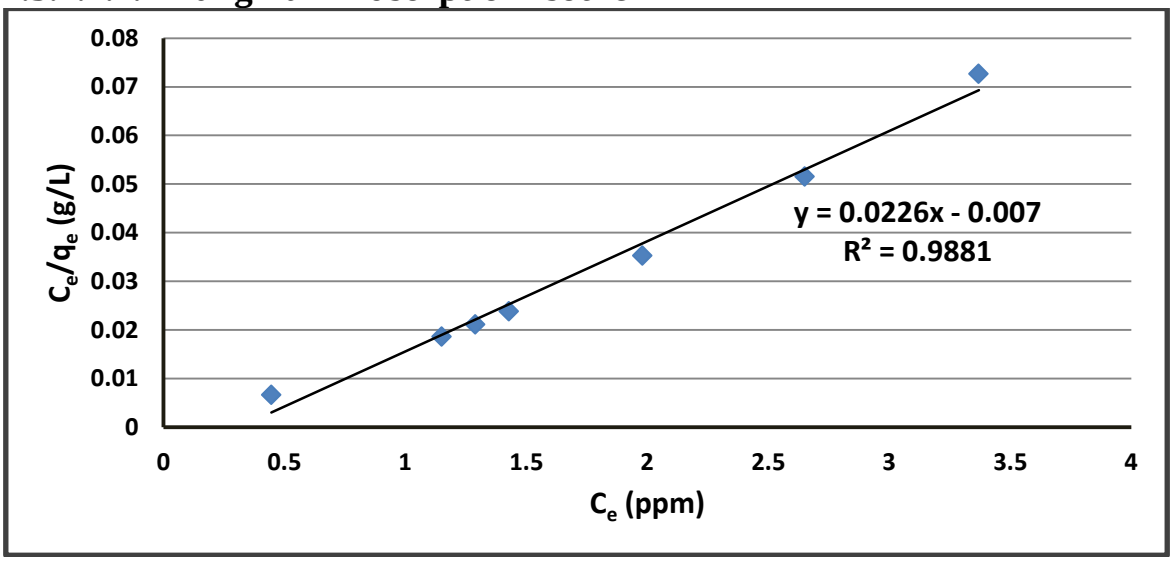

Figure 4.50: Langmuir plot for the adsorption of Cd(II) on (Si-o-NO_2) (time = 50 minute, pH = 5, temperature = 25 °C, adsorbent dose = 4 mg, volume = 7 mL).

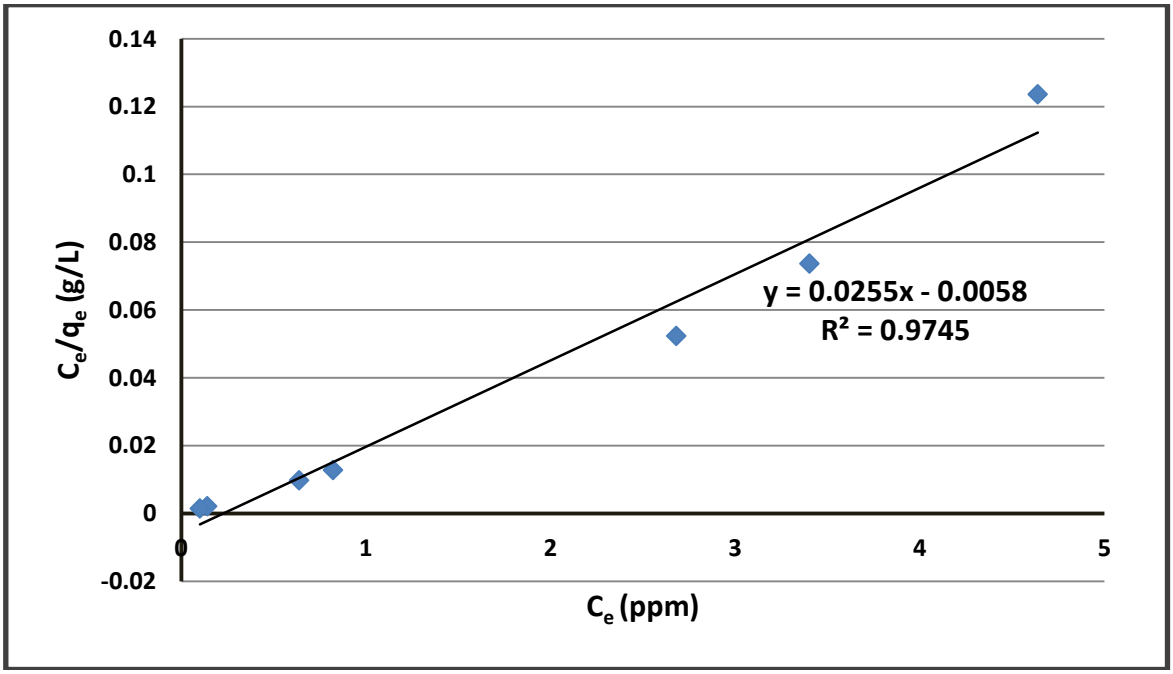

Figure 4.51: Langmuir plot for the adsorption of Cd(II) on (Si-m-NO_2) (time = 10 minute, pH = 6, temperature = 10 °C, adsorbent dose = 4 mg, volume = 7 mL).

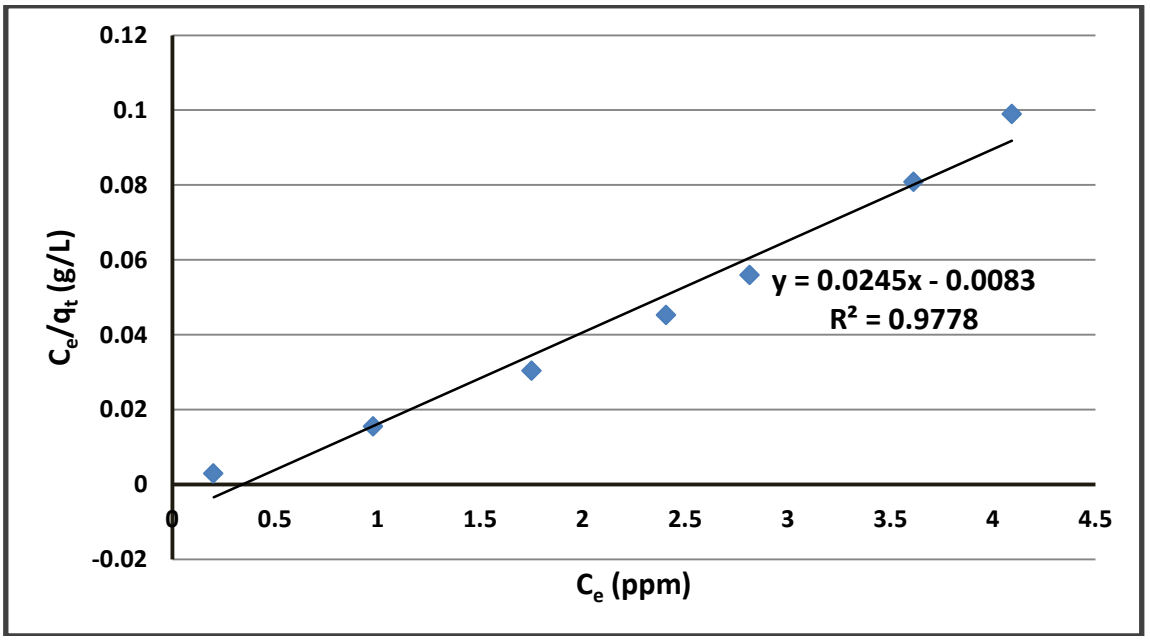

Figure 4.52: Langmuir plot for the adsorption of Cd(II) on (Si-p-NO_2) (time = 5 minute, pH = 7, temperature = 15 °C, adsorbent dose = 1 mg, volume = 7 mL).

4.3.1.1.1.2 Freundlich Adsorption Isotherm

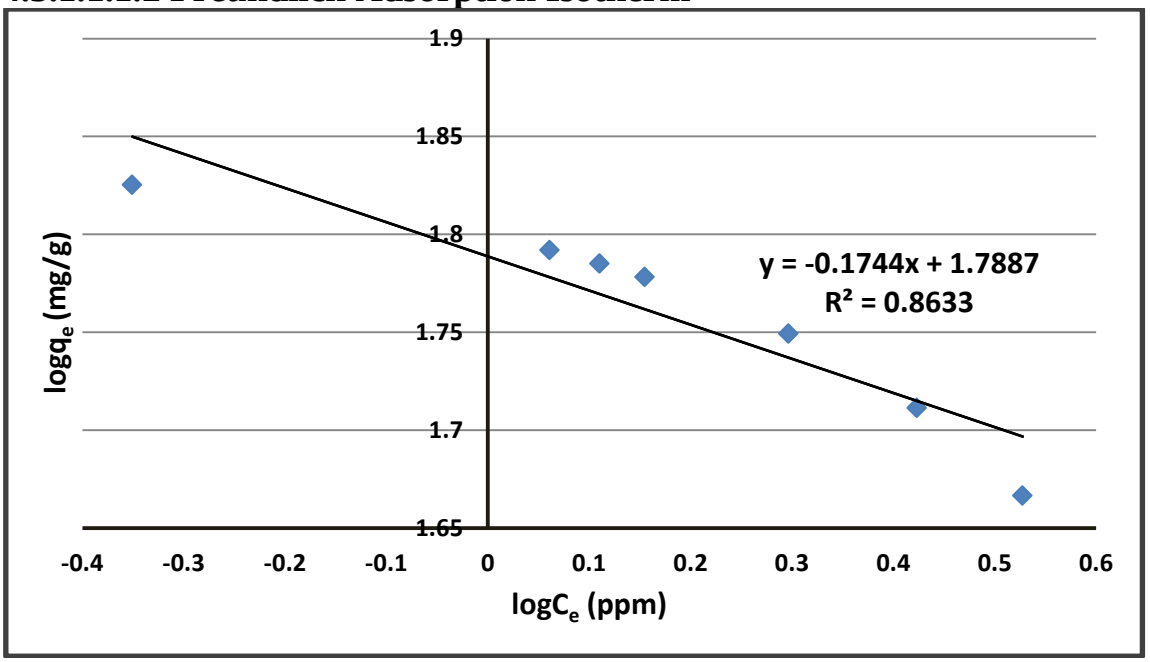

Figure 4.53: Freundlich plot for the adsorption of Cd(II) on (Si-o-NO_2) (time = 50 minute, pH = 5, temperature = 25 °C, adsorbent dose = 4 mg, volume = 7 mL).

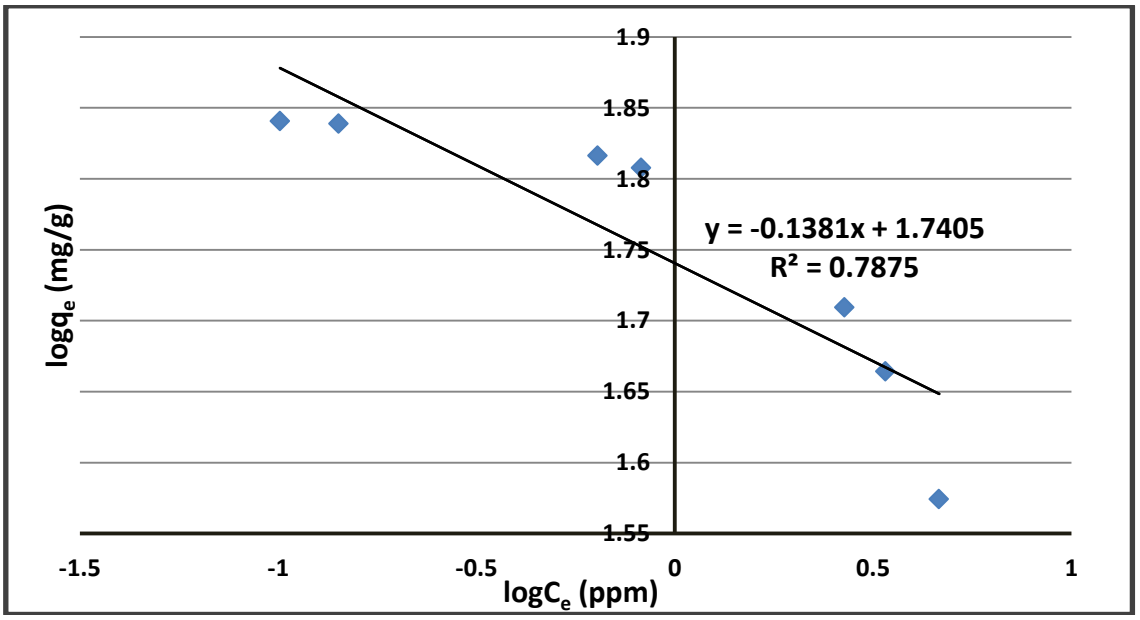

Figure 4.54: Freundlich plot for the adsorption of Cd(II) on (Si-m-NO_2) (time = 10 minute, pH = 6, temperature = 10 °C, adsorbent dose = 4 mg, volume = 7 mL).

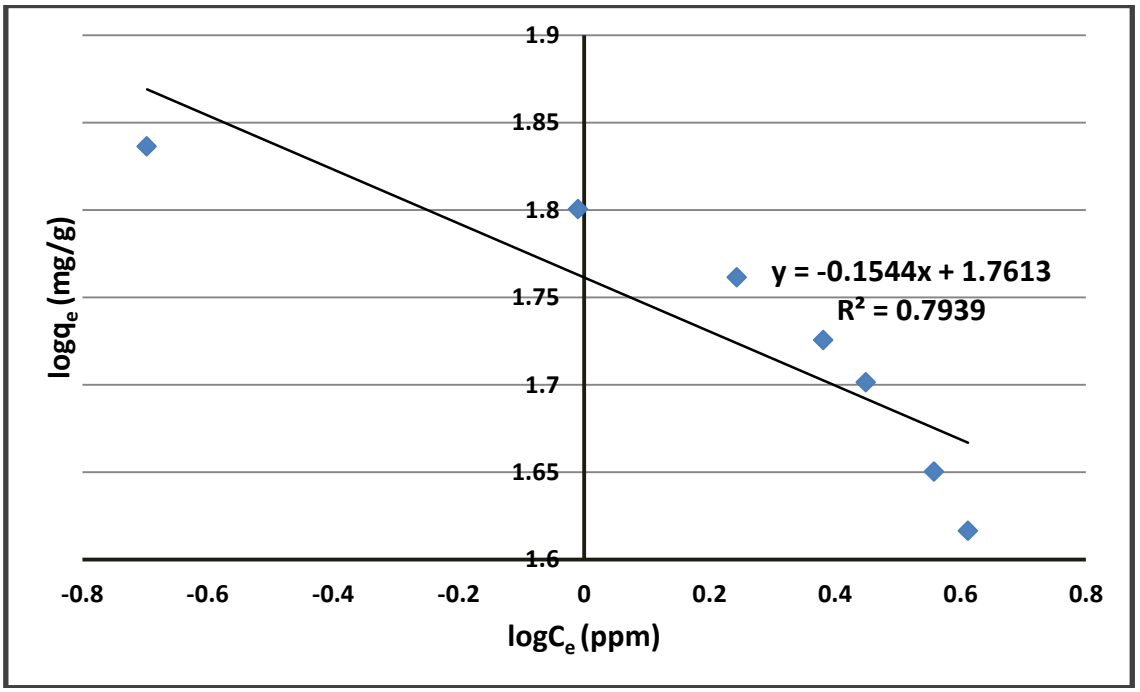

Figure 4.55: Freundlich plot for the adsorption of Cd(II) on (Si-p-NO_2) (time = 5 minute, pH = 7, temperature = 15 °C, adsorbent dose = 1 mg, volume = 7 mL).

As shown from the previous figures, the values of R^2 using Langmuir adsorption isotherm are approximately 1. This means that the adsorption of

Cd(II) on ortho-, meta, or para-nitrophenyl silicas is chemical adsorption and follows Langmuir equation. Hence, this is strong evidence on the presence of real chemical bonds between the adsorbate and the adsorbent.

The following table represents the values of Langmuir and Freundlich isotherm parameters for the adsorption of Cd(II) on (Si-o-NO_2), (Si-m-NO_2) and (Si-p-NO_2).

Table 4.9: The parameters of Langmuir and Freundlich isotherms for the adsorption of Cd(II) on (Si-o-NO_2), (Si-m-NO_2) and (Si-p-NO_2).

Adsorbents	Adsorption of Cd(II)			
	Equilibrium Isotherm Models			
	Langmuir Isotherm		Freundlich Isotherm	
	Q_o (mg/g)	b (L/mg)	K_F (mg/g)	n (g/L)
Si-o-NO_2	44.247	-3.228	61.475	-5.734
Si-m-NO_2	39.216	-4.396	55.017	-7.241
Si-p-NO_2	40.816	-2.952	57.716	-6.477

4.3.1.1.2 Adsorption Kinetic Models

The experimental kinetic data for Cd(II) adsorption on the prepared polymers are fitted with pseudo first-order, pseudo second-order and intra-particle diffusion kinetic models in order to investigate the mechanism of each adsorption process.

The kinetics parameters and correlation coefficients have been calculated from the linear plots of $\log(q_e - q_t)$ versus t for pseudo first order model, (t/q_t) versus t for pseudo second-order model, and q_t versus t for intra-particle diffusion kinetic model, as shown in the following Figures (4.56-4.64).

4.3.1.1.2.1 Pseudo First-Order Kinetics

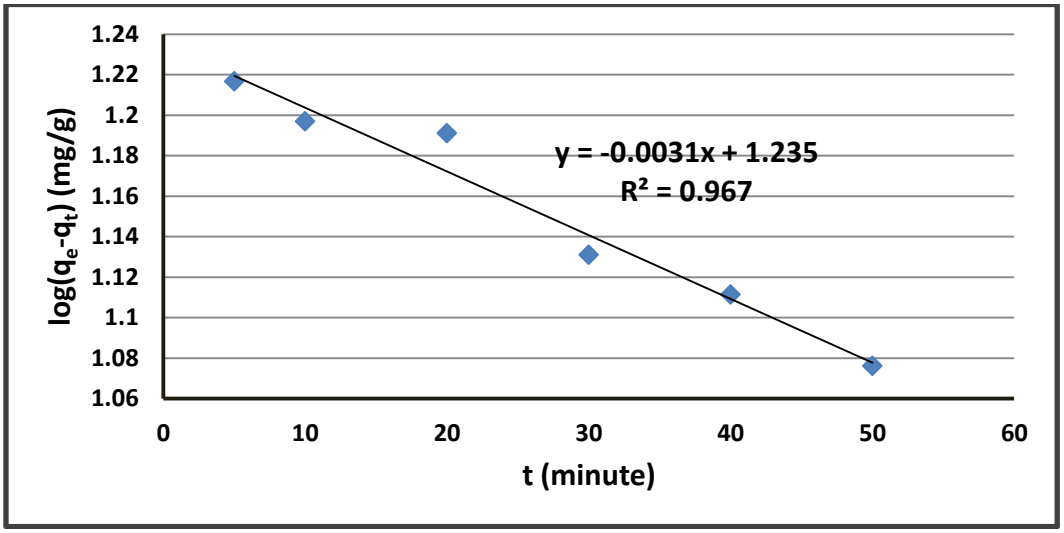

Figure 4.56: Pseudo first-order kinetic model for the adsorption of Cd(II) on (Si-o-NO_2) (C_I = 10 ppm, pH = 6, temperature = 20 °C, adsorbent dose = 1 mg, volume = 7 mL).

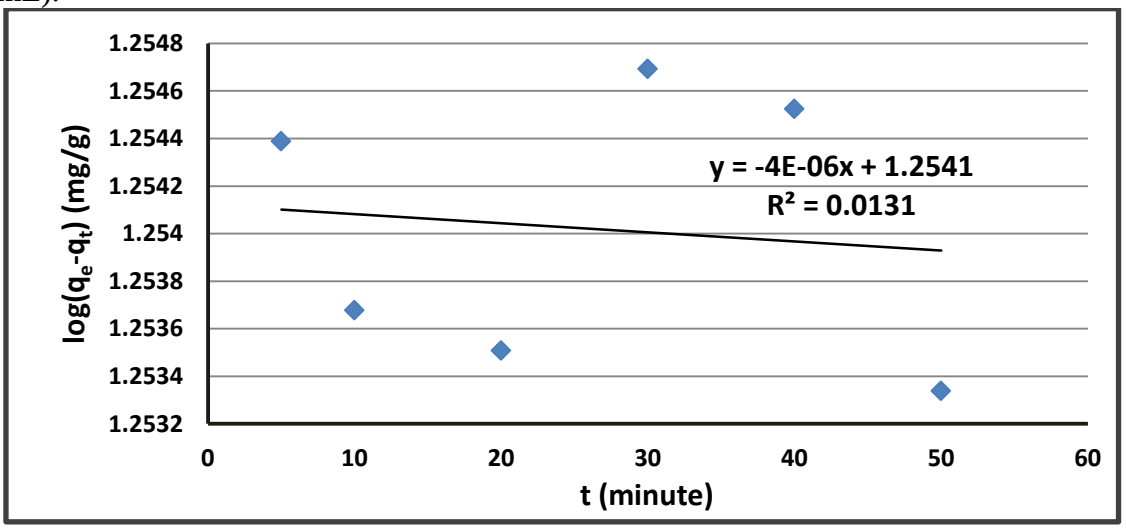

Figure 4.57: Pseudo first-order kinetic model for the adsorption of Cd(II) on (Si-m-NO_2) (C_I = 10 ppm, pH = 6, temperature = 20 °C, adsorbent dose = 1 mg, volume = 7 mL).

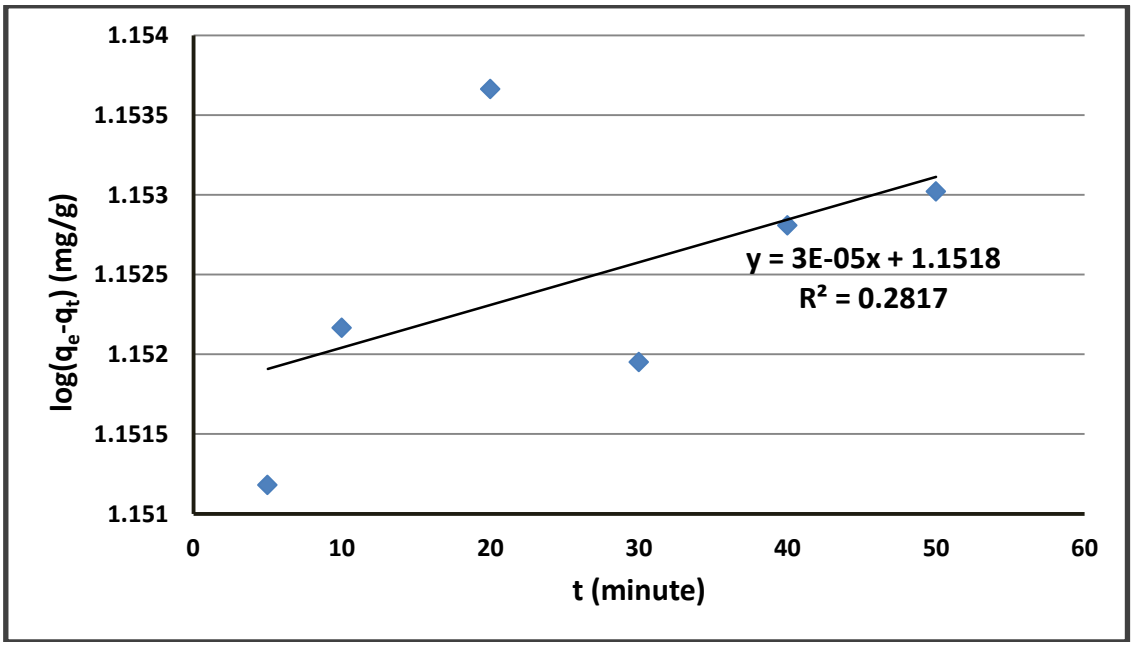

Figure 4.58: Pseudo first-order kinetic model for the adsorption of Cd(II) on (Si-p-NO_2) (C_I = 10 ppm, pH = 6, temperature = 20 °C, adsorbent dose = 1 mg, volume = 7 mL).

4.3.1.1.2.2 Pseudo Second-Order Kinetics

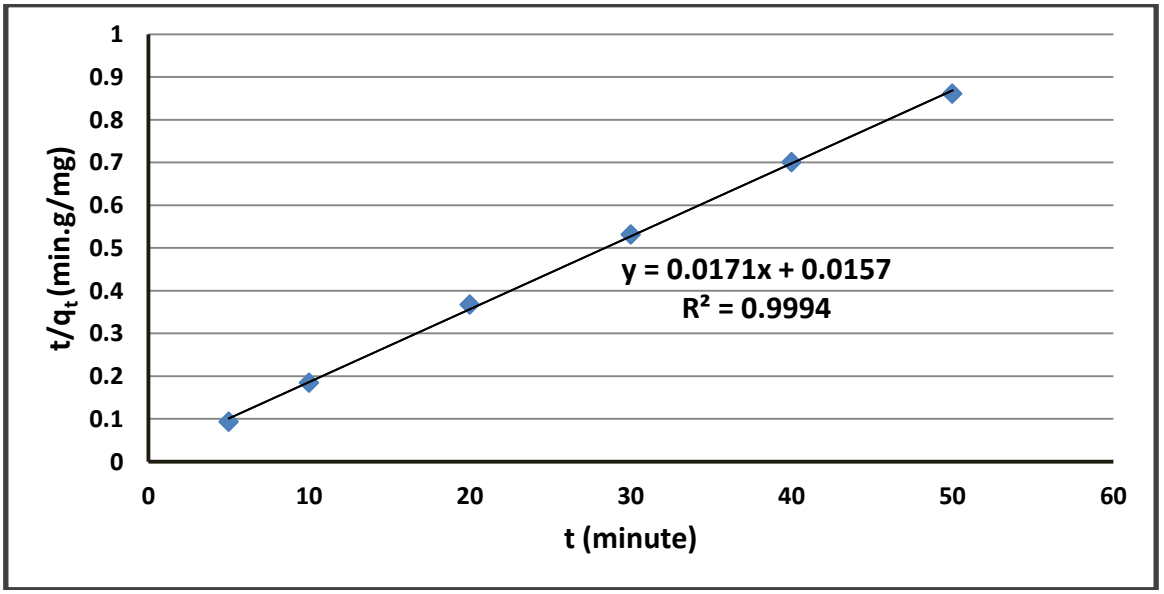

Figure 4.59: Pseudo second-order kinetic model for the adsorption of Cd(II) on (Si-o-NO_2) (C_I = 10 ppm, pH = 6, temperature = 20 °C, adsorbent dose = 1 mg, volume = 7 mL).

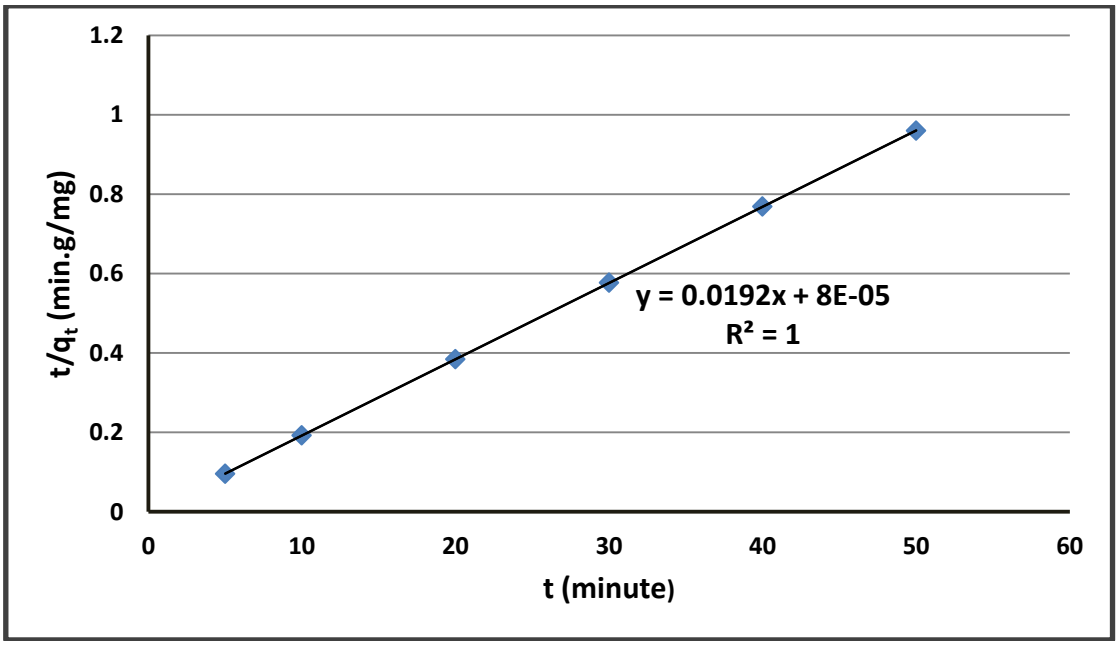

Figure 4.60: Pseudo second-order kinetic model for the adsorption of Cd(II) on (Si-m-NO_2) (C_I = 10 ppm, pH = 6, temperature = 20 °C, adsorbent dose = 1 mg, volume = 7 mL).

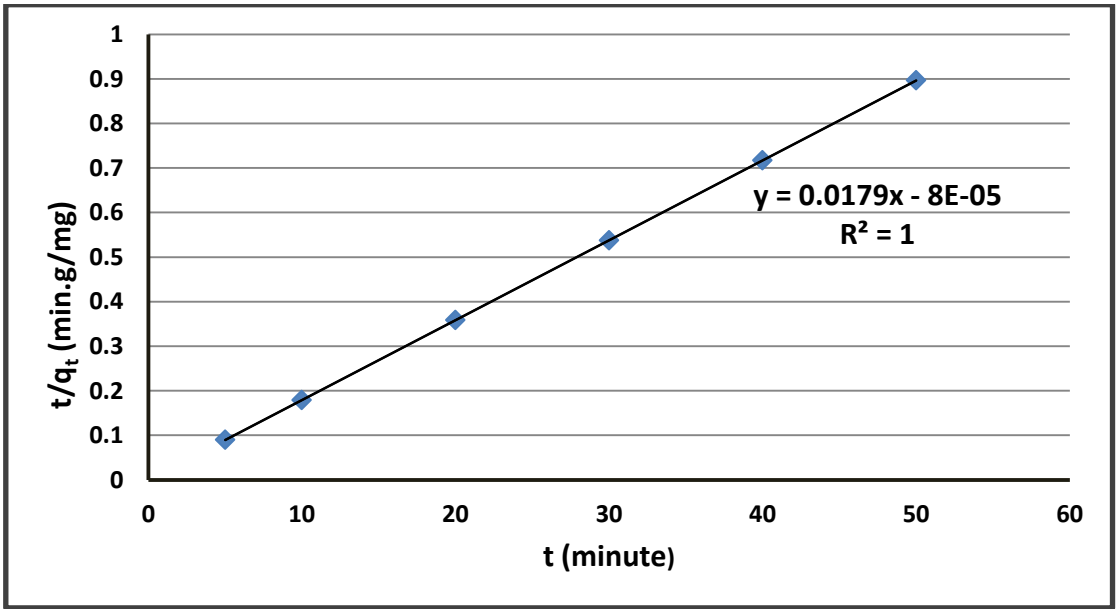

Figure 4.61: Pseudo second-order kinetic model for the adsorption of Cd(II) on (Si-p-NO_2) (C_I = 10 ppm, pH = 6, temperature = 20 °C, adsorbent dose = 1 mg, volume = 7 mL).

4.3.1.1.2.3 Intra-Particle Diffusion Kinetic Model

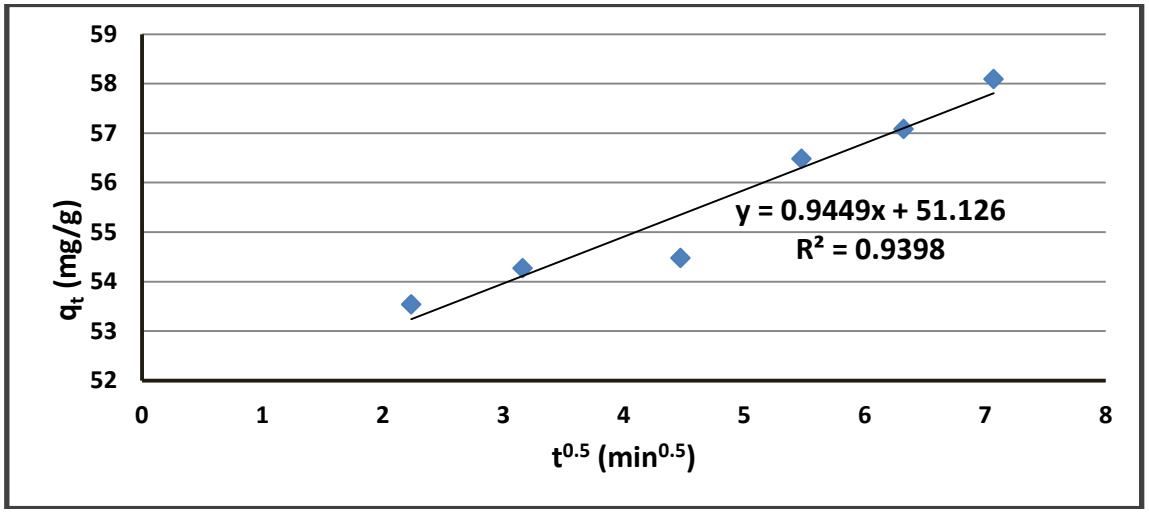

Figure 4.62: Intra-particle diffusion kinetic model for the adsorption of Cd(II) on (Si-o-NO_2) (C_I = 10 ppm, pH = 6, temperature = 20 °C, adsorbent dose = 1 mg, volume = 7 mL).

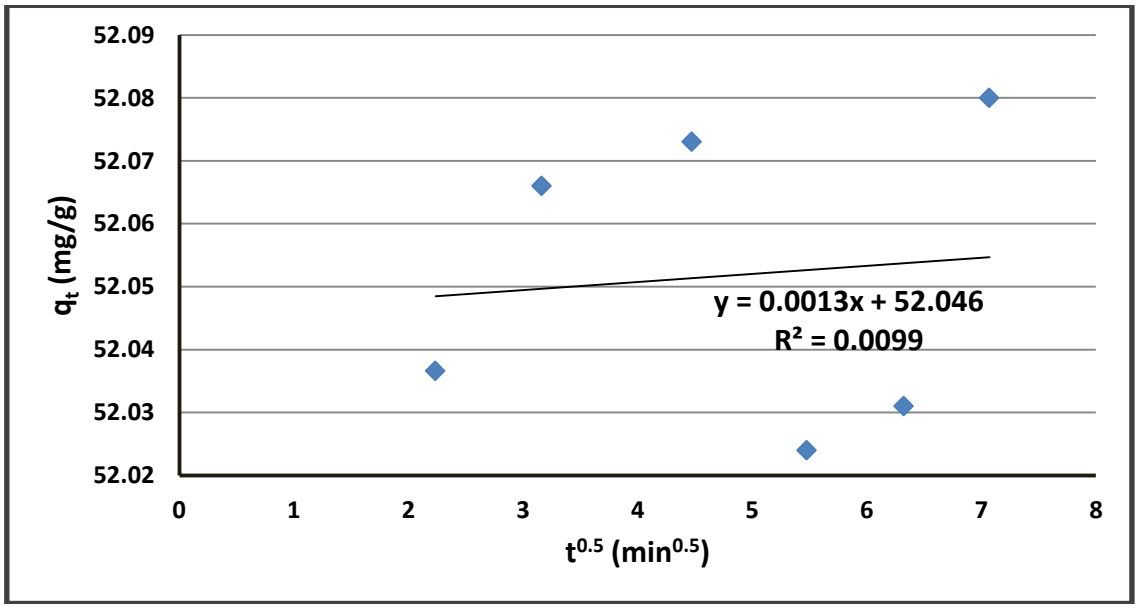

Figure 4.63: Intra-particle diffusion kinetic model for the adsorption of Cd(II) on (Si-m-NO_2) (C_I = 10 ppm, pH = 6, temperature = 20 °C, adsorbent dose = 1 mg, volume = 7 mL).

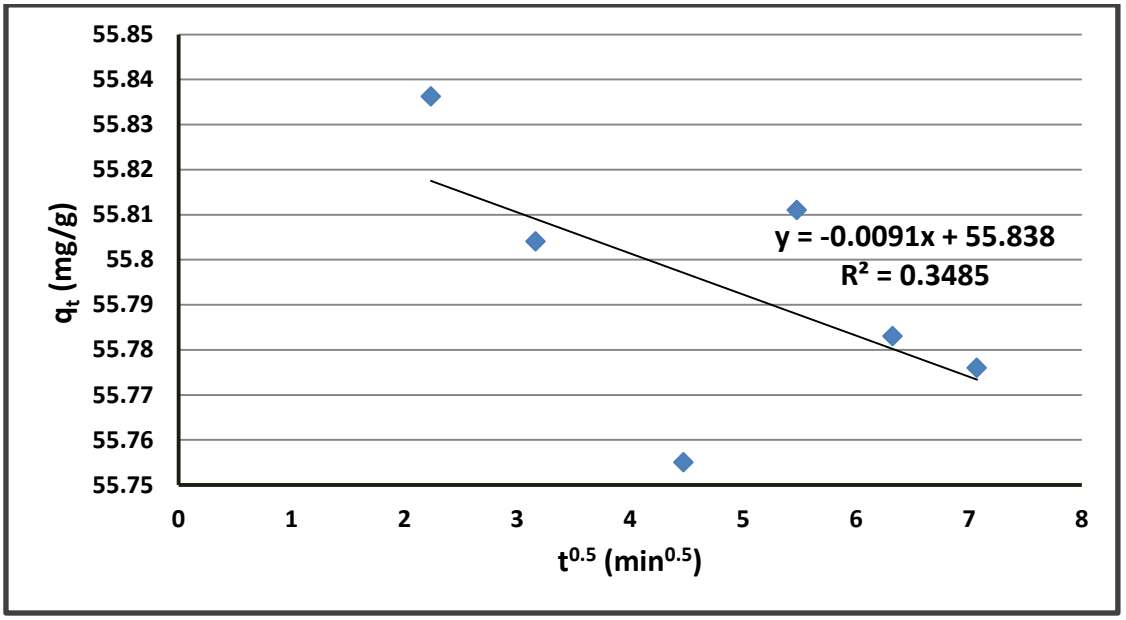

Figure 4.64: Intra-particle diffusion kinetic model for the adsorption of Cd(II) on (Si-p-NO_2) (C_I = 10 ppm, pH = 6, temperature = 20 °C, adsorbent dose = 1 mg, volume = 7 mL).

According to the values for the correlation coefficient using the previous kinetic models. It is showed the adsorption of Cd(II) on (Si-o-NO_2), (Si-m-NO_2) or (Si-p-NO_2) followed the mechanism of pseudo second-order kinetic model. Such that, the values of R^2 in this kinetic model are approximately one.

The following table shows the kinetic parameters of pseudo first-order, pseudo second-order and intra-particle diffusion kinetic models for the adsorption of Cd(II) on (Si-o-NO_2), (Si-m-NO_2) and (Si-p-NO_2).

Table 4.10: The parameters of pseudo first-order, pseudo second-order and intra-particle diffusion kinetic models for the adsorption of Cd(II) on (Si-o-NO_2), (Si-m-NO_2) and (Si-p-NO_2).

Adsorbents	Adsorption of Cd(II)					
	Adsorption Kinetic Models					
	Pseudo First-Order Kinetics		Pseudo Second-Order Kinetics		Intra-Particle Diffusion Kinetics	
	q_e (mg/g)	K_1 ($mg.g^{-1}.min^{-1}$)	q_e (mg/g)	K_2 ($g.mg^{-1}.min^{-1}$)	C (mg/g)	K_p ($mg.g^{-1}.min^{-0.5}$)
Si-o-NO_2	17.179	$7.149*10^{-3}$	58.479	0.0186	51.126	0.945
Si-m-NO_2	17.952	-	52.083	-	52.046	0.0013
Si-p-NO_2	14.184	-	55.866	-	55.838	-0.0091

Comparing the value of q_e (experimentally) for all adsorption processes that equals 70, with the values of q_e (calculated) in pseudo first-order and pseudo second-order kinetic adsorption models, we conclude that the experimental values for all adsorptions are closer to the values of q_e (calculated) in pseudo second-order adsorption model. Hence, proving that this model represents the mechanism of the adsorption.

4.3.1.1.3 Adsorption Thermodynamics

By using the thermodynamic equation of Van't Hoff plot. The thermodynamic parameters (ΔH and ΔS) for the adsorption of cadmium ions on (Si-o-NO_2), (Si-m-NO_2) or (Si-p-NO_2) can be calculated from the slope and y-intercept of the graph of In K_d versus (1/T), as shown in

the following Figures (4.65-4.67).

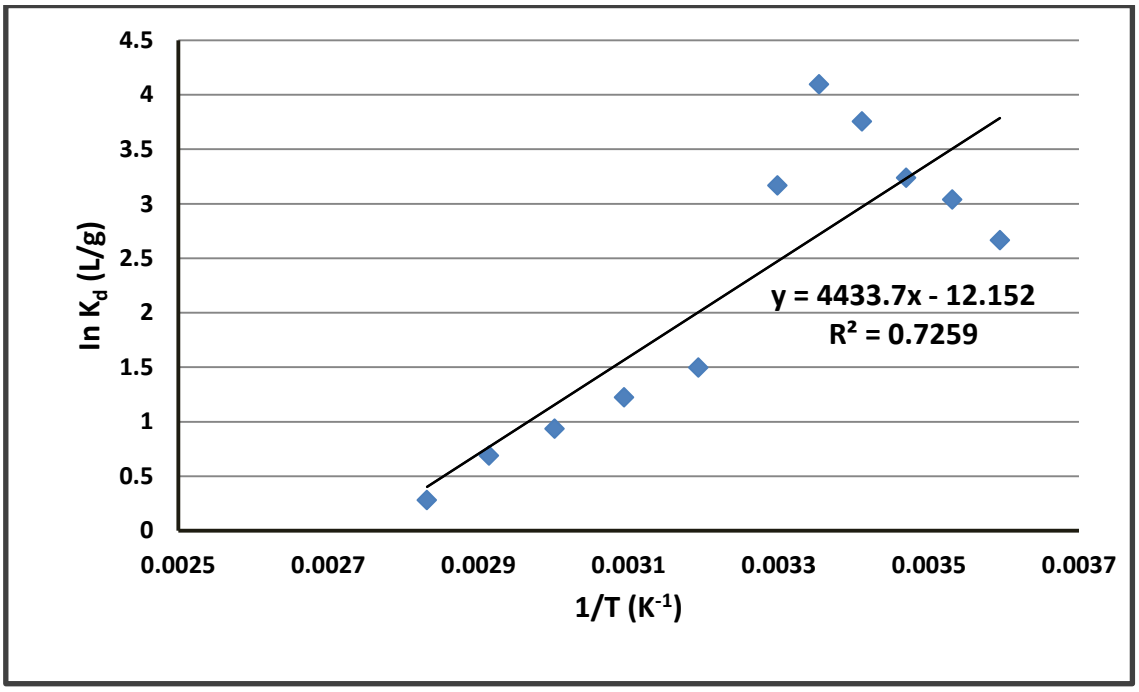

Figure 4.65: Van't Hoff plot for the adsorption of Cd(II) on (Si-o-NO_2) (time = 50 minute, C_I = 10 ppm, pH = 5, adsorbent dose = 1 mg, volume = 7 mL).

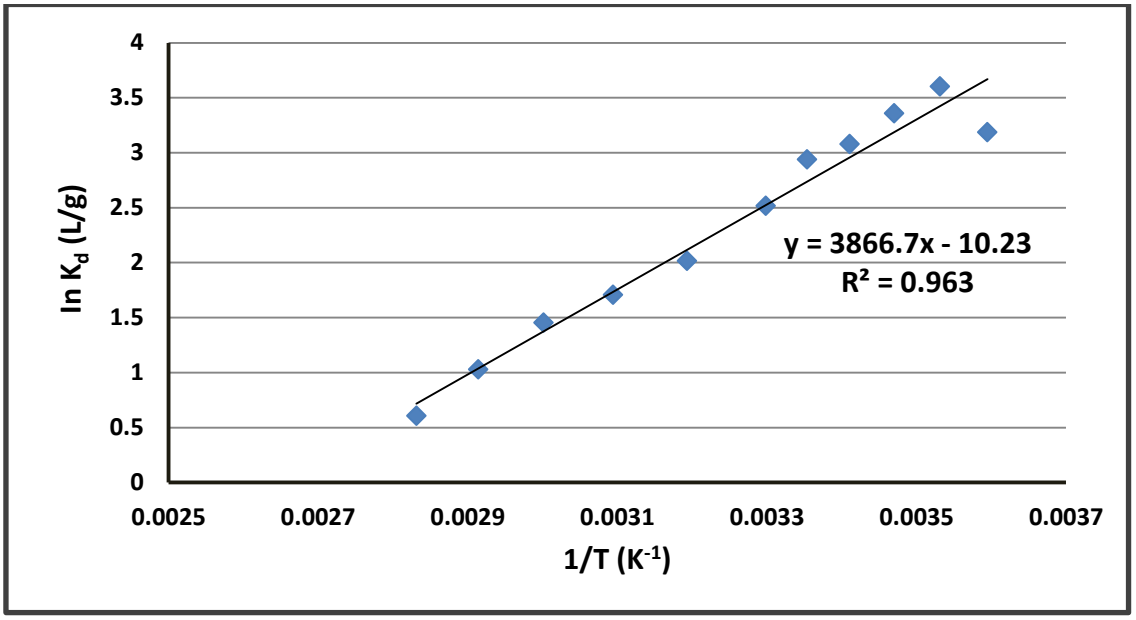

Figure 4.66: Van't Hoff plot for the adsorption of Cd(II) on (Si-m-NO_2) (time = 10 minute, C_I = 10 ppm, pH = 6, adsorbent dose = 1 mg, volume = 7 mL).

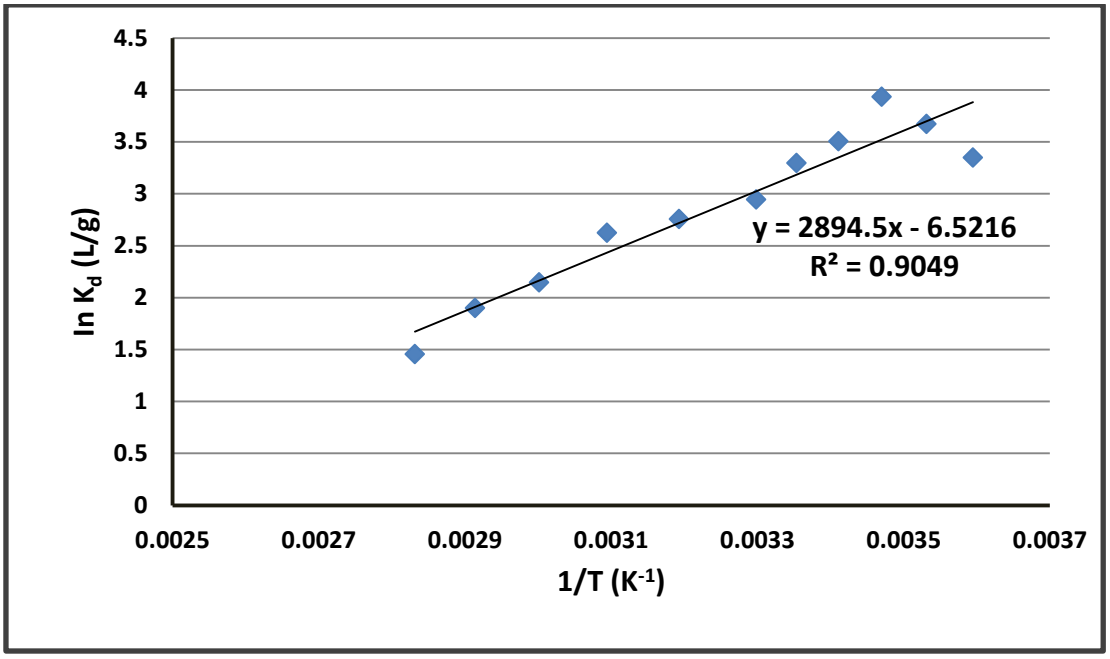

Figure 4.67: Van't Hoff plot for the adsorption of Cd(II) on (Si-p-NO_2) (time = 5 minute, C_I = 10 ppm, pH = 7, adsorbent dose = 1 mg, volume = 7 mL).

The following table represents the values of the thermodynamic parameters (ΔS and ΔH) for the adsorption of Cd(II) on ortho-, meta-, or para-nitrophenyl silicas.

Table 4.11: The thermodynamic parameters for the adsorption of Cd(II) on (Si-o-NO_2), (Si-m-NO_2) and (Si-p-NO_2).

Adsorbents	Adsorption of Cd(II)	
	Adsorption Thermodynamics	
	ΔH (kJ)	ΔS (J/K)
Si-o-NO_2	36.861	-101.032
Si-m-NO_2	32.148	-85.052
Si-p-NO_2	24.065	-54.221

As shown in this table, the adsorption of Cd(II) on (Si-o-NO_2), (Si-m-NO_2) or (Si-p-NO_2) adsorbent is endothermic process (ΔH > 0) and non spontaneous (ΔS < 0).

4.3.1.2 Adsorption of Lead

4.3.1.2.1 Equilibrium Isotherm Models

In order to determine the best adsorption isotherm for the adsorption of lead ions onto ortho-, meta-, or para-nitrophenyl silicas, the observed data were fitted to Langmuir and Freundlich isotherms which describe the relationship between the amounts of Pb(II) adsorbed and its equilibrium concentration in solution. The adsorption parameters were investigated by plotting C_e/q_e versus C_e for Langmuir adsorption isotherm, and $logq_e$ versus $logC_e$ for Freundlich adsorption isotherm, as shown in the following Figures (4.68-4.73).

4.3.1.2 .1.1 Langmuir Adsorption Isotherm

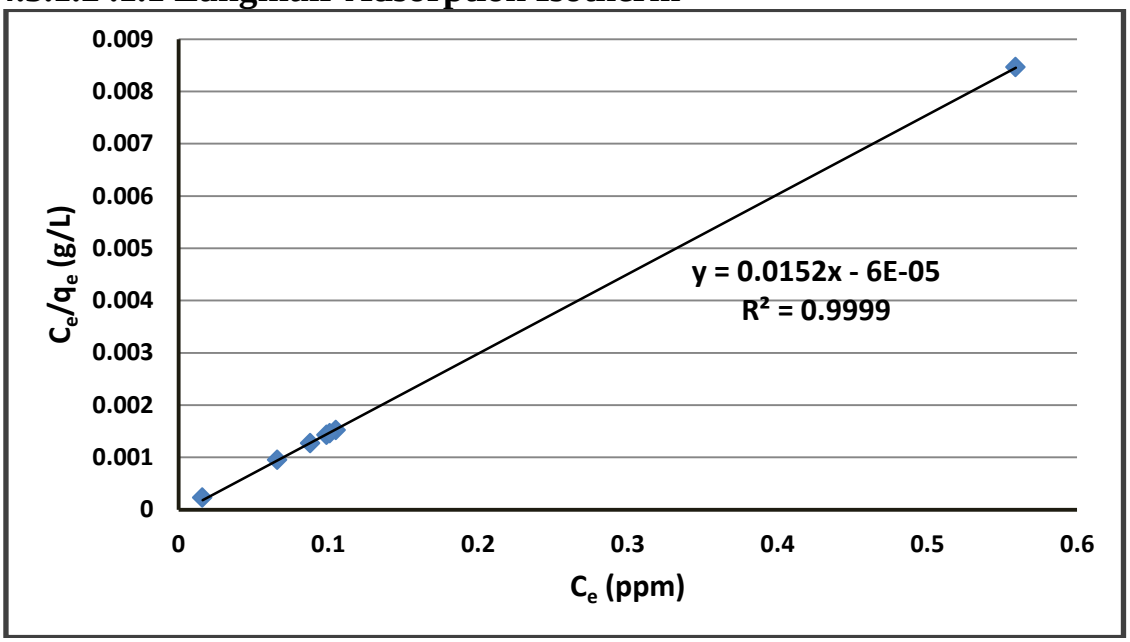

Figure 4.68: Langmuir plot for the adsorption of Pb(II) on (Si-o-NO_2) (time = 30 minute, pH = 8, temperature = 10 °C, adsorbent dose = 5 mg, volume = 7 mL).

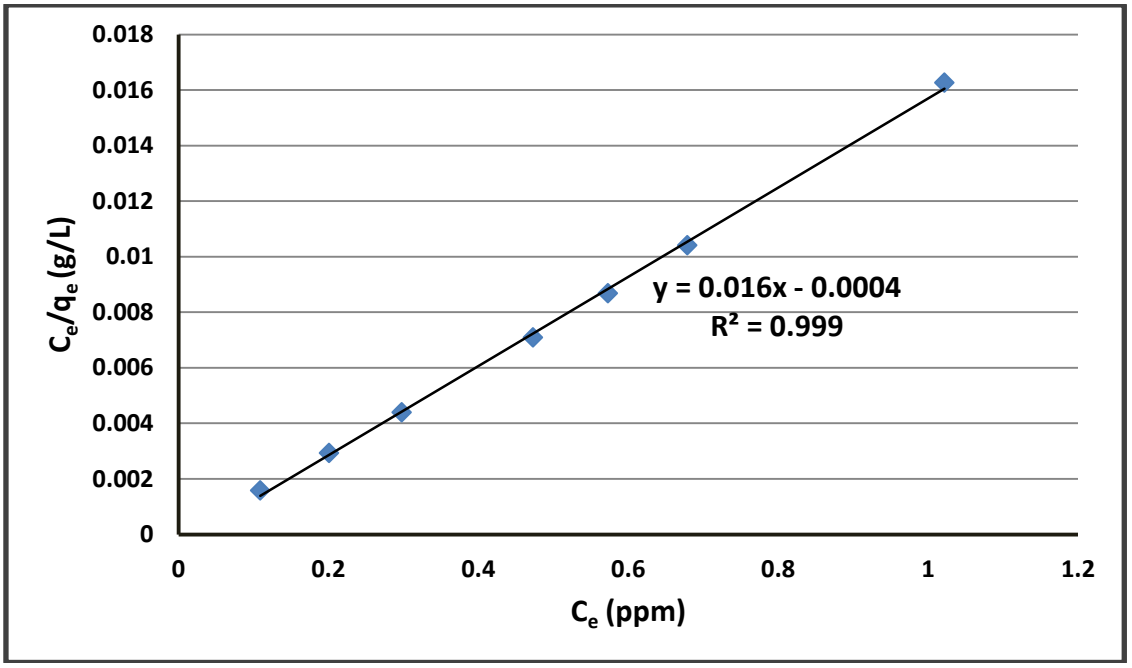

Figure 4.69: Langmuir plot for the adsorption of Pb(II) on (Si-m-NO_2) (time = 5 minute, pH = 7, temperature = 15 °C, adsorbent dose = 3 mg, volume = 7 mL).

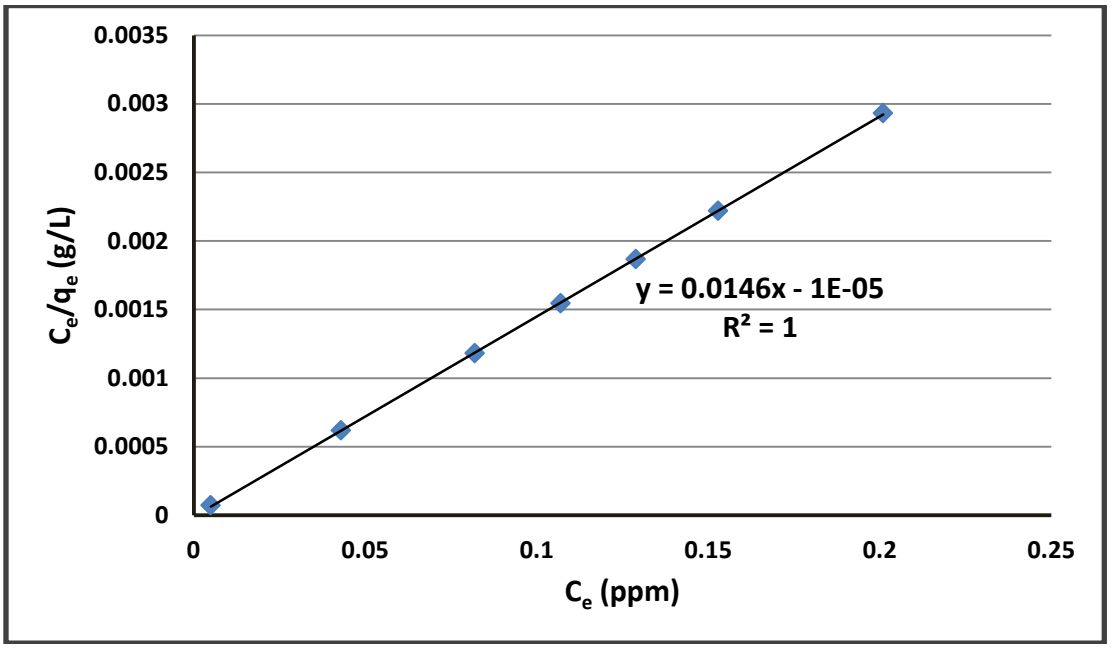

Figure 4.70: Langmuir plot for the adsorption of Pb(II) on (Si-p-NO_2) (time = 1 minute, pH = 8, temperature = 20 °C, adsorbent dose = 5 mg, volume = 7 mL).

4.3.1.2.1.2 Freundlich Adsorption Isotherm

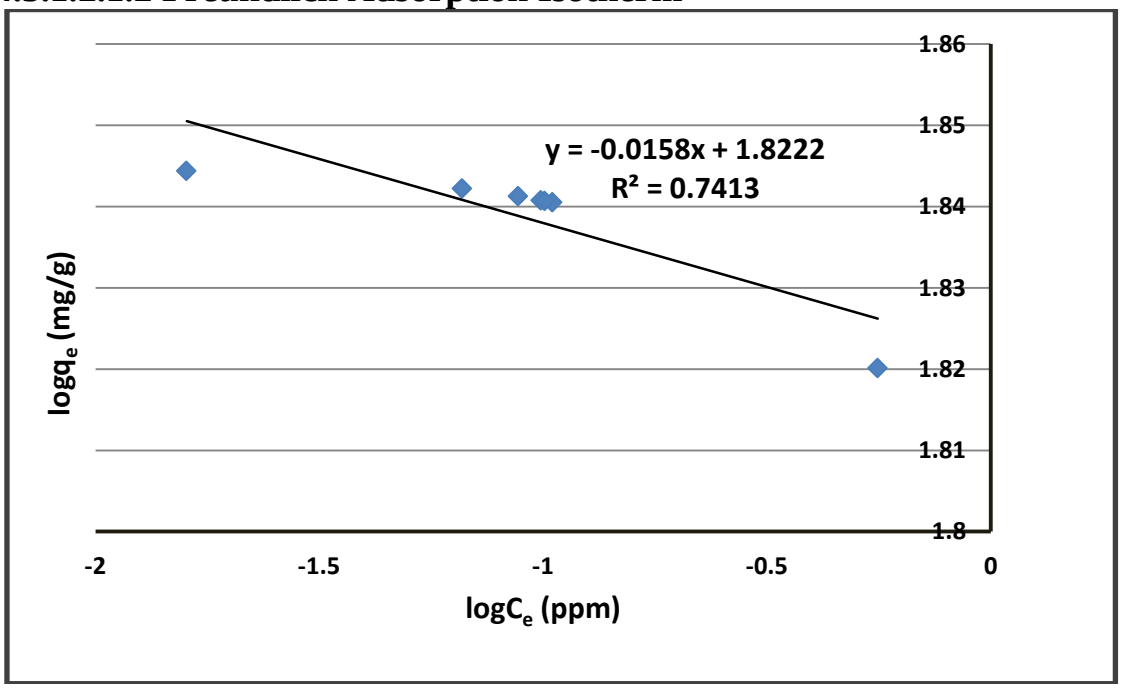

Figure 4.71: Freundlich plot for the adsorption of Pb(II) on (Si-o-NO_2) (time = 30 minute, pH = 8, temperature = 10 °C, adsorbent dose = 5 mg, volume = 7 mL).

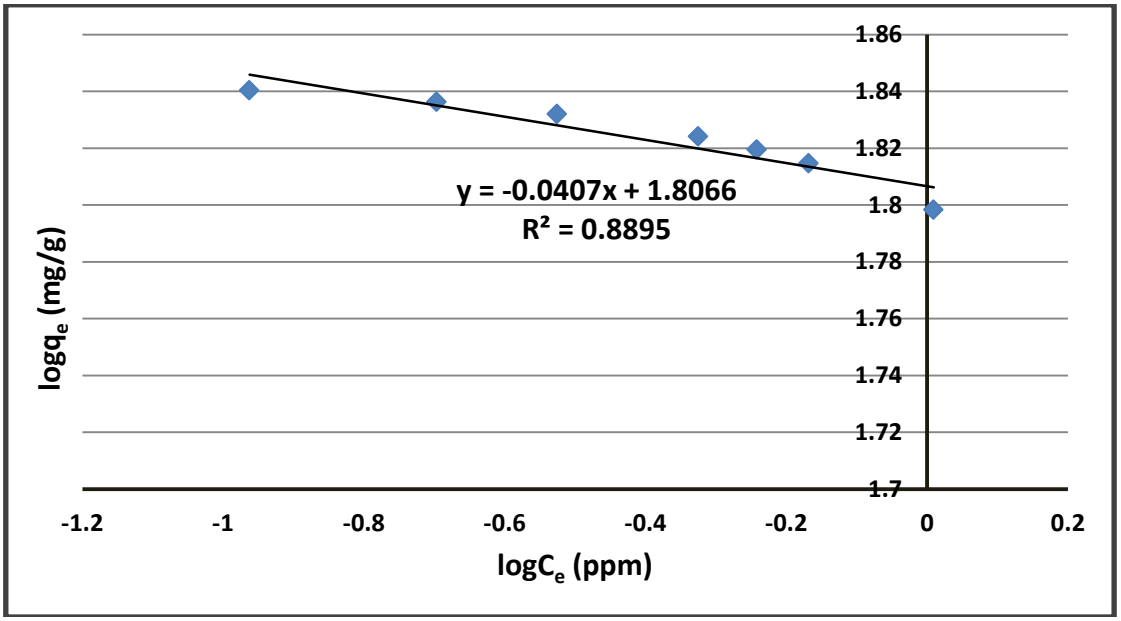

Figure 4.72: Freundlich plot for the adsorption of Pb(II) on (Si-m-NO_2) (time = 5 minute, pH = 7, temperature = 15 °C, adsorbent dose = 3 mg, volume = 7 mL).

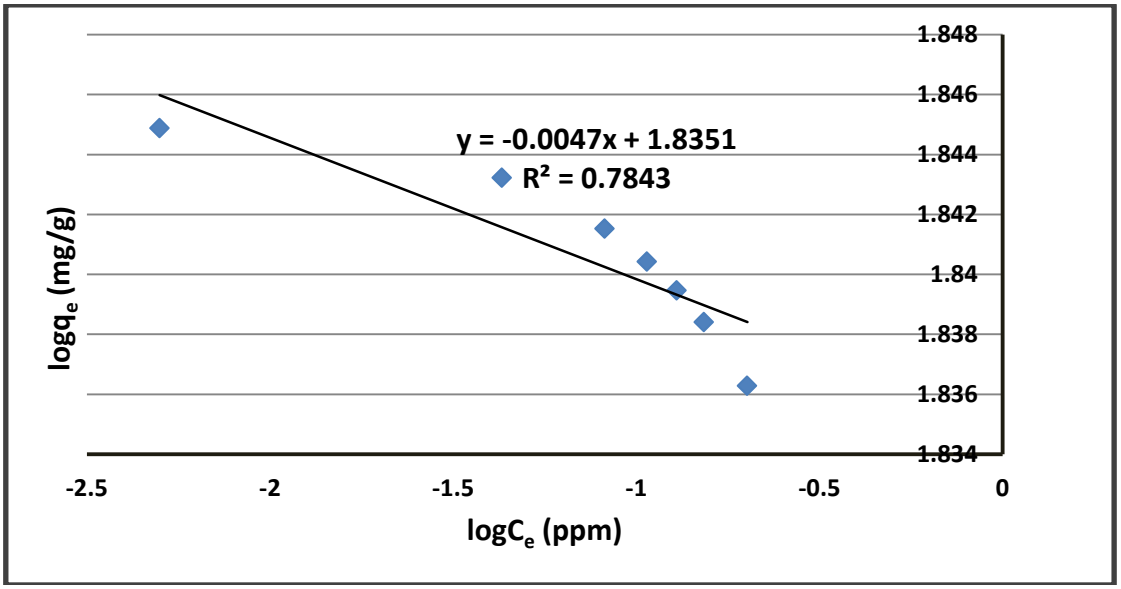

Figure 4.73: Freundlich plot for the adsorption of Pb(II) on (Si-p-NO_2) (time = 1 minute, pH = 8, temperature = 20 °C, adsorbent dose = 5 mg, volume = 7 mL).

As shown from the previous figures, the values of R^2 using Langmuir adsorption isotherm are approximately one. This means that the adsorption of Pb(II) on ortho-, meta, or para-nitrophenyl silica is chemical adsorption and follows Langmuir equation.

The following table represents the values of Langmuir and Freundlich isotherm parameters for the adsorption of Pb(II) on (Si-o-NO_2), (Si-m-NO_2) and (Si-p-NO_2).

Table 4.12: The parameters of Langmuir and Freundlich isotherms for the adsorption of Pb(II) on (Si-o-NO_2), (Si-m-NO_2) and (Si-p-NO_2).

Adsorbents	Adsorption of Pb(II)			
	Equilibrium Isotherm Models			
	Langmuir Isotherm		Freundlich Isotherm	
	Q_o (mg/g)	b (L/mg)	K_F (mg/g)	n (g/L)
Si-o-NO_2	65.789	-	66.405	-63.291
Si-m-NO_2	62.500	-40.000	64.062	-24.570
Si-p-NO_2	68.493	-	68.407	-212.766

4.3.1.2 .2 Adsorption Kinetic Models

The experimental kinetic data for Pb(II) adsorption on the prepared polymers are fitted with pseudo first-order, pseudo second-order and intra-particle diffusion kinetic models in order to investigate the mechanism of each adsorption process.

The kinetics parameters and correlation coefficients have been calculated from the linear plots of $\log(q_e - q_t)$ versus t for pseudo first order model, (t/q_t) versus t for pseudo second-order model, and q_t versus t for intra-particle diffusion kinetic model, as shown in the following Figures (4.74-4.82).

4.3.1.2 .2.1 Pseudo First-Order Kinetics

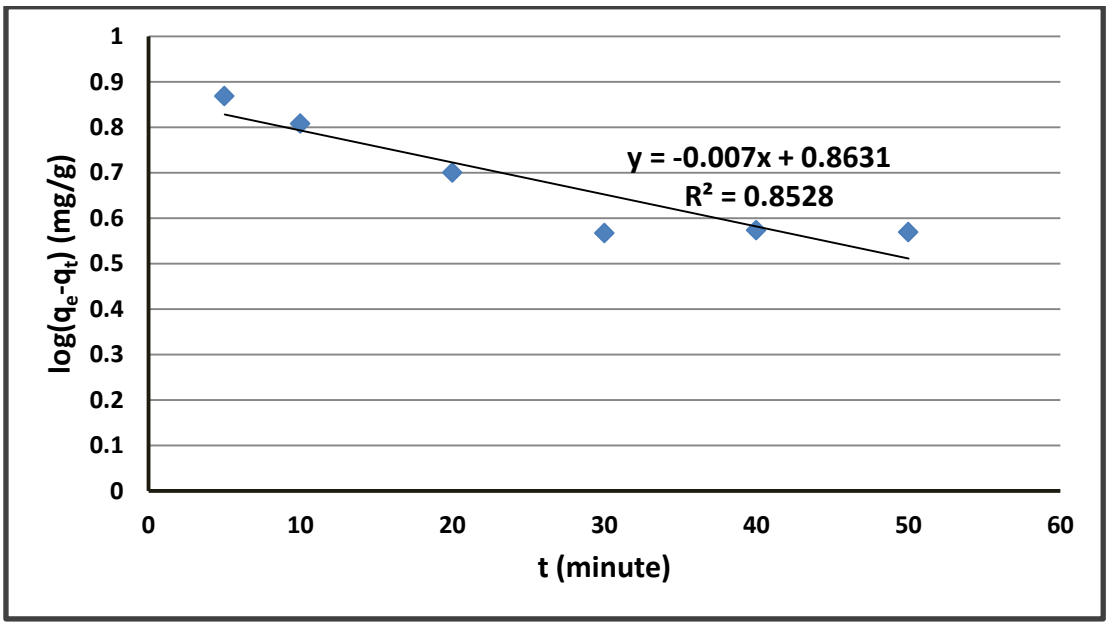

Figure 4.74: Pseudo first-order kinetic model for the adsorption of Pb(II) on (Si-o-NO_2) (C_I = 10 ppm, pH = 6, temperature = 20 °C, adsorbent dose = 1 mg, volume = 7 mL).

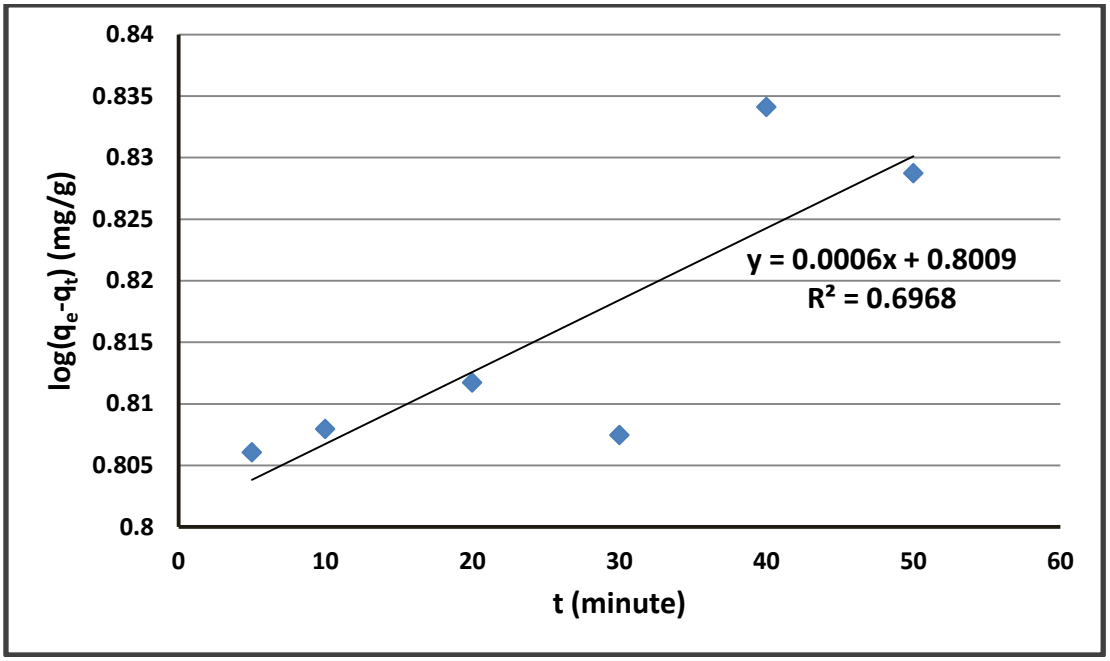

Figure 4.75: Pseudo first-order kinetic model for the adsorption of Pb(II) on (Si-m-NO_2) (C_I = 10 ppm, pH = 6, temperature = 20 °C, adsorbent dose = 1 mg, volume = 7 mL).

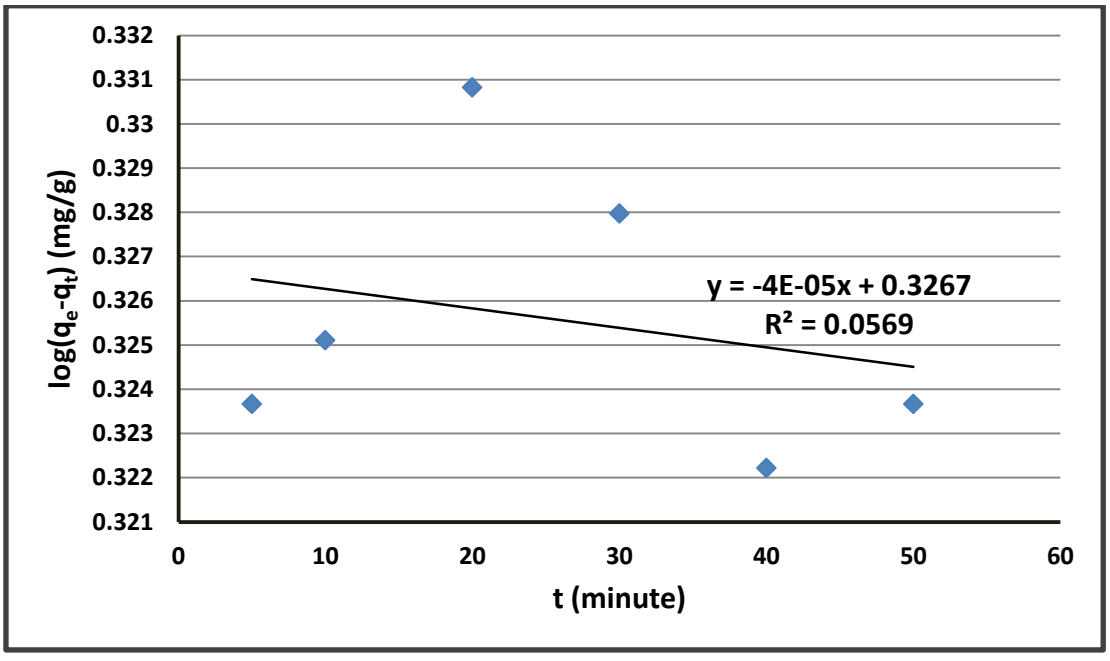

Figure 4.76: Pseudo first-order kinetic model for the adsorption of Pb(II) on (Si-p-NO_2) (C_I = 10 ppm, pH = 6, temperature = 20 °C, adsorbent dose = 1 mg, volume = 7 mL).

4.3.1.2 .2.2 Pseudo Second-Order Kinetics

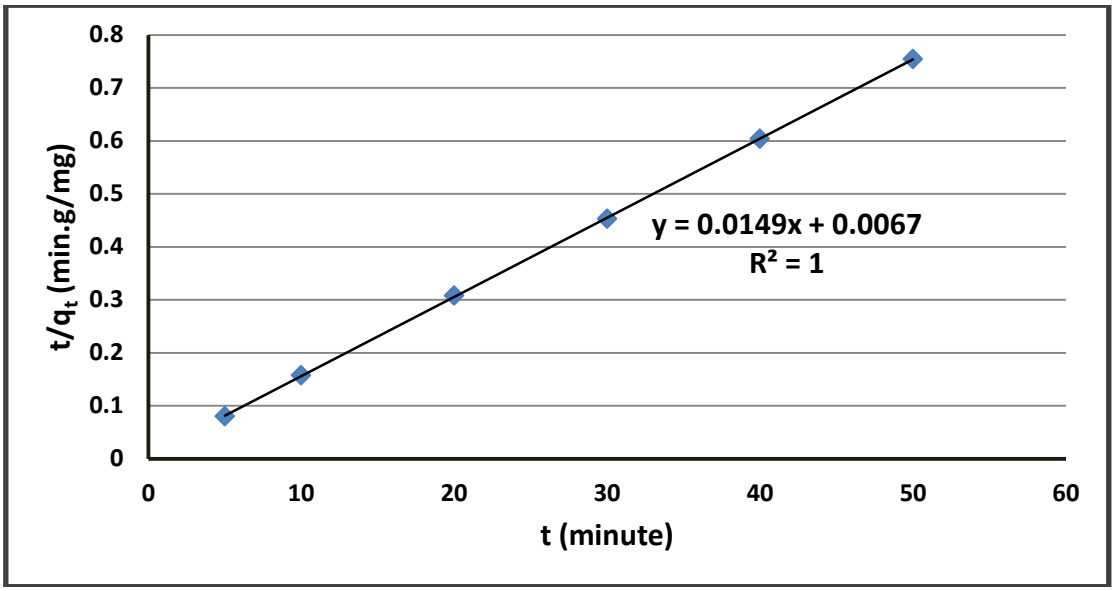

Figure 4.77: Pseudo second-order kinetic model for the adsorption of Pb(II) on (Si-o-NO_2) (C_I = 10 ppm, pH = 6, temperature = 20 °C, adsorbent dose = 1 mg, volume = 7 mL).

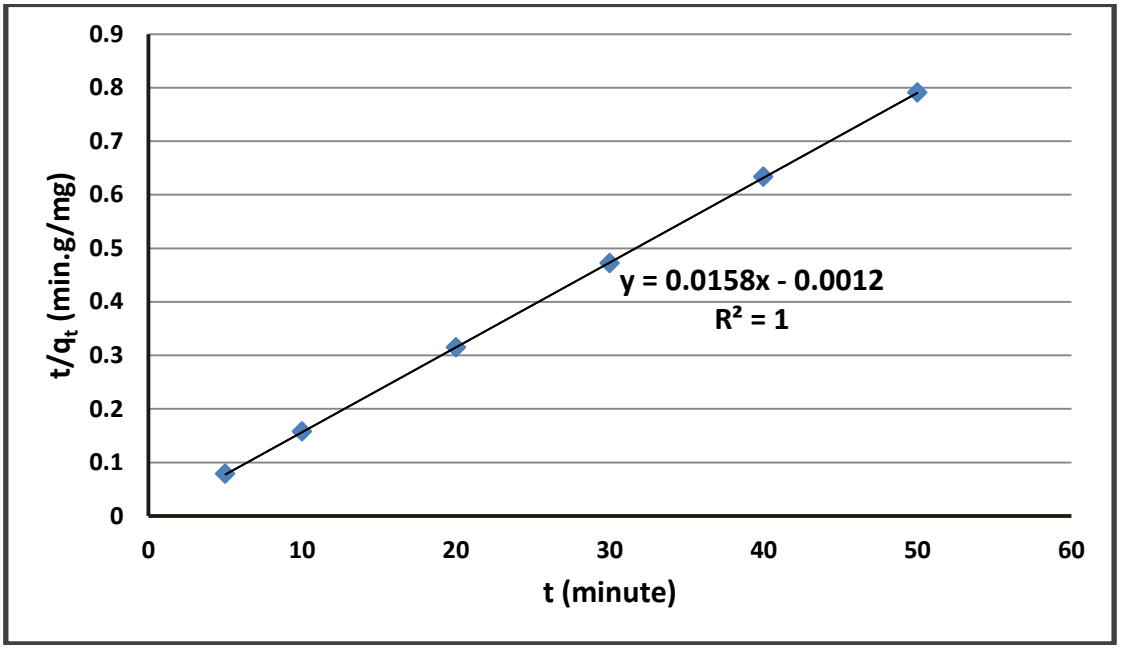

Figure 4.78: Pseudo second-order kinetic model for the adsorption of Pb(II) on (Si-m-NO_2) (C_I = 10 ppm, pH = 6, temperature = 20 °C, adsorbent dose = 1 mg, volume = 7 mL).

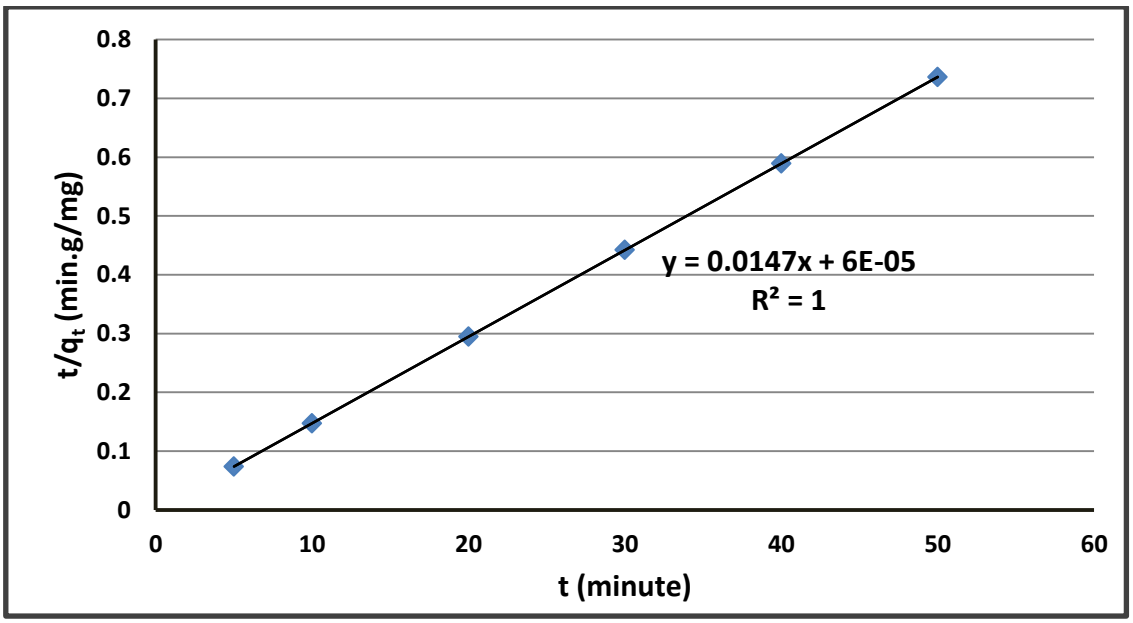

Figure 4.79: Pseudo second-order kinetic model for the adsorption of Pb(II) on (Si-p-NO_2) (C_I = 10 ppm, pH = 6, temperature = 20 °C, adsorbent dose = 1 mg, volume = 7 mL).

4.3.1.2 .2.3 Intra-Particle Diffusion Kinetic Model

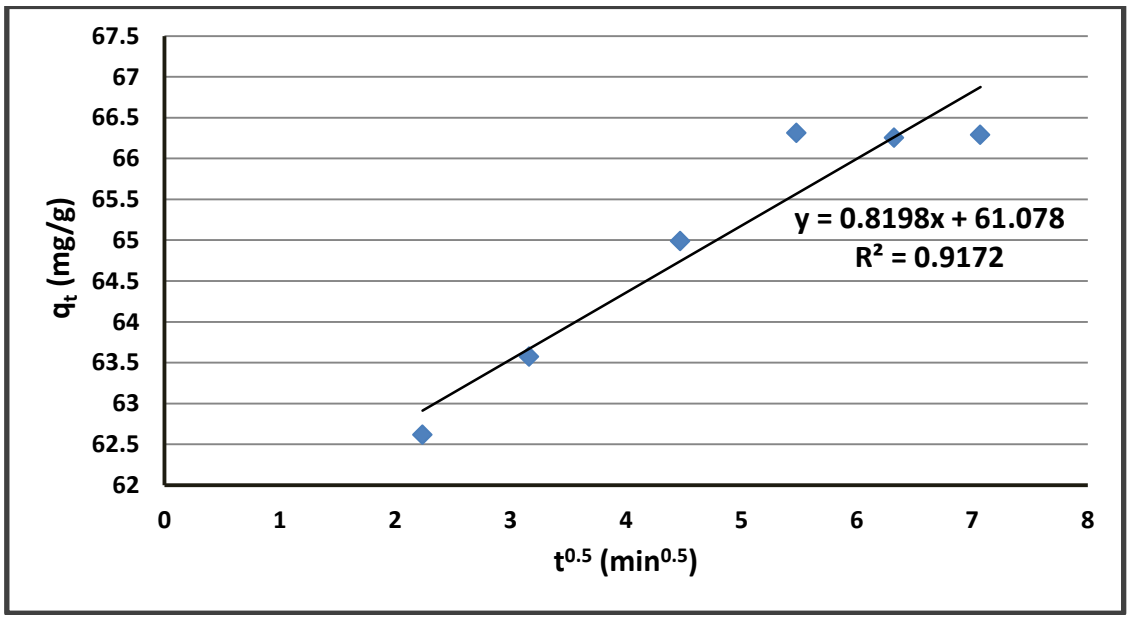

Figure 4.80: Intra-particle diffusion kinetic model for the adsorption of Pb(II) on (Si-o-NO_2) (C_I = 10 ppm, pH = 6, temperature = 20 °C, adsorbent dose = 1 mg, volume = 7 mL).

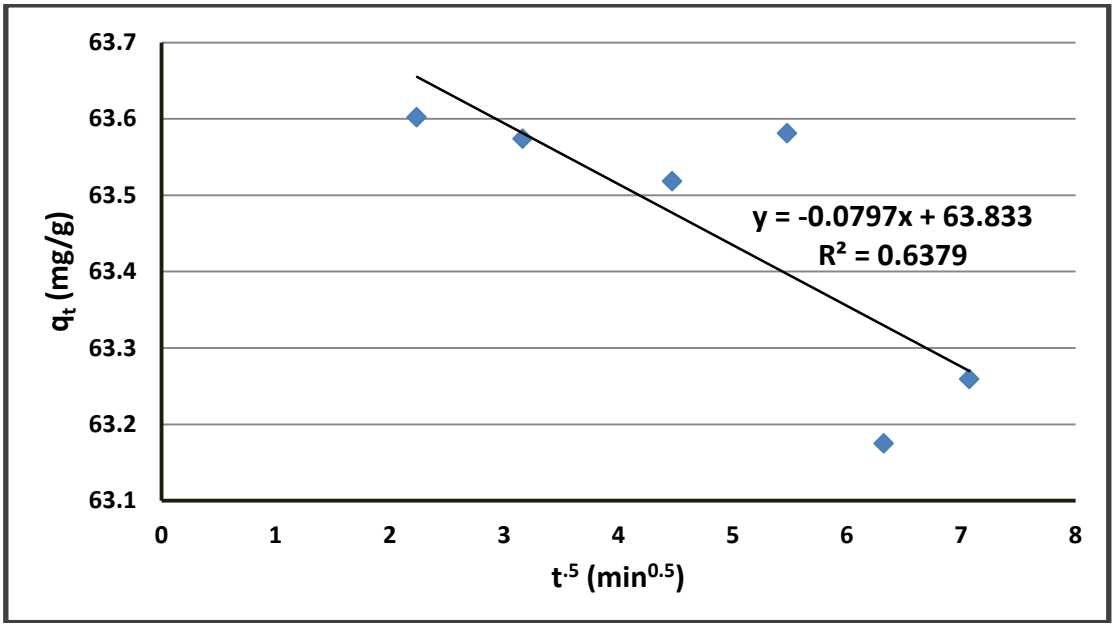

Figure 4.81: Intra-particle diffusion kinetic model for the adsorption of Pb(II) on (Si-m-NO_2) (C_I = 10 ppm, pH = 6, temperature = 20 °C, adsorbent dose = 1 mg, volume = 7 mL).

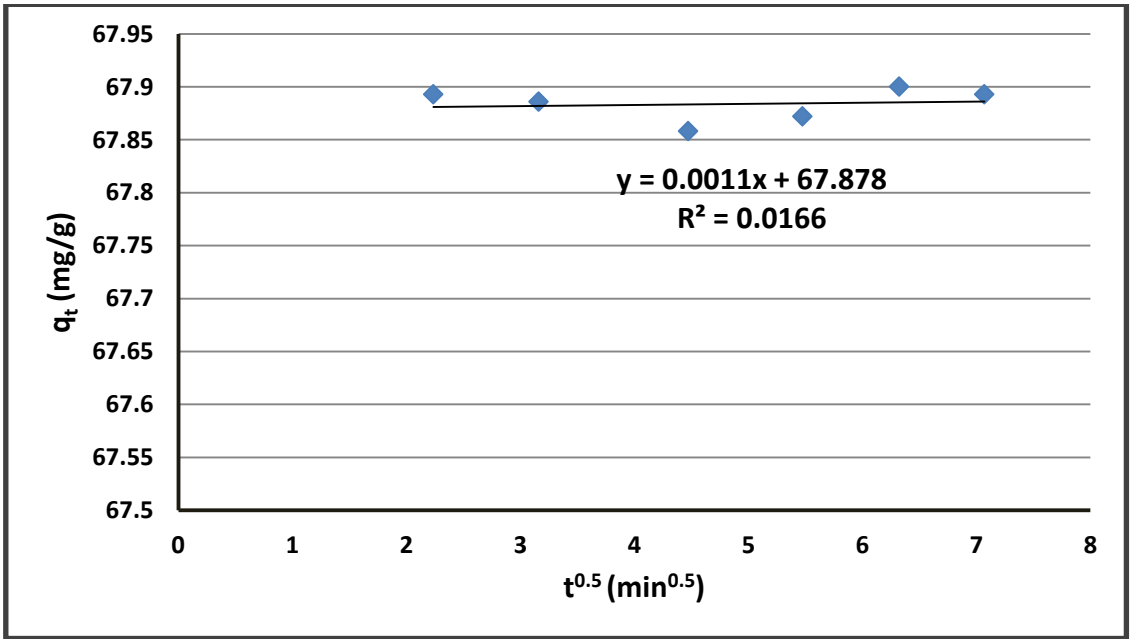

Figure 4.82: Intra-particle diffusion kinetic model for the adsorption of Pb(II) on (Si-p-NO_2) (C_I = 10 ppm, pH = 6, temperature = 20 °C, adsorbent dose = 1 mg, volume = 7 mL).

According to the values for the correlation coefficient using the previous kinetic models. It is showed the adsorption of Pb(II) on (Si-o-NO_2), (Si-m-NO_2) or (Si-p-NO_2) followed the mechanism of pseudo second-order kinetic model. Such that, the values of R^2 in this kinetic model are approximately one.

The following table shows the kinetic parameters of pseudo first-order, pseudo second-order and intra-particle diffusion kinetic models for the adsorption of Pb(II) on (Si-o-NO_2), (Si-m-NO_2) and (Si-p-NO_2).

Table 4.13: The parameters of pseudo first-order, pseudo second-order and intra-particle diffusion kinetic models for the adsorption of Pb(II) on (Si-o-NO_2), (Si-m-NO_2) and (Si-p-NO_2).

Adsorbents	Adsorption of Pb(II)					
	Adsorption Kinetic Models					
	Pseudo First-Order Kinetics		Pseudo Second-Order Kinetics		Intra-Particle Diffusion Kinetics	
	q_e (mg/g)	K_1 ($mg.g^{-1}.min^{-1}$)	q_e (mg/g)	K_2 ($g.mg^{-1}.min^{-1}$)	C (mg/g)	K_p ($mg.g^{-1}.min^{-0.5}$)
Si-o-NO_2	7.296	0.0162	67.114	0.0331	61.078	0.8198
Si-m-NO_2	6.323	$-1.382*10^{-3}$	63.291	-0.208	63.833	-0.0799
Si-p-NO_2	2.122	-	68.027	-	67.878	0.0011

Comparing the value of q_e (experimentally) for all adsorption processes that equal 70, with the values of q_e (calculated) in pseudo first-order and pseudo second-order kinetic adsorption models, we conclude that the experimental values for all adsorptions are closer to the values of q_e (calculated) in pseudo second-order adsorption model. Hence, proving that this model represents the mechanism of the adsorption.

4.3.1.2.3 Adsorption Thermodynamics

By using the thermodynamic equation of Van't Hoff plot. The

thermodynamic parameters (ΔH and ΔS) for the adsorption of lead ions on (Si-o-NO_2), (Si-m-NO_2) or (Si-p-NO_2) can be calculated from the slope and y-intercept of the graph of In K_d versus (1/T), as shown in the following Figures (4.83-4.85).

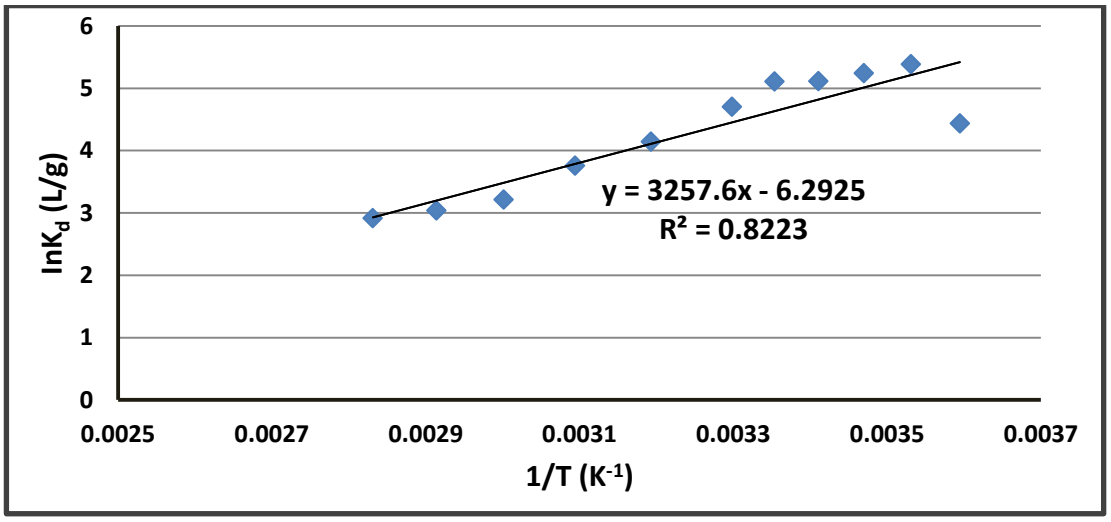

Figure 4.83: Van't Hoff plot for the adsorption of Pb(II) on (Si-o-NO_2) (time = 30 minute, C_I = 10 ppm, pH = 8, adsorbent dose = 1 mg, volume = 7 mL).

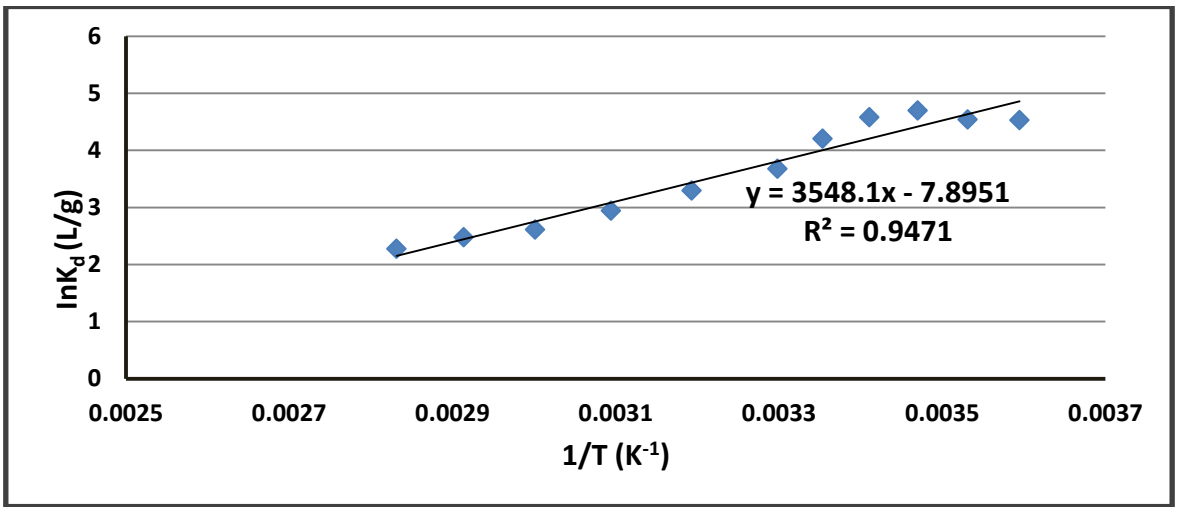

Figure 4.84: Van't Hoff plot for the adsorption of Pb(II) on (Si-m-NO_2) (time = 5 minute, C_I = 10 ppm, pH = 7, adsorbent dose = 1 mg, volume = 7 mL).

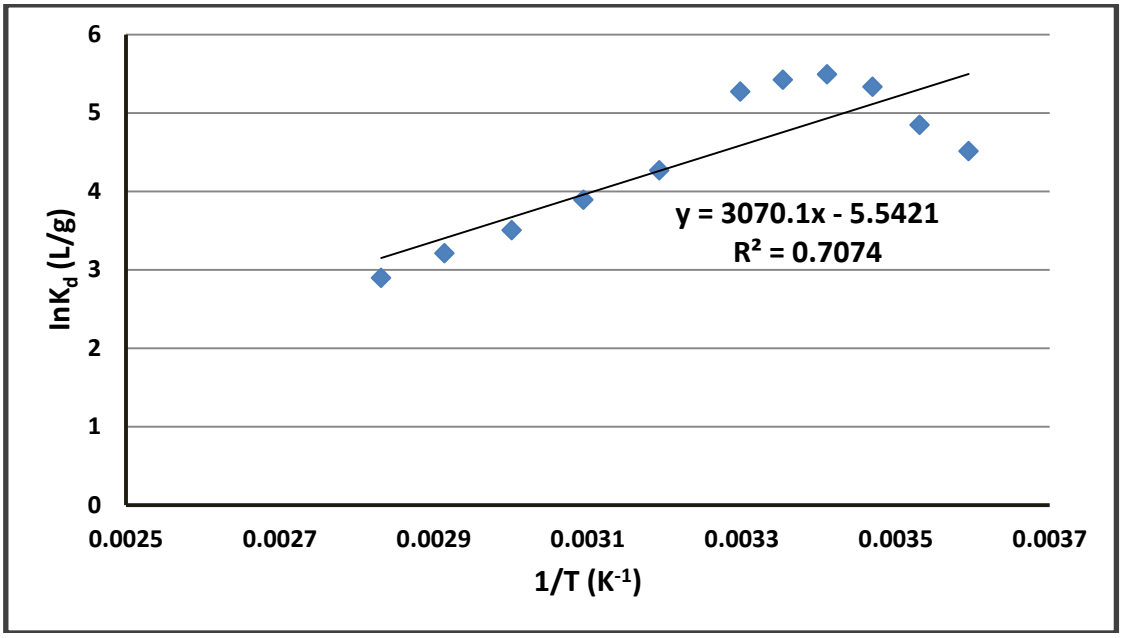

Figure 4.85: Van't Hoff plot for the adsorption of Pb(II) on (Si-p-NO_2) (time = 1 minute, C_I = 10 ppm, pH = 8, adsorbent dose = 1 mg, volume = 7 mL).

The following table represents the values of the thermodynamic parameters (ΔS and ΔH) for the adsorption of Pb(II) on ortho-, meta-, or para-nitrophenyl silicas.

Table 4.14: The thermodynamic parameters for the adsorption of Pb(II) on (Si-o-NO_2), (Si-m-NO_2) and (Si-p-NO_2).

Adsorbents	Adsorption of Pb(II)	
	Adsorption Thermodynamics	
	ΔH (kJ)	ΔS (J/K)
Si-o-NO_2	27.084	-52.316
Si-m-NO_2	29.499	-65.639
Si-p-NO_2	25.525	-46.077

As shown in this table, the adsorption of Pb(II) on (Si-o-NO_2), (Si-m-NO_2) or (Si-p-NO_2) adsorbent is endothermic process (ΔH > 0) and non spontaneous (ΔS < 0).

4.3.1.3 Adsorption of Nickel

4.3.1.3.1 Equilibrium Isotherm Models

In order to determine the best adsorption isotherm for the adsorption of nickel ions onto ortho-, meta-, or para-nitrophenyl silicas, the observed data were fitted to Langmuir and Freundlich isotherms which describe the relationship between the amounts of Ni(II) adsorbed and its equilibrium concentration in solution.

The adsorption parameters were investigated by plotting C_e/q_e versus C_e for Langmuir adsorption isotherm, and $\log q_e$ versus $\log C_e$ for Freundlich adsorption isotherm, as shown in the following Figures (4.86-4.91).

4.3.1.3 .1.1 Langmuir Adsorption Isotherm

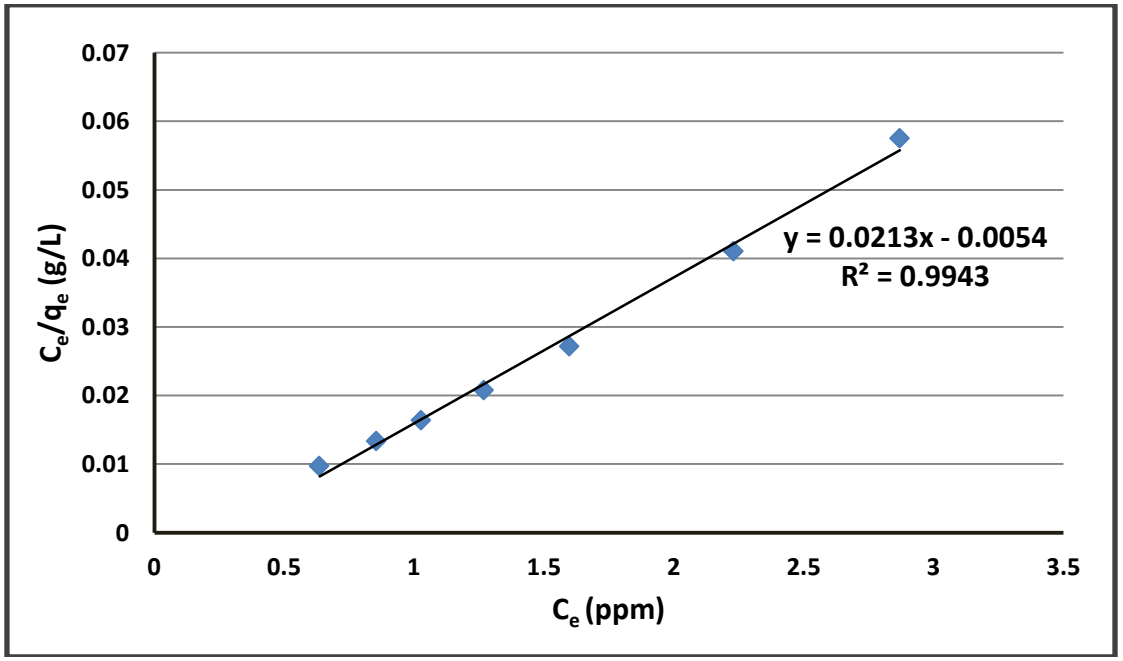

Figure 4.86: Langmuir plot for the adsorption of Ni(II) on (Si-o-NO_2) (time = 10 minute, pH = 7, temperature = 25 °C, adsorbent dose = 2 mg, volume = 7 mL).

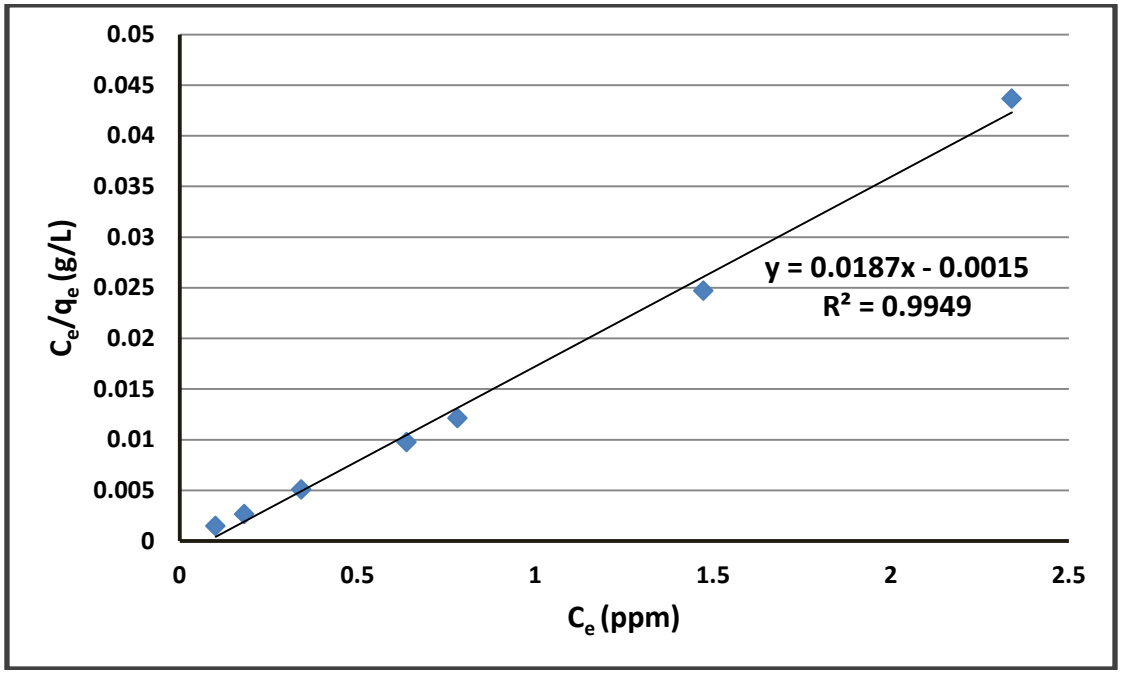

Figure 4.87: Langmuir plot for the adsorption of Ni(II) on (Si-m-NO_2) (time = 20 minute, pH = 7, temperature = 10 °C, adsorbent dose = 5 mg, volume = 7 mL).

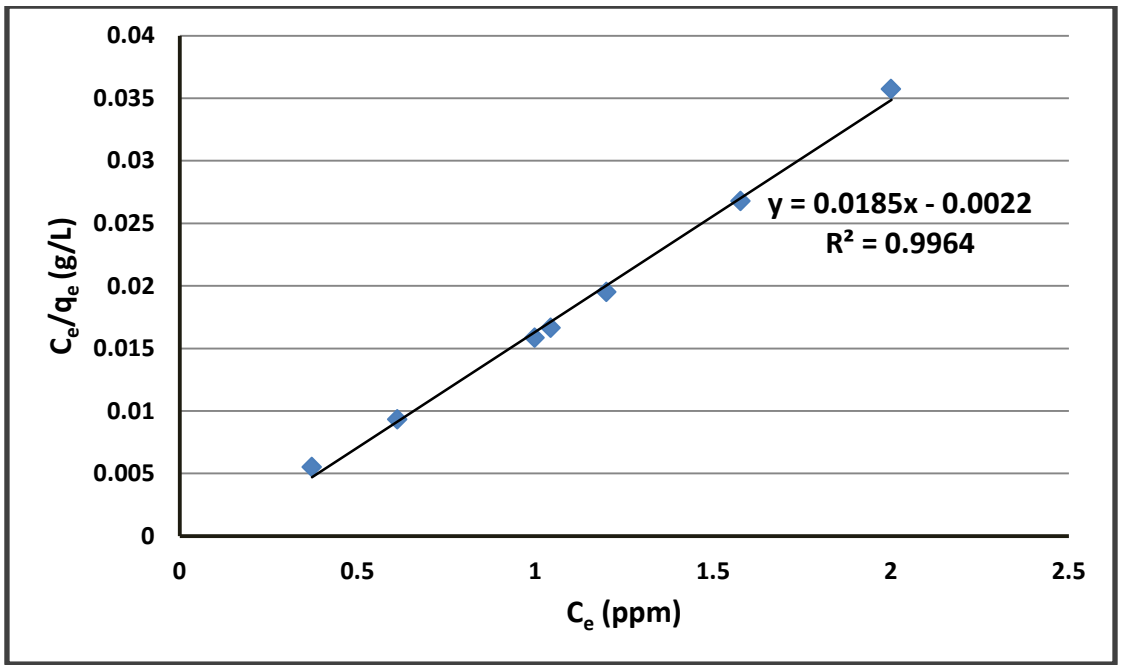

Figure 4.88: Langmuir plot for the adsorption of Ni(II) on (Si-p-NO_2) (time = 10 minute, pH = 8, temperature = 20 °C, adsorbent dose = 1 mg, volume = 7 mL).

4.3.1.3 .1.2 Freundlich Adsorption Isotherm

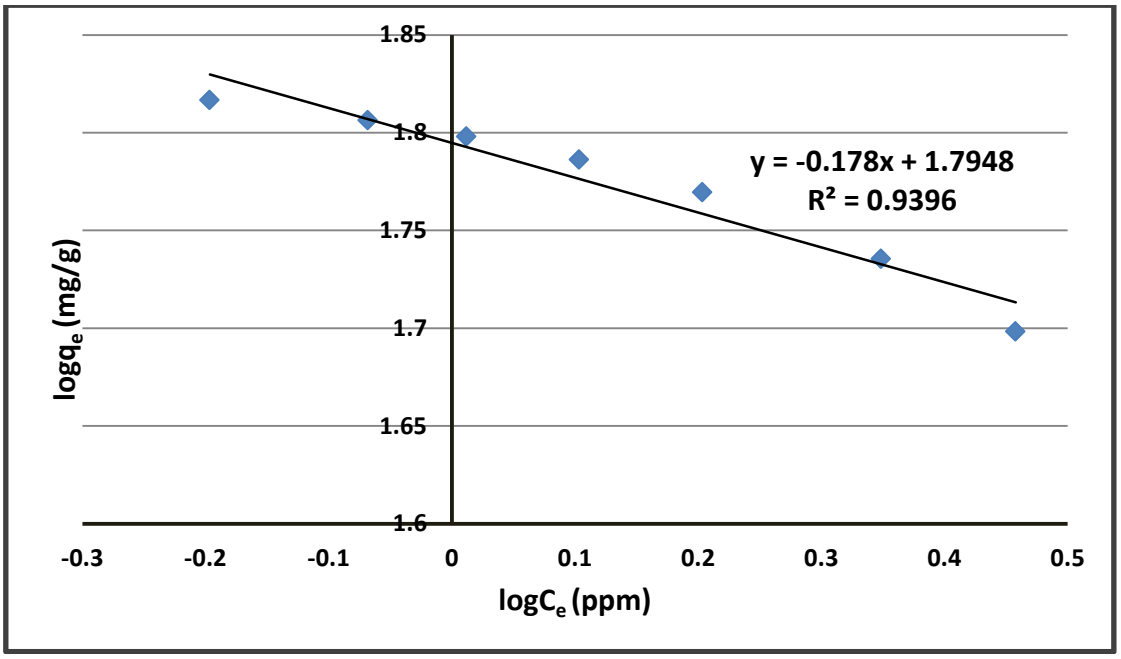

Figure 4.89: Freundlich plot for the adsorption of Ni(II) on (Si-o-NO_2) (time = 10 minute, pH = 7, temperature = 25 °C, adsorbent dose = 2 mg, volume = 7 mL).

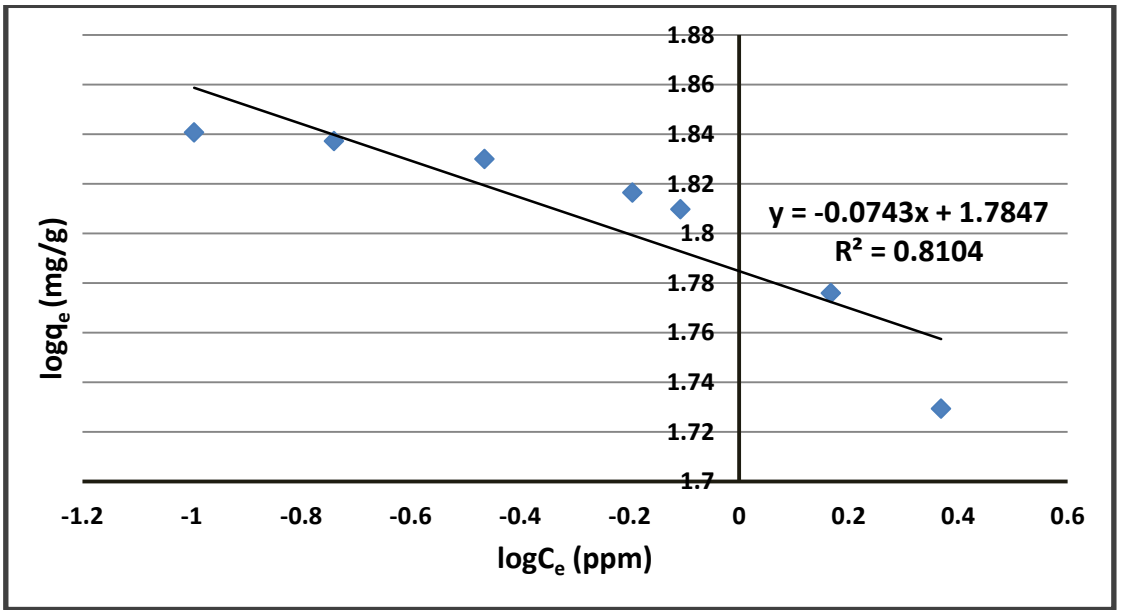

Figure 4.90: Freundlich plot for the adsorption of Ni(II) on (Si-m-NO_2) (time = 20 minute, pH = 7, temperature = 10 °C, adsorbent dose = 5 mg, volume = 7 mL).

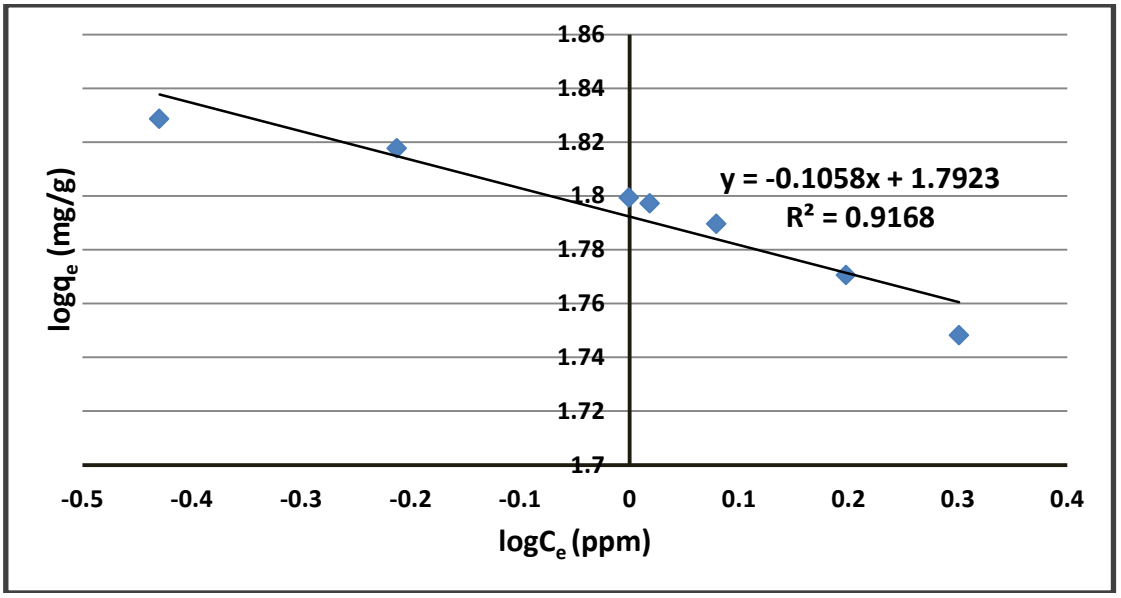

Figure 4.91: Freundlich plot for the adsorption of Ni(II) on (Si-p-NO_2) (time = 10 minute, pH = 8, temperature = 20 °C, adsorbent dose = 1 mg, volume = 7 mL).

As shown from the previous figures, the values of R^2 using Langmuir adsorption isotherm are approximately one. This means that the adsorption of Ni(II) on ortho-, meta, or para-nitrophenyl silica is chemical adsorption and follows Langmuir equation.

The following table represents the values of Langmuir and Freundlich isotherm parameters for the adsorption of Ni(II) on (Si-o-NO_2), (Si-m-NO_2) and (Si-p-NO_2) adsorbents.

Table 4.15: The parameters of Langmuir and Freundlich isotherms for the adsorption of Ni(II) on (Si-o-NO_2), (Si-m-NO_2) and (Si-p-NO_2).

Adsorbents	Adsorption of Ni(II)			
	Equilibrium Isotherm Models			
	Langmuir Isotherm		Freundlich Isotherm	
	Q_o (mg/g)	b (L/mg)	K_F (mg/g)	n (g/L)
Si-o-NO_2	46.948	-3.944	62.345	-5.618
Si-m-NO_2	53.476	-12.466	60.912	-13.459
Si-p-NO_2	54.054	-8.409	61.987	-9.452

4.3.1.3 .2 Adsorption Kinetic Models

The experimental kinetic data for Ni(II) adsorption on the prepared polymers are fitted with pseudo first-order, pseudo second-order and intra-particle diffusion kinetic models in order to investigate the mechanism of each adsorption process.

The kinetics parameters and correlation coefficients have been calculated from the linear plots of $\log(q_e - q_t)$ versus t for pseudo first order model, (t/q_t) versus t for pseudo second-order model, and q_t versus t for intra-particle diffusion kinetic model, as shown in the following Figures (4.92-4.100).

4.3.1.3 .2.1 Pseudo First-Order Kinetics

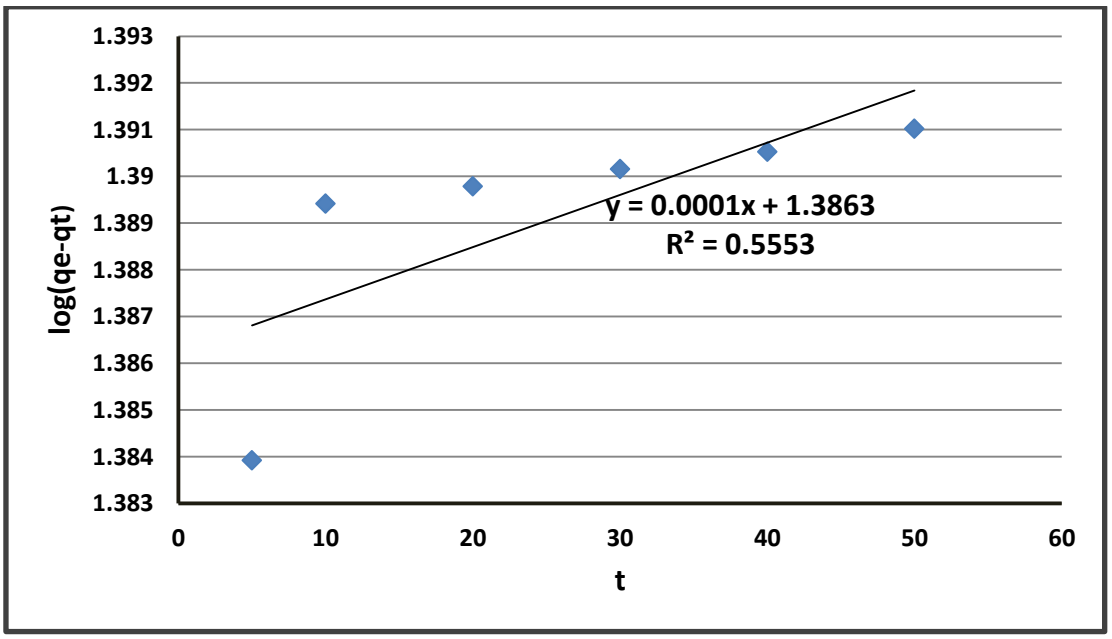

Figure 4.92: Pseudo first-order kinetic model for the adsorption of Ni(II) on (Si-o-NO_2) (C_I = 10 ppm, pH = 6, temperature = 20 °C, adsorbent dose = 1 mg, volume = 7 mL).

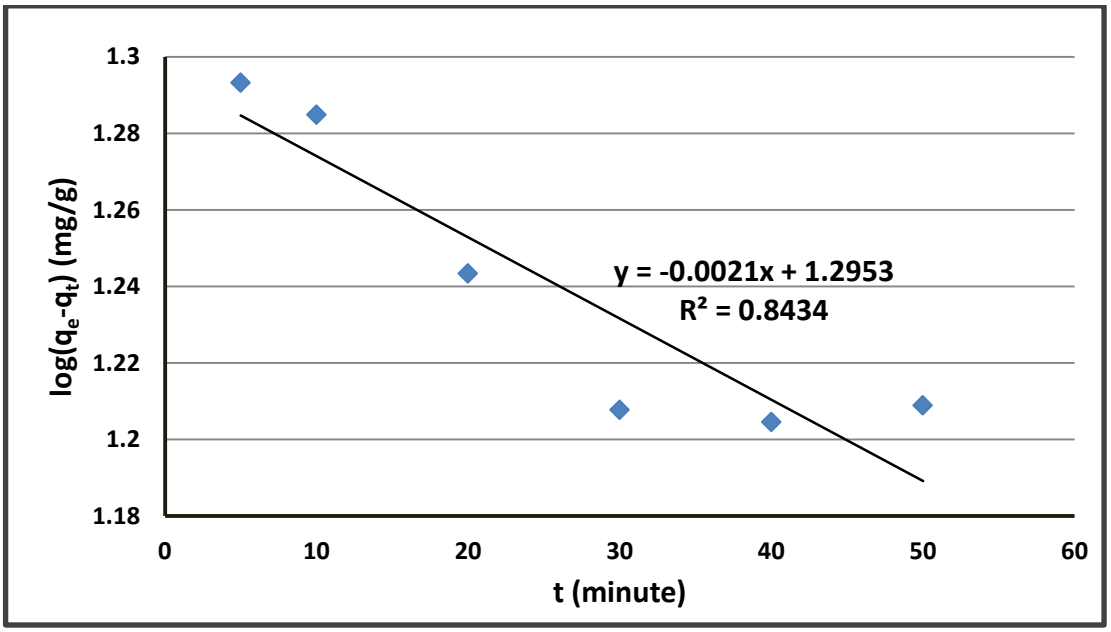

Figure 4.93: Pseudo first-order kinetic model for the adsorption of Ni(II) on (Si-m-NO_2) (C_I = 10 ppm, pH = 6, temperature = 20 °C, adsorbent dose = 1 mg, volume = 7 mL).

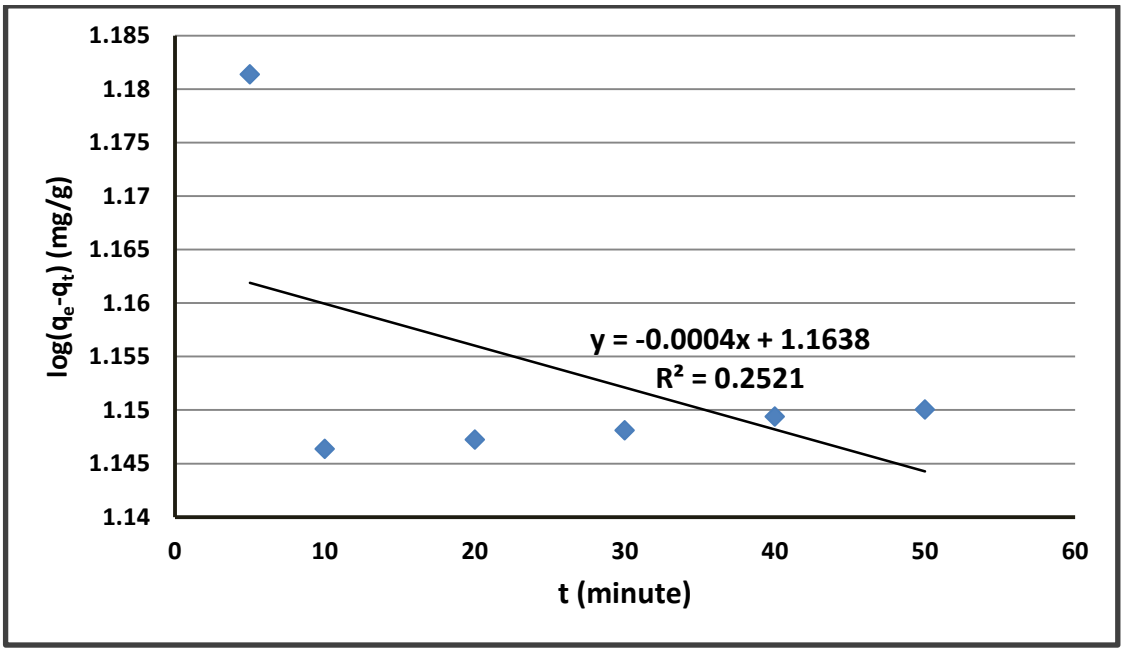

Figure 4.94: Pseudo first-order kinetic model for the adsorption of Ni(II) on (Si-p-NO_2) (C_I = 10 ppm, pH = 6, temperature = 20 °C, adsorbent dose = 1 mg, volume = 7 mL).

4.3.1.3 .2.2 Pseudo Second-Order Kinetics

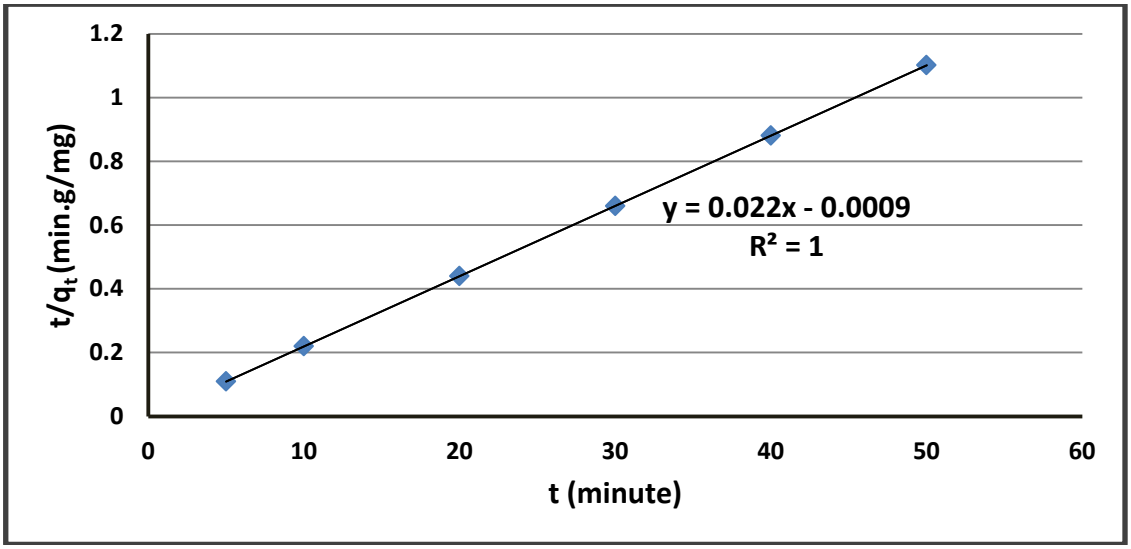

Figure 4.95: Pseudo second-order kinetic model for the adsorption of Ni(II) on (Si-o-NO_2) (C_I = 10 ppm, pH = 6, temperature = 20 °C, adsorbent dose = 1 mg, volume = 7 mL).

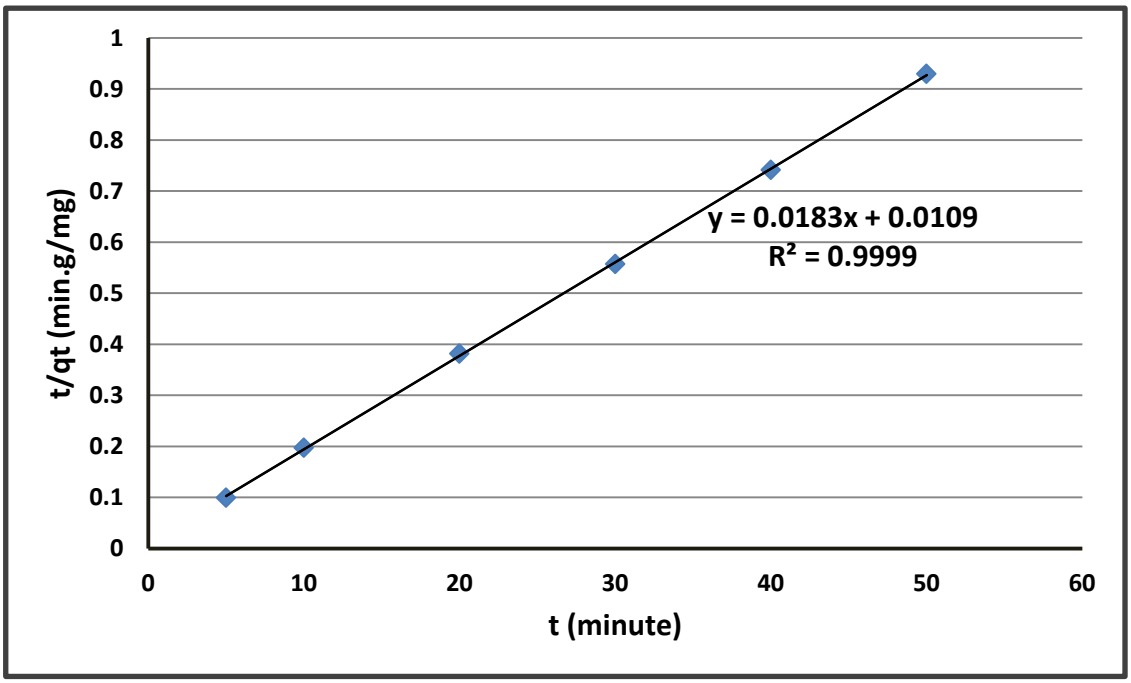

Figure 4.96: Pseudo second-order kinetic model for the adsorption of Ni(II) on (Si-m-NO_2) (C_I = 10 ppm, pH = 6, temperature = 20 °C, adsorbent dose = 1 mg, volume = 7 mL).

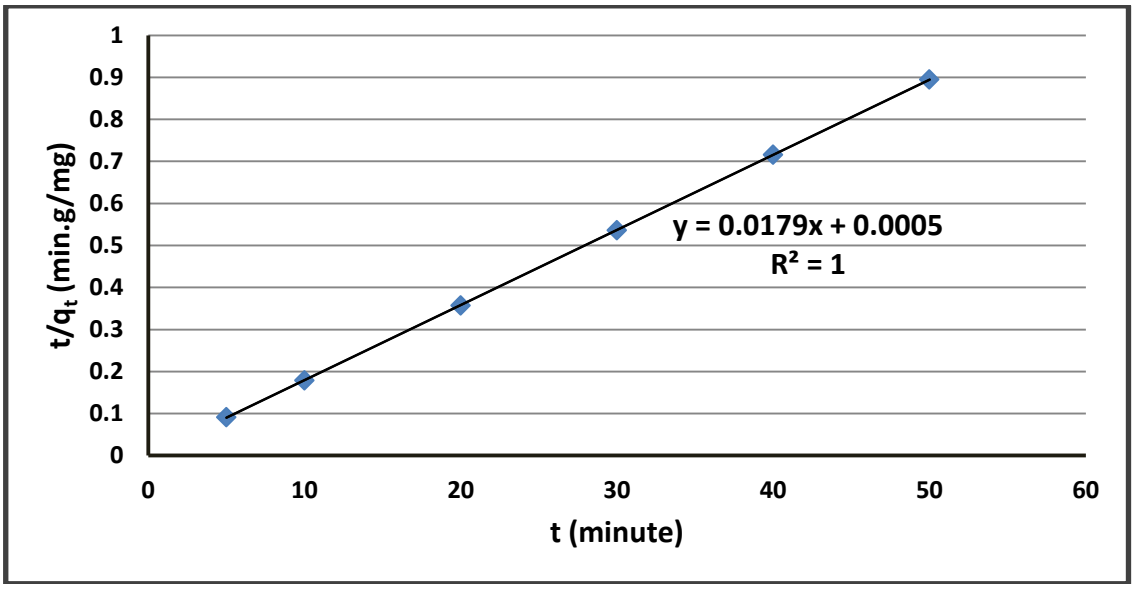

Figure 4.97: Pseudo second-order kinetic model for the adsorption of Ni(II) on (Si-p-NO_2) (C_I = 10 ppm, pH = 6, temperature = 20 °C, adsorbent dose = 1 mg, volume = 7 mL).

4.3.1.3 .2.3 Intra-Particle Diffusion Kinetic Model

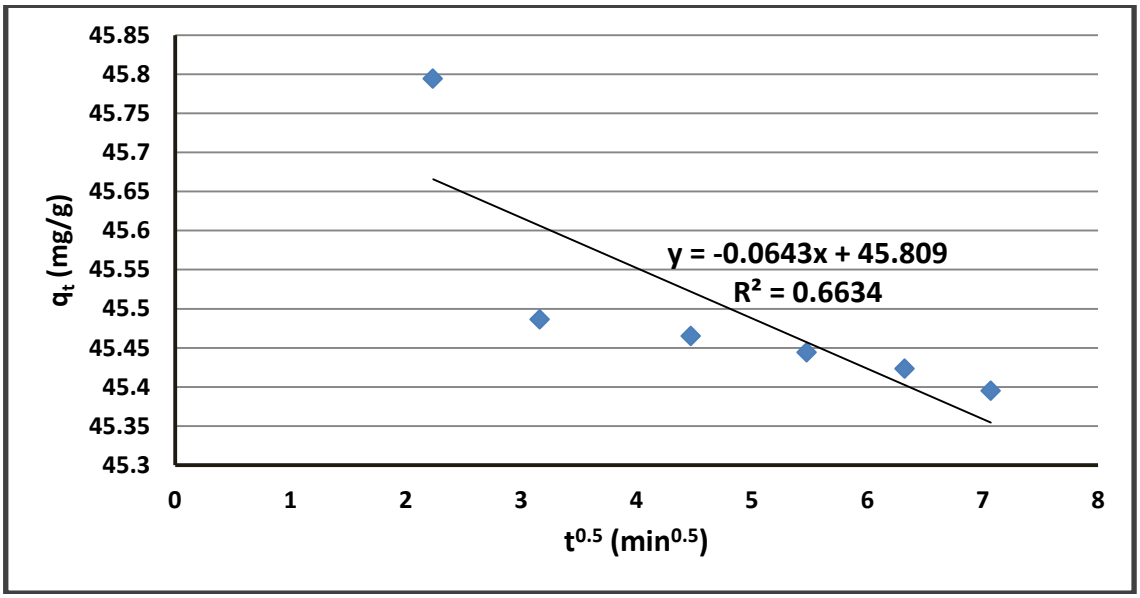

Figure 4.98: Intra-particle diffusion kinetic model for the adsorption of Ni(II) on (Si-o-NO_2) (C_I = 10 ppm, pH = 6, temperature = 20 °C, adsorbent dose = 1 mg, volume = 7 mL).

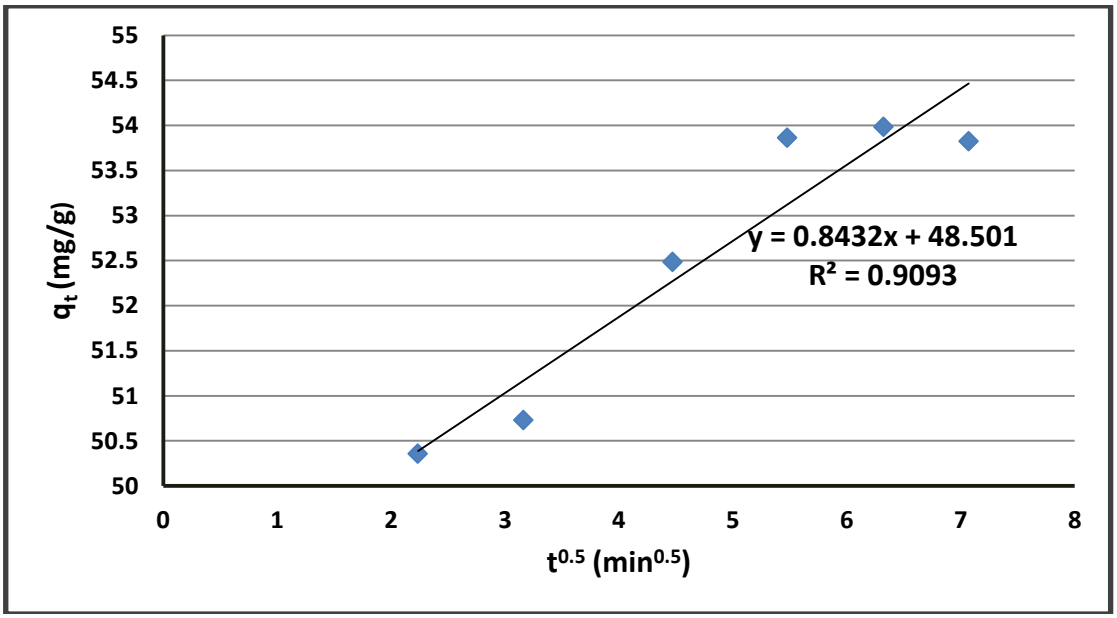

Figure 4.99: Intra-particle diffusion kinetic model for the adsorption of Ni(II) on (Si-m-NO_2) (C_I = 10 ppm, pH = 6, temperature = 20 °C, adsorbent dose = 1 mg, volume = 7 mL).

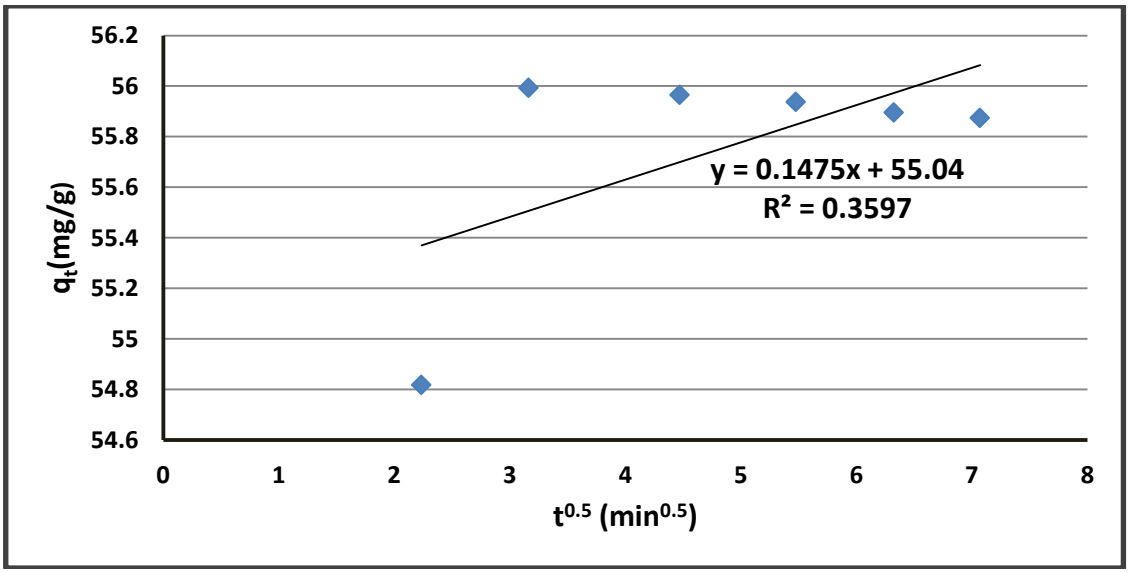

Figure 4.100: Intra-particle diffusion kinetic model for the adsorption of Ni(II) on (Si-p-NO_2) (C_I = 10 ppm, pH = 6, temperature = 20 °C, adsorbent dose = 1 mg, volume = 7 mL).

According to the values for the correlation coefficient using the previous kinetic models. It is showed the adsorption of Ni(II) on (Si-o-NO_2), (Si-m-NO_2) or (Si-p-NO_2) followed the mechanism of pseudo second-order kinetic model. Such that, the values of R^2 in this kinetic model are approximately one.

The following table shows the kinetic parameters of pseudo first-order, pseudo second-order and intra-particle diffusion kinetic models for the adsorption of Ni(II) on (Si-o-NO_2), (Si-m-NO_2) and (Si-p-NO_2).

Table 4.16: The parameters of pseudo first-order, pseudo second-order and intra-particle diffusion kinetic models for the adsorption of Ni(II) on (Si-o-NO_2), (Si-m-NO_2) and (Si-p-NO_2).

Adsorbents	Adsorption of Ni(II)					
	Adsorption Kinetic Models					
	Pseudo First-Order Kinetics		Pseudo Second-Order Kinetics		Intra-Particle Diffusion Kinetics	
	q_e (mg/g)	K_1 ($mg.g^{-1}.min^{-1}$)	q_e (mg/g)	K_2 ($g.mg^{-1}.min^{-1}$)	C (mg/g)	K_p ($mg.g^{-1}.min^{-0.5}$)
Si-o-NO_2	24.339	$-2.303*10^{-4}$	45.454	-0.538	45.809	-0.0643
Si-m-NO_2	19.738	$4.836*10^{-3}$	54.645	0.0307	48.501	0.8432
Si-p-NO_2	14.581	$9.212*10^{-4}$	55.866	0.641	55.040	0.1475

Comparing the value of q_e (experimentally) for all adsorption processes that equals 70, with the values of q_e (calculated) in pseudo first-order and pseudo second-order kinetic adsorption models, we conclude that the experimental values for all adsorptions are closer to the values of q_e (calculated) in pseudo second-order adsorption model. Hence, proving that this model represents the mechanism of the adsorption.

4.3.1.3 .4 Adsorption Thermodynamics

By using the thermodynamic equation of Van't Hoff plot. The thermodynamic parameters (ΔH and ΔS) for the adsorption of nickel ions on (Si-o-NO_2), (Si-m-NO_2) and (Si-p-NO_2) can be calculated from the slope and y-intercept of the graph of In K_d versus (1/T), as shown in the following Figures (4.101-4.103).

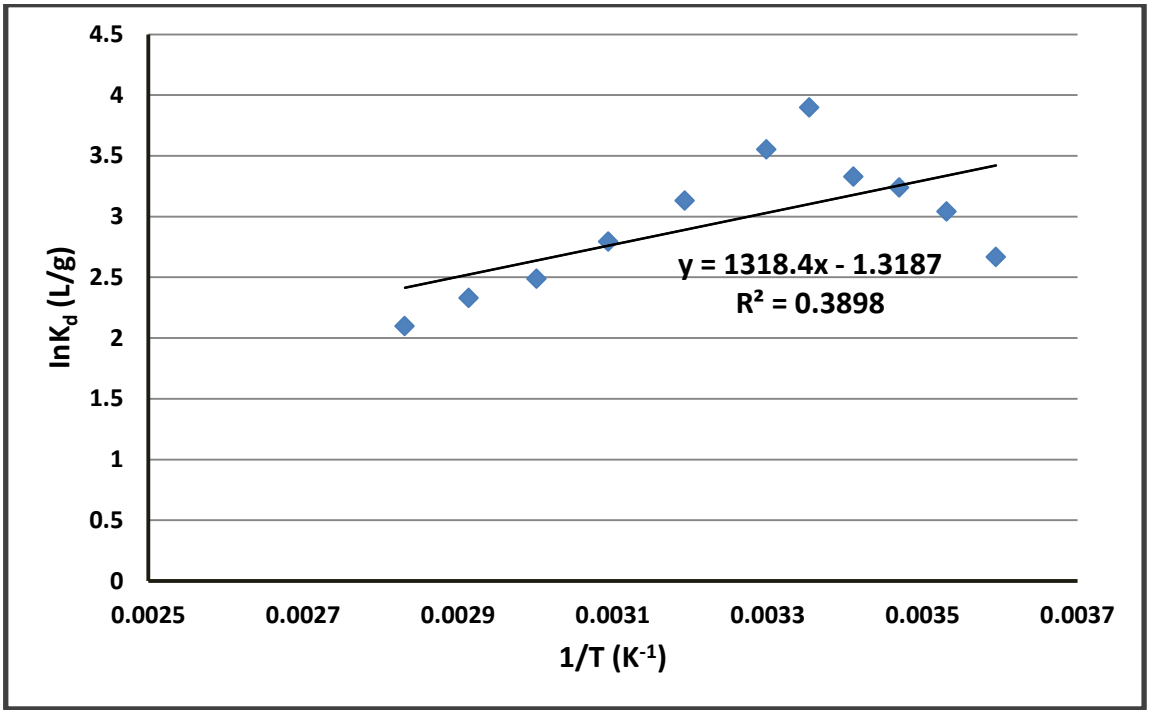

Figure 4.101: Van't Hoff plot for the adsorption of Ni(II) on (Si-o-NO_2) (time = 10 minute, C_I = 10 ppm, pH = 7, adsorbent dose = 1 mg, volume = 7 mL).

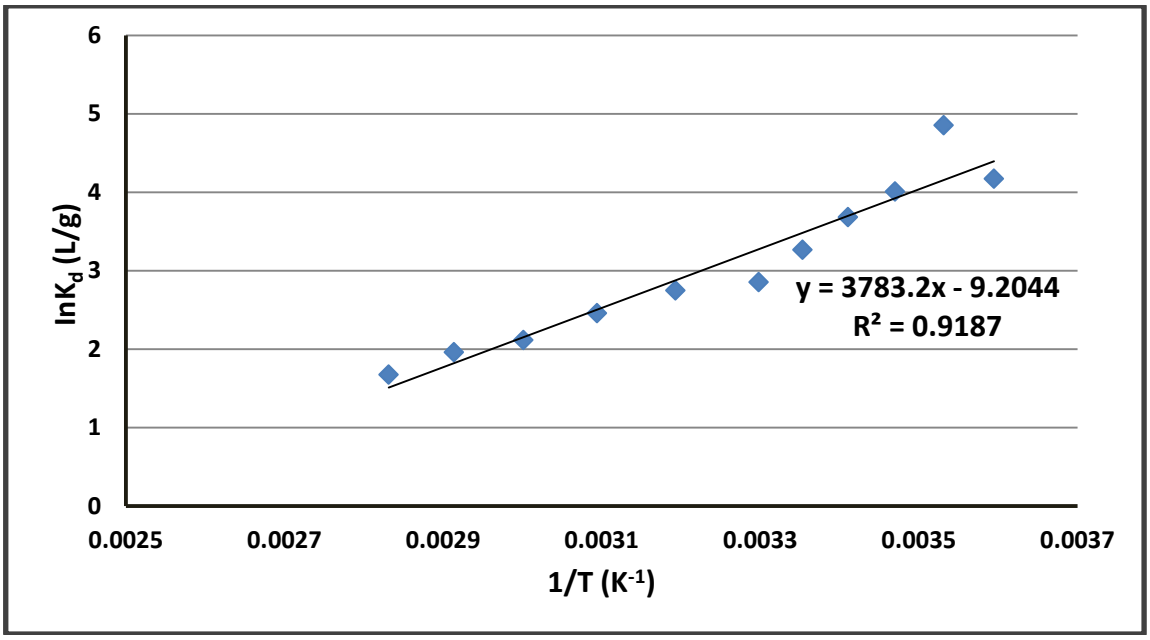

Figure 4.102: Van't Hoff plot for the adsorption of Ni(II) on (Si-m-NO_2) (time = 20 minute, C_I = 10 ppm, pH = 7, adsorbent dose = 1 mg, volume = 7 mL).

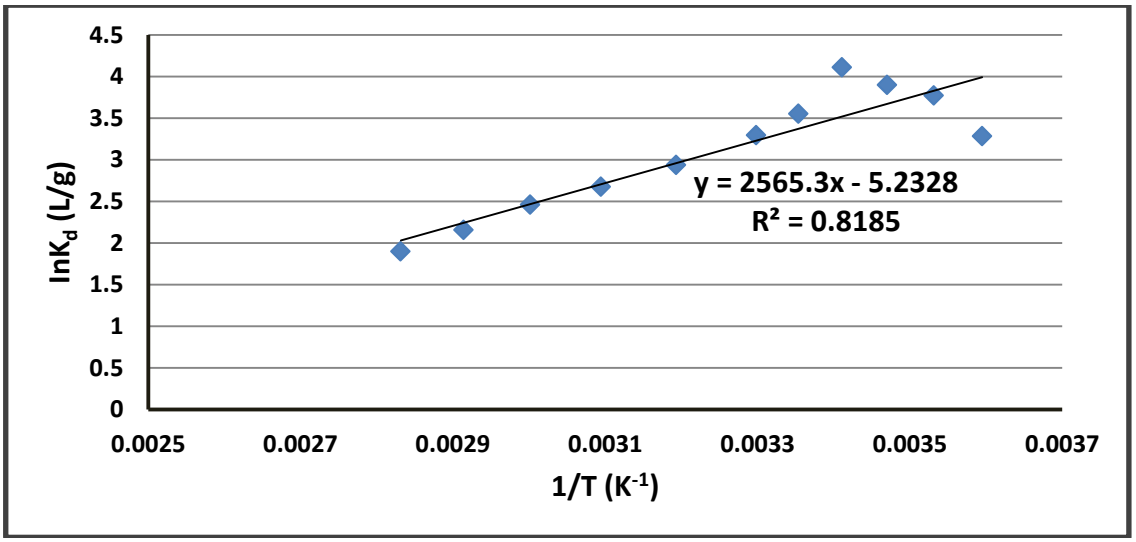

Figure 4.103: Van't Hoff plot for the adsorption of Ni(II) on (Si-p-NO_2) (time = 10 minute, C_I = 10 ppm, pH = 8, adsorbent dose = 1 mg, volume = 7 mL).

The following table represents the values of the thermodynamic parameters (ΔS and ΔH) for the adsorption of Ni(II) on ortho-, meta-, or para-nitrophenyl silicas.

Table 4.17: The thermodynamic parameters for the adsorption of Ni(II) on (Si-o-NO_2), (Si-m-NO_2) and (Si-p-NO_2).

Adsorbents	Adsorption of Ni(II)	
	Adsorption Thermodynamics	
	ΔH (kJ)	ΔS (J/K)
Si-o-NO_2	10.961	-10.964
Si-m-NO_2	31.453	-76.525
Si-p-NO_2	21.328	-43.505

As shown in this table, the adsorption of Ni(II) on (Si-o-NO_2), (Si-m-NO_2) or (Si-p-NO_2) adsorbent is endothermic process ($\Delta H > 0$) and non spontaneous ($\Delta S < 0$).

4.3.2 Using the same Adsorbent with Different Adsorbates

4.3.2.1 Adsorption on (Si-o-NO_2)

The parameters for the adsorption of Cd(II), Pb(II) and Ni(II) on (Si-o-NO_2) were investigated, as shown in Tables (4.18-4.20).

4.3.2.1.1 Equilibrium Isotherm Models

Table 4.18: The parameters of Langmuir and Freundlich isotherms for the adsorption of Cd(II), Pb(II) and Ni(II) on (Si-o-NO_2).

Adsorbates	Adsorption on (Si-o-NO_2)			
	Equilibrium Isotherm Models			
	Langmuir Isotherm		Freundlich Isotherm	
	Q_o (mg/g)	b (L/mg)	K_F (mg/g)	n (g/L)
Cd(II)	44.247	-3.228	61.475	-5.734
Pb(II)	65.789	-	66.405	-63.291
Ni(II)	46.948	-3.944	62.345	-5.618

4.3.2.1.2 Adsorption Kinetic Models

Table 4.19: The parameters of pseudo first-order, pseudo second-order and intra-particle diffusion kinetic models for the adsorption of Cd(II), Pb(II) and Ni(II) on (Si-o-NO_2).

Adsorbates	Adsorption on (Si-o-NO_2)					
	Adsorption Kinetic Models					
	Pseudo First-Order Kinetics		Pseudo Second-Order Kinetics		Intra-Particle Diffusion Kinetics	
	q_e (mg/g)	K_1 ($mg.g^{-1}.min^{-1}$)	q_e (mg/g)	K_2 ($g.mg^{-1}.min^{-1}$)	C (mg/g)	K_p ($mg.g^{-1}.min^{-0.5}$)
Cd(II)	17.179	$7.149*10^{-3}$	58.479	0.0186	51.126	0.945
Pb(II)	7.296	0.0162	67.114	0.0331	61.078	0.8198
Ni(II)	24.339	$-2.303*10^{-4}$	45.454	-0.538	45.809	-0.0643

4.3.2.1.3 Adsorption Thermodynamics

Table 4.20: The thermodynamic parameters for the adsorption of Cd(II), Pb(II) and Ni(II) on (Si-o-NO_2).

Adsorbates	Adsorption on (Si-o-NO_2)	
	Adsorption Thermodynamics	
	ΔH (kJ)	ΔS (J/K)
Cd(II)	36.861	-101.032
Pb(II)	27.084	-52.316
Ni(II)	10.961	-10.964

4.3.2.2 Adsorption on (Si-m-NO_2)

The parameters for the adsorption of Cd(II), Pb(II) and Ni(II) on (Si-m-NO_2) were investigated, as shown in Tables (4.21-4.23).

4.3.2.2.1 Equilibrium Isotherm Models

Table 4.21: The parameters of Langmuir and Freundlich isotherms for the adsorption of Cd(II), Pb(II) and Ni(II) on (Si-m-NO_2).

Adsorbates	Adsorption on (Si-m-NO_2)			
	Equilibrium Isotherm Models			
	Langmuir Isotherm		Freundlich Isotherm	
	Q_o (mg/g)	b (L/mg)	K_F (mg/g)	n (g/L)
Cd(II)	39.216	-4.396	55.017	-7.241
Pb(II)	62.500	-40.000	64.062	-24.570
Ni(II)	53.476	-12.466	60.912	-13.459

4.3.2.2.2 Adsorption Kinetic Models

Table 4.22: The parameters of pseudo first-order, pseudo second-order and intra-particle diffusion kinetic models for the adsorption of Cd(II), Pb(II) and Ni(II) on (Si-m-NO_2).

Adsorbates	Adsorption on (Si-m-NO_2)					
	Adsorption Kinetic Models					
	Pseudo First-Order Kinetics		Pseudo Second-Order Kinetics		Intra-Particle Diffusion Kinetics	
	q_e (mg/g)	K_1 ($mg.g^{-1}.min^{-1}$)	q_e (mg/g)	K_2 ($g.mg^{-1}.min^{-1}$)	C (mg/g)	K_p ($mg.g^{-1}.min^{-0.5}$)
Cd(II)	17.952	-	52.083	-	52.046	0.0013
Pb(II)	6.323	$-1.382*10^{-3}$	63.291	-0.208	63.833	-0.0799
Ni(II)	19.738	$4.836*10^{-3}$	54.645	0.0307	48.501	0.8432

4.3.2.2.3 Adsorption Thermodynamics

Table 4.23: The thermodynamic parameters for the adsorption of Cd(II), Pb(II) and Ni(II) on (Si-m-NO_2).

Adsorbates	Adsorption on (Si-m-NO_2)	
	Adsorption Thermodynamics	
	ΔH (kJ)	ΔS (J/K)
Cd(II)	32.148	-85.052
Pb(II)	29.499	-65.639
Ni(II)	31.453	-76.525

4.3.2.3 Adsorption on (Si-p-NO_2)

The parameters for the adsorption of Cd(II), Pb(II) and Ni(II) on (Si-p-NO_2) were investigated, as shown in Tables (4.24-4.26).

4.3.2.3.1 Equilibrium Isotherm Models

Table 4.24: The parameters of Langmuir and Freundlich isotherms for the adsorption of Cd(II), Pb(II) and Ni(II) on (Si-p-NO_2).

Adsorbates	Adsorption on (Si-p-NO_2)			
	Equilibrium Isotherm Models			
	Langmuir Isotherm		Freundlich Isotherm	
	Q_o (mg/g)	b (L/mg)	K_F (mg/g)	n (g/L)
Cd(II)	40.816	-2.952	57.716	-6.477
Pb(II)	68.493	-	68.407	-212.766
Ni(II)	54.054	-8.409	61.987	-9.452

4.3.2.3.2 Adsorption Kinetic Models

Table 4.25: The parameters of pseudo first-order, pseudo second-order and intra-particle diffusion kinetic models for the adsorption of Cd(II), Pb(II) and Ni(II) on (Si-p-NO_2).

Adsorbates	Adsorption on (Si-p-NO_2)					
	Adsorption Kinetic Models					
	Pseudo First-Order Kinetics		Pseudo Second-Order Kinetics		Intra-Particle Diffusion Kinetics	
	q_e (mg/g)	K_1 ($mg.g^{-1}.min^{-1}$)	q_e (mg/g)	K_2 ($g.mg^{-1}.min^{-1}$)	C (mg/g)	K_p ($mg.g^{-1}.min^{-0.5}$)
Cd(II)	14.184	-	55.866	-	55.838	-0.0091
Pb(II)	2.122	-	68.027	-	67.878	0.0011
Ni(II)	14.581	$9.212*10^{-4}$	55.866	0.641	55.040	0.1475

4.3.2.3.3 Adsorption Thermodynamics

Table 4.26: The thermodynamic parameters for the adsorption of Cd(II), Pb(II) and Ni(II) on (Si-p-NO_2).

Adsorbates	Adsorption on (Si-p-NO_2)	
	Adsorption Thermodynamics	
	ΔH (kJ)	ΔS (J/K)
Cd(II)	24.065	-54.221
Pb(II)	25.525	-46.077
Ni(II)	21.328	-43.505

Conclusion

The synthesis and characterization of the new polysiloxane modified surfaces including (Si-o-NO_2), (Si-m-NO_2) and (Si-p-NO_2) showed that these polymers have very good thermal and chemical stabilities, and hence they can be used as perfect adsorbents to uptake Cd(II), Pb(II) and Ni(II) from groundwater.

The observed results of this research include the following:

1. The maximum extent of adsorption was for (Si-p-NO_2) polymer in the presence of lead ions. This adsorption needed only 1 minute of shaking to have 99.95% as percent of Pb(II) removal. For cadmium and nickel ions, the maximum percent of removal was 98.99% in the presence of (Si-m-NO_2) adsorbent.
2. The results showed that all adsorptions followed Langmuir adsorption and the mechanism of all reactions followed pseudo second-order kinetic adsorption model.
3. The thermodynamic parameters of all the adsorptions proved that these processes are endothermic ($\Delta H > 0$) and non spontaneous ($\Delta S < 0$).
4. The regenerated polymers showed good percentage removal for Cd(II), Pb(II) and Ni(II).
5. The synthesized adsorbents have high adsorption efficiency and showed perfect strong complexation properties with heavy metal ions.

Recommendations for Future Works

1. Using the synthesized adsorbents to remove other toxic heavy metal ions rather than cadmium, lead and nickel ions form water.
2. Up taking of toxic metal ions from water using others modified polymer surfaces and compare between the adsorption efficiency between them and the synthesized polymers in this research.
3. Using the synthesized polymers for water purification in Hebron, due to the presence of many factories which contribute in a pronounced increase in the pollution with toxic metal ions.
4. A column containing the synthesized modified silicas whether as a filling or as a cover can be designed, and hence this technique can be used to clean up polluted water.
5. A complexation reaction of the synthesized polymers with a metal ion such as Cu(II) or Cd(II) can be used in order to remove other pollutants from wastewater like nitrate (NO_3^{-1}) or nitrite (NO_2^{-1}).

References

[1] B.J. Nebel, R.T. Wright, **Environmental Science**, fifth edition, Prentice-Hall, Inc., New Jersey, 1996, pp. 348-349.

[2] A. Denizli, G. O¨ zkan, M.Y. Arica. **Preparation and characterization of magnetic polymethylmethacrylate microbeads carrying ethylene diamine for removal of Cu(II),** Cd(II), Pb(II) and Hg(II) from aqueous solutions, J. Appl. Polym. Sci. 78, 2000, pp. 81-89.

[3] S.R. Shukla, R.S. Pai, A.D. **Shendarkar. Adsorption of Ni(II), Zn(II) and Fe(II) on modified coir fibres**, Sep. Purif. Technol. 47, 2006, pp. 141-147.

[4] R.-S. Juang, H.-C. Kao, W. Chen. **Column removal of Ni(II) from synthetic electroplating waste water using a strong-acid resin**, Sep. Purif. Technol. 49, 2006, pp. 36-42.

[5] A.M. Donia, A.A. Atia, K.Z. **Elwakeel. Gold(II) recovery using synthetic resins with amine, thio and amine/mercaptan functionalities,** Sep. Purif. Technol. 42, 2005, pp. 111-116.

[6] C.-Y. Chen, C.-L. Chiang, P.-C. **Huang. Adsorptions of heavy metal ions by a magnetic chelating resin containing hydroxy and iminodiacetate groups**, Sep. Purif. Technol. 50, 2006, pp. 15-21.

[7] C.-Y. Chen, S.-Y. Chen. **Adsorption properties of a chelating resin containing hydroxy group and iminodiacetic acid for copper ions**, J. Appl. Polym. Sci. 94, 2004, pp. 2123-2130.

[8] W. Li, H. Zhao, P.R. Teasdale, R. John, S. Zhang. **Synthesis and characterization of a polyacrylamide-polyacrylic acid copolymer**

hydrogel for environmental analysis of Cu and Cd, React. Funct. Polym. 52, 2002, pp. 31-41.

[9] A.G. Kılıc¸, S. Malcı, O¨ . C¸ elikbıc¸ak, N. S¸ ahiner, B. Salih. **Gold recovery onto poly(acrylamide-allylthiourea) hydrogels synthesized by treating with gamma radiation,** Anal. Chim. Acta 547, 2005, pp. 18-25.

[10] H.A. Essawy, H.S. Ibrahim. **Synthesis and characterization of poly(vinylpyrrolidone-co-methylacrylate) hydrogel for removal and recovery of heavy metal ions from wastewater,** React. Funct. Polym. 61, 2004, pp. 421-432.

[11] N. Pekel, H. Savas, O. G¨uven. **Complex formation and adsorption of V^{+3}, Cr^{+3} and Fe^{3+} ions with poly(N-vinylimidazole),** Colloid Polym. Sci. 280, 2002, pp. 46-51.

[12] C. Zhang, X. Li, J. Pang. **Synthesis and adsorption properties of magnetic resin microbeads with amine and mercaptan as chelating groups**, J. Appl. Polym. Sci. 82, 2001, pp. 1587-1592.

[13] A.M. Donia, A.A. Atia, H.A. El-Boraey, D.H. Mabrouk. **Adsorption of Ag(I) on glycidyl methacrylate/N,N_methylene bis-acrylamide chelating resins with embedded iron oxide,** Sep. Purif. Technol. 48, 2006, pp. 281-287.

[14] A.M. Donia, A.A. Atia, H.A. El-Boraey, D.H. Mabrouk. **Uptake studies of copper(II) on glycidyl methacrylate chelating resin containing Fe_2O_3 particles,** Sep. Purif. Technol. 49, 2006, pp. 64-70.

[15] A.A. Atia, A.M. Donia, K.Z. Elwakeel. **Selective separation of mercury(II) using a synthetic resin containing amine and mercaptan as chelating groups,** React. Funct. Polym. 65, 2005, pp. 267-275.

[16] K.H. Reddy, A.R. Reddy. **Removal of heavy metal ions using the chelating polymers derived by the condensation of poly(3-hydroxy-4-acetylphenl methacrylate) with different diamine**, J. Appl. Polym. Sci. 88, 2003, pp. 414-421.

[17] A. Dis¸budak, S. Bektas¸, S. Patir, O¨ . Genc¸, A. Denizli. **Cysteine-metal affinity chromatography: determination of heavy metal adsorption properties**, Sep. Purif. Technol. 26, 2002, pp. 273-281.

[18] J. Shao, Y. Yang, C. Shi. **Preparation and adsorption properties for metal ions of chitin modified by l-cysteine**, J. Appl. Polym. Sci. 88, 2003, pp. 2575-2579.

[19] R.R. Navarro, K.Tatsumi, K. Sumi, M. Matsumura. **Role of anions on heavy metal sorption of cellulose modified with poly(glycidyl methacrylate) and polyethyleneimine,** Water Res. 35, 2001, pp. 2724-2730.

[20] R.R. Navarro, K. Sumi, M. Matsumura. **Heavy metal sequestration properties of a new amine-type chelating adsorbent**, Water Res. 38, 1998, pp. 195-201.

[21] R.R.Navarro, K. Sumi, M. Matsumura. **Improved metal affinity of chelating adsorbents through graft polymerization**, Water Res. 33, 1999, pp. 2037-2044.

[22] L. Wang, S. P. Good, K. K. **Caylor, Geophys**. Res. Lett. 41, 2014, pp. 6753-6757.

[23] Mumford AC, Barringer JL, Benzel WM, Reilly PA, Young L. **Microbial transformations of Arsenic: mobilization from glauconitic sediments to water,** Water Res 46, 2012, pp. 2859-2868.

[24] Schilling, K. E. **Investigating local variation in groundwater recharge along a topographic gradient, Walnut Creek**, Iowa, USA, Hydrogeol. J. Schofield, N. J. Tree planting for dryland salinity. 17, 2009, pp. 397-407.

[25] Boufekane, A., & Saighi, O. ***Assessment of Groundwater Pollution by Nitrates using Intrinsic Vulnerability Methods: A Case Study of the Nil Valley Groundwater (Jijel, North-East Algeria).*** **African Journal of Environmental Science and Technology**, 7(10), 2013, pp. 949-960.

[26] WHO. **Guidelines for Drinking Water Quality**, third edition, World Health Organization Press, 20 Avenue Appia, 1211 Geneva 27, Switzerland, 2008.

[27] Schuster-Wallace, C. J., Grover, V. I., Adeel, Z., Confalonieri, U., & Elliot, S. ***Safe water as the key to global health. United Nations University International Network on Water***, **Environment and Health (UNUINWEH), Hamilton**, ON, 2008.

[28] Reddy, V. R., & Behera, B. ***Analysis Impact of Water Pollution on Rural Communities: An Economic Analysis,*** **Ecological Economics**, 58, 2006, pp. 520-537.

[29] Ragossnig, A. M., & Vujic, G. **Challenges in Technology Transfer from Developed to Developing Countries,** Waste Management and Research, 33(2), 2015, pp. 93-95.

[30] Osibanjo, O., & Adie, G. U. ***Impact of Effluent from Bodija Abattoir on the Physico-chemical Parameters of Oshunkaye Stream in Ibadan City, Nigeria***, **African Journal of Biotechnology**, 6(15), 2007, pp. 1806-1811.

[31] Hailin, Y., Ligang, X., Chang, Y., & Jiaxing, X. **Evaluation of groundwater vulnerability with improved DRASTIC method**, Procedia Environ Sci, 10, 2011, pp. 2690-2695.

[32] Eugene, L. R., Shylla, R., & Singh, O. P. ***Assessment of Ground Water Quality from Dug Wells in West Jaintia Hills District, Meghalaya, India*, International Journal of Environmental Sciences**, 5(3), 2014, pp. 544-552.

[33] Adekunle, I. M., Adetunji, M. T., Gbadebo, A. M., & Banjoko, O. B. ***Assessment of Groundwater Quality in a Typical Settlement in Southwest Nigeria,*** **International Journal of Environmental Research and Public Health**, 4(4), 2007, pp. 307-318.

[34] D. Ghosh, H. Solanki, M.K. Purkait. **Removal of Fe(II) from tap water by electrocoagulation technique**, J. Hazard. Mater. 155, 2008, pp. 135–143.

[35] Collin, M. L., & Melloul, A. J. ***Assessing Groundwater Vulnerability to Pollution to Promote Sustainable Urban and Rural Development***, **Journal of Cleaner Production**, 11, 2003, pp. 727-736.

[36] World Health Organization. **Guidelines for Drinking-Water Quality: Recommendations-Addendum,** Vol. 1, Third Edition, 2008.

[37] M. G. Donat, L. V. Alexander, H. Yang et al. ***Updated analyses of temperature and precipitation extreme indices since the beginning of the twentieth century: the HadEX2 dataset,*** **Journal of Geophysical Research,** vol. 118, no. 5, 2013, pp. 2098-2118.

[38] V. Stankovic, D. Bozic, I. Manasijevic, G. Bogdanovic. **Direct electrowinning of copper from mine waters**, in: **First Regional Symposium on Electrochemistry of South-East Europe**, Rovinj, Croatia, 2008.

[39] B. Yasemin, T. Zeki. **Removal of heavy metals from aqueous solution by sawdust adsorption**, J. Environ. Sci. 19, 2007, pp. 160-166.

[40] D. Feng, C. Aldrich. **Adsorption of heavy metals by biomaterials derived from the marine alga Ecklonia maxima, Hydrometallurgy** 73, 2004, pp. 1-10.

[41] D. Mohan, S. Chander. **Removal and recovery of metal ions from acid mine drainage using lignite low cost sorbent,** J. Hazard. Mater. B137, 2006, pp. 1545-1553.

[42] W.S.W. Ngah, M.A.K.M. Hanafiah. **Removal of heavy metal ions from wastewater by chemically modified plant wastes as adsorbents: a review, Bioresour**. Technol. 99, 2008, pp. 3935-3948.

[43] N. Fiol, I. Villaescusa, M. Martinez, N. Miralles, J. Poch, J. Serarols. **Sorption of Pb(II), Ni(II), Cu(II) and Cd(II) from aqueous solution by olive stone waste,** Sep. Purif. Technol. 50, 2006, pp. 132-140.

[44] J. Febrianto, A.N. Kosasih, J. Sunarso, Y. Ju, N. Indraswati, S. Ismadji. **Equilibrium and kinetic studies in adsorption of heavy metals using biosorbent: a summary of recent studies**, J. Hazard. Mater. 162, 2009, pp. 616-645.

[45] D. Lu, Q. Cao, X. Li, X. Cao, F. Cao, W. Shao. **Kinetics and equilibrium of Cu(II) adsorption onto chemically modified orange peel cellulose biosorbents,** Hydrometallurgy. 95, 2009, pp. 145-152.

[46] S. Larous, A. Meniai, M.B. Lehocine. **Experimental study of the removal of copper from aqueous solutions by adsorption using sawdust**, Desalination 185, 2005, pp. 483-490.

[47] L. Tofan, C. Paduraru, D. Bilbia, M. Rotoriu. **Thermal power plants ash as sorbent for the removal of Cu(II) and Zn(II) ions from wastewaters**, J. Hazard. Mater. 156, 2008, pp. 1-8.

[48] A.K. Meena, G.K. Mishra, K. Satish, C. Rajagopal, P.N. Nagar. **Adsorption of cadmium ions from aqueous solution using different adsorbents,** Indian J. Sci Ind. Res. 63, 2004, pp. 410-416.

[49] Ameh PO. **Modeling of the adsorption of Cu(II) and Cd(II) from aqueous solution by Iraqi Palm-Date activated carbon**, Intl. J. Modern chem. 2013, pp. 136-144.

[50] Cheung W, Porter JF and McKay G. **Sorption kinetic analysis for removal of cadmium ion from effluents using bone char,** Water Res. 35, 2001, pp. 605-621.

[51] SINGANAN M. **Removal of Lead(II) and Cadmium(II) ions from wastewater using activated biocarbon**, Sci. Asia 37, 115, 2011.

[52] Ajmal MR, Rao A, Ahmad J and Ahmad R. **Adsorption studies on rice husk: removal and recovery of Cd(II) from waste water**, Biosource Tech. 86, 2003, pp. 147-149.

[53] Garg U, Kaur MP, Jawa GK, Sud D, Garg V.K. ***Removal of cadmium (II) from aqueous solutions by adsorption on agricultural waste biomass,*** **Journal of Hazards Mater**. 154(1-3), 2008, pp. 1149-1157.

[54] Amarasinghe BMWPK, Williams RA. **Tea waste as a low cost adsorbent for the removal of Cu and Pb from wastewater,** Chem. Eng. J, 2007, pp. 299-309.

[55] Zahra N. **Lead Removal from Water by Low Cost Adsorbents a Review Pak,** J. Anal. Environ. Chem.13(1), 2012, pp. 1-8.

[56] Gupta, VK, Ali I. ***Removal of lead and chromium from wastewater using bagasse fly ash, A sugar industry waste,*** **Journal of Colloid Interface Science**, 2004, pp. 321-328.

[57] D. He, S. Gu, M. Ma. **Simultaneous removal and recovery of cadmium (II) and CN from simulated electroplating rinse wastewater by a strip dispersion hybrid liquid membrane (SDHLM) containing double carrier,** J. Membr. Sci. 305, 2007, pp. 36-47.

[58] Vijayaraghavan K, Jegan J, Palanivelu K, Velan M et al. ***Removal of nickel(II) ions from aqueous solution using crab shell particles in a packed bed upflow column,*** **Journal of Hazardous Materials**. 113(1-3), 2004, pp. 223-230.

[59] Faghihnasiri S, Baei MS, Ardjmand M. ***Kinetic Isotherm Study of Nickel Adsorption from Colored Wastewater Using Polypyrrole/ Polyvinyl Alcohol Composite***, **Middle-East Journal of Scientific Research.** 15(10), 2013, pp. 1345-1352.

[60] Vijayaraghavan K, Jegan J, Palanivelu K, Velan M et al. **Biosorption of cobalt(II) and nickel(II) by seaweeds: batch and column studies, Separation and Purification Technology.** 44(1), 2005, pp. 53-59.

[61] ***Eisazadeh H. Effect of various agents on removal of Nickel from aqueous solution using Polypyrrole as an adsorbent***, **Journal of Engineering Science and Technology.** 7(5), 2012, pp. 540-550.

[62] M.N. Rashed. **Adsorption Technique for the Removal of Organic Pollutants from Water and Wastewater, Organic Pollutants Monitoring, Risk and Treatment".** Prof. M. Nageeb Rashed (Ed.). 2013.

[63] **A. Dąbrowski. Adsorption—From Theory to Practice, Advances in a Colloid and Interface Science**. 93, 2001, pp. 135-224.

[64] J. S. Piccin and et al. ***Adsorption Isotherms and Thermochemical Data of FD&C RED N° 40 Binding by Chitosan,*** **Brazilian Journal of Chemical Engineering,** Vol. 28, No. 02, 2011, pp. 295-304.

[65] M. Ghiaci, A. Abbaspur, R. Kia, F. **Seyedeyn-Azad. Equilibrium isotherm studies for the sorption of benzene, toluene, and phenol onto Organozeolites and as-synthesized MCM-41,** Separation and Purification Technology J. 40, 2004, pp. 217–229.

[66] M.C. Ncibi. ***Applicability of some statistical tools to predict optimum adsorption isotherm after linear and non-linear regression analysis,*** **Journal of Hazardous Materials**. 153, 2008, pp. 207–212.

[67] Sylvester O. Adejo and Mbanefo M. Ekwenchi. ***Proposing a new empirical adsorption isotherm known as Adejo-Ekwenchi isotherm,*** **Journal of Applied Chemistry**, 2014, pp. 66-71.

[68] K.Y. Foo and B.H. Hameed***. Insights into the modeling of adsorption isotherm systems***, **Chemical Engineering Journal** 156, 2010, pp. 2-10.

[69] H. Qiu, L. Lv, B. Pan, Q. Zhang, W. Zhang, Q. ***Zhang. Critical Review in Adsorption Kinetic Models,*** **Journal of Zhejiang University Science A**. 10, 2009, pp. 716-724.

[70] J. He, S. Hong, L. Zhang, F. Gan, Y. Ho. **Equilibrium and Thermodynamic Parameters of Adsorption of Methylene Blue onto Rectorite, Fresenius Environmental Bulletin.** 19, 2010, pp. 2651-2656.

[71] D. Sridev, K. Rajendran. **Synthesis and Optical Characteristics of ZnO Nanocrystals, Bulletin of Materials Science**. 32, 2009, pp. 165-168.

[72] **Lucia Ferrari and et al. Interaction of cement model systems with super plasticizers investigated by atomic force microscopy, zeta potential, and adsorption measurements**, J Colloid Interface Sci., 2010, pp. 15-24.

[73] BAI Y., BARTKIEWICZ B. **Removal of Cadmium from wastewater using ion exchange resin amberjet 1200H columns**, Pol. J. Environ. Stud. 18, 1191, 2009.

[74] A. Agrawal, K. Sahu. ***Kinetics and isotherm studies of cadmium adsorption on manganese nodule residue***, **Journal of Hazardous Materials.** 137, 2009, pp. 915-924.

[75] Y. Li, S. Wang, Z. Luan, J. Ding, C. Xu, D. Wu. **Adsorption of Cadmium (II) from aqueous solution by surface oxidized carbon Nanotubes.** J. of Elsevier. 41,2003, pp. 1057–1062.

[76] J. Lin, L. Wang. **Comparison between linear and non-linear forms of pseudo-first-order and pseudo-second-order adsorption kinetic models for the removal of Methylene blue by activated carbon**. J. of Environ Sci. Engin. 83, 2009, pp. 11-17.

[77] M. Ugurlu, A. Gurses, M. Acıkyıldız. **Comparison of textile dyeing effluent adsorption on commercial activated carbon and activated carbon prepared from olive stone by ZnCl2 activation**. Microporous and Mesoporous Materials. 111, 2008, pp. 228-235.

[78] E. Elmolla, M. ***Chaudhuri. Improvement of biodegradability of synthetic amoxicillin wastewater by Photo-Fenton process.*** **World Applied Science Journal**. 5, 2009, pp. 53-58.

[79] I. Tan, B. Hameed, A. Ahmad. **Equilibrium and Kinetic studies on basic dye adsorption by oil palm fiber activated carbon**, J. Chem. Eng. 127, 2007, pp. 111-119.

[80] Nizam M. El-Ashgar and Salman M. **Saadeh. Preparation of Immobilized-Polysiloxane Salicylaldehyde Propylimine and Its Application**, J. Al-Aqsa Unv.10, 2006.

[81] SG. Dubois, C. Reyé, R. J. P. Corriu and C. ***Chuit. Organic-Inorganic Hybrid Materials. Preparation and Properties of Dibenzo-18-Crown-6 Ether-Bridged Poly-silsesquioxanes,*** **Journal of Materials Chemistry,** Vol.10, 2000, pp. 1091-1098

[82] S. Radi, S. Tighadouini, Y. ***Toubi and M. Bacquet. Polysiloxane Surface Modified with Bipyrazolic Tripodal Receptor for Quantitative Lead Adsorption,*** **Journal of Hazardous Materials**, Vol. 185, No. 1, 2011, pp. 494-501.

[83] Mehdi Rahimi , Mehdi Vadi. ***Langmuir, Freundlich and Temkin Adsorption Isotherms of Propranolol on Multi-Wall Carbon Nanotubes.*** **Journal of Modern Drug Discovery and Drug Delivery Research,** 2014.

[84] Dada, A.O and et al. Langmuir, Freundlich, ***Temkin and Dubinin-Radushkevich Isotherms Studies of Equilibrium Sorption of Zn^{2+} Unto Phosphoric Acid Modified Rice Husk,*** **IOSR Journal of Applied Chemistry,** 2012, pp. 38-45.

[85] X. Li and F. Xue. **Removal of Cu(II) from Aqueous Solution by Adsorption onto Functionalized SBA-16 Mesoporous Silica,**

Microporous and Mesoporous Materials, Vol. 116, No. 1-3, 2008, pp. 116-122.

[86] R. Qu, M. Wang, C. Sun, Y. Zhang, C. Ji, H. Chen, Y. Meng and P. Yin**. Chemical Modification of Silica-Gel with Hydroxyl- or Amino-Terminated Polyamine for Adsorption of Au(III).** Applied Surface Science, Vol. 255, No. 5, 2008, pp. 3361-3370.

[87] S. Radi, A. Ramdani, Y. Lekchiri, M. Morcellet, G. Crini, L. ***Janus and M. Bacquet. Immobilization of Pyrazole Compounds on Silica Gels and Their Preliminary Use in Metal Ion Extraction.*** **New Journal of Chemistry,** Vol. 27, No. 8, 2003, pp. 1224-1227.

[88] S. Radi, A. Attayibat, A. Ramdani and M. Bacquet. ***Synthesis and Characterization of Novel Silica Gel Supported N-Pyrazole Ligand for Selective Elimination of Hg(II),*** **European Polymer Journal,** Vol. 44, No. 10, 2008, pp. 3163-3168.

[89] D. P. Quintanilla, I. Hierro, M. Fajardo and I. Sierra. ***Adsorption of Cadmium(II) from Aqueous Media onto a Mesoporous Silica Chemically Modified with 2-Mercaptopyrimidine,*** **Journal of Materials Chemistry**, Vol. 16, 2006, pp. 1757-1764.

[90] D. P. Quintanilla, A. Sánchez, I. Hierro, M. Fajardo and I. ***Sierra. Preparation, Characterization, and Zn^{2+} Adsorption Behavior of Chemically Modified MCM-41 with 5-Mercapto-1-Methyltetrazole***, **Journal of Colloid and Interface Science**, Vol. 313, No. 2, 2007, pp. 551-562.

[91] S. Radi, Y. Toubi, M. Bacquet, S. Degoutin and F. **Cazier. 1-(Pyridin-2-yl) Imine Functionalized Silica Gel: Synthesis, Characterization, and Preliminary Use in Metal Ion Extraction,** Separation Science and Technology, Vol. 48, No. 9, 2013, pp. 1349.

[92] ***Smaail Radi and et al. New Polysiloxane Surfaces Modified with ortho-, meta- or para-Nitrophenyl Receptors for Copper Adsorption***, **Journal of Surface Engineered Materials and Advanced Technology.** 4, 2014, pp. 21-28.

[93] Radi, Y. Toubi and M. Bacquet. **Synthesis of Pyridin-3-Yl-Functionalized Silica as a Chelating Sorbent for Solid-Phase Adsorption of Hg(II), Pb(II), Zn(II), and Cd(II) from Water,** Research on Chemical Intermediates, Vol. 39, No. 8, 2013, pp. 3791-3802.

[94] S. Radi and A. Attayibat. **Functionalized SiO2 With S-Donor Thiophene: Synthesis, Characterization, and Its Heavy Metals Adsorption, Phosphorus, Sulfur, and Silicon and the Related Elements,** Vol. 185, No. 10, 2010, pp. 2003-2013.

[95] S. Radi, A. Attayibat, A. Ramdani, Y. Lekchiri and M. **Bacquet. Synthesis and Characterization of a New Material Based on Porous Silica—Chemically Immobilized C,N-Pyridylpyrazole for Heavy Metals Adsorption, Materials Chemistry and Physics,** Vol. 111, No. 2-3, 2008, pp. 296-300.

جامعة النجاح الوطنية

كلية الدراسات العليا

تنقية المياه الجوفية من الفلزات السامة بواسطة المتصلات المتعددة المثبتة و المعلقة

إعداد

بيان محمد محمود خلف

إشراف

أ.د. شحدة جودة

أ.د. إسماعيل وراد

قدمت هذه الأطروحة استكمالاً لمتطلبات الحصول على درجة الماجستير في الكيمياء بكلية الدراسات العليا في جامعة النجاح الوطنية ، نابلس ، فلسطين.

2016

تنقية المياه الجوفية من الفلزات السامة بواسطة المتصلات المتعددة المثبتة و المعلقة

إعداد

بيان محمد محمود خلف

إشراف

أ.د. شحدة جودة

أ.د. اسماعيل وراد

الملخص

تهدف هذه الدراسة إلى تنقية المياه الجوفية من أيونات الفلزات الثقيلة السامّة بواسطة المُتصلات المتعددّة المُثبتة و المُعلقّة ؛ حيث أنّ المياه الجوفية المستخدمة في هذا البحث كانت من بلدة برقين في فلسطين ، في البداية تم تحضير محاليل معيارية معروفة التراكيز من أملاح مختلفة لكل من أيونات الكادميوم و الرصاص و النيكل، و بعدها تمت إزالة هذه العناصر السامّة بالإعتماد على طريقة الإمتزاز ، حيث حُضّرت ثلاثة بُوليمرات ذات خصائص سطحية ممتازة و هذه المواد هي:

($Si-o-NO_2$) و($Si-m-NO_2$) و($Si-p-NO_2$) ، و من ثم تم فحص صفات هذه المركبات و ثباتية كلٍ منها كيميائياً و حرارياً باستخدام تقنيات و أجهزة عديدة أثبتت أنّ هذه البوليمرات ذات قدرة كبيرة على إزالة الفلزات السامة من المياه الجوفية ، مما يعني كفاءتها كمواد مازة.

تم اختبار العديد من الظروف المختلفة مثل : زمن التحريك ، درجة الحرارة ، درجة الحموضة ، التركيز الإبتدائي للمادة المُمتزة ، و كمية المادة المازة ، و ذلك من أجل معرفة الظروف المثالية التي تؤدي إلى أكبر نسبة إزالة للعناصر الفلزية السامّة بطريقة فعالة.

أشارت النتائج أنّ عملية الإمتزاز كانت أفضل عند درجات الحرارة المنخفضة حيث أنّ درجة الحرارة المثالية لأغلب عمليات الإمتزاز كانت عند درجة حرارة الغرفة أو أقل من ذلك ؛ وبالنسبة لدرجة الحموضة المثالية فكانت تتراوح بشكل عام ما بين 5 و 8 ؛ أما بالنسبة لوقت

الإتصال الأمثل ما بين المادة المازة و المُمتزة فكان قليل جداً لأغلب العمليات ، و كان الوقت الأطول هو 50 دقيقة و ذلك عند استخدام أيونات الكادميوم مع مادة ($Si-o-NO_2$).

أشارت النتائج النهائية أنّ أعلى نسبة إزالة لكل من أيونات النيكل و الكادميوم هي % 98.99 و ذلك بوجود المادة المازة ($Si-m-NO_2$) ، أما بالنسبة لأيونات الرصاص فكانت النسبة 99.95% باستخدام المادة المازة ($Si-p-NO_2$).

بعد ذلك ، تم تطبيق عمليات الإمتزاز المختلفة على نماذج الإمتزاز ثابتة الحرارة (Langmuir and Freundlich Isotherms) ، حيث تم ملاحظة أنّ كل عمليات الإمتزاز كانت تابعة لنموذج (Langmuir) و بالتالي فهي إمتزازات كيميائية ، مما يدل على وجود روابط كيميائية حقيقية بين كل من المادة المازة و المُمتزة.

من أجل معرفة ميكانيكية كل من تفاعلات الإمتزاز ؛ تم تطبيق هذه العمليات على نماذج الإمتزاز الحركية و هي:

(pseudo first-order, pseudo second-order and intra-particle diffusion kinetic adsorption models)

و بالإعتماد على قيمة معامل الإرتباط لكل عملية إمتزاز ؛ كانت النتائج تشير أنّ كل تفاعلات الإمتزاز تابعة لنموذج (pseudo second-order kinetics).

و أيضاً تم رسم مخطط (Van't Hoff) من أجل معرفة دلائل الديناميكا الحرارية لعمليات الإمتزاز المختلفة ، و أشارت النتائج أنّ جميع هذه العمليات ماصة للحرارة ($\Delta H > 0$) و لا تحدث بصورة تلقائية ($\Delta S < 0$) ، في النهاية تم إعادة استخدام المواد المازة مرة أخرى من أجل معرفة أثر ذلك على نسبة إزالة الأيونات الفلزية السامّة.

بشكل عام ؛ أشارت نتائج هذا البحث أنّ المواد المازة التي تم تحضيرها كانت فعالة جداً في إزالة أيونات الكادميوم و الرصاص و النيكل من المياه الجوفية.